(12)

WT-935 (EX)
EXTRACTED VERSION

AD A995085

OPERATION CASTLE

Project 2.7
Distribution of Radioactive Fallout By Survey and Analyses of Sea Water

AD338336L

March-May 1954

Headquarters Field Command
Armed Forces Special Weapons Project
Sandia Base, Albuquerque, New Mexico

April 14, 1959

NOTICE

This is an extract of WT-935, Operation CASTLE, which remains classified SECRET/RESTRICTED DATA as of this date.

DTIC
ELECTE
JUN 4 1981
S D
D

Extract version prepared for:

Director
DEFENSE NUCLEAR AGENCY
Washington, D.C. 20305

1 April 1981

Approved for public release;
distribution unlimited.

DTIC FILE COPY

81 6 03 087

UNCLASSIFIED

SECURITY CLASSIFICATION OF THIS PAGE (When Data Entered)

REPORT DOCUMENTATION PAGE

READ INSTRUCTIONS BEFORE COMPLETING FORM

1. REPORT NUMBER: WT-935 (EX) (18) DOE

2. GOVT ACCESSION NO.: AD-A995 085

3. RECIPIENT'S CATALOG NUMBER:

4. TITLE (and Subtitle): (6)
Operation CASTLE. Project 2.7, Distribution of Radioactive Fallout by Survey and Analyses of Sea Water.

5. TYPE OF REPORT & PERIOD COVERED:

6. PERFORMING ORG. REPORT NUMBER: WT-935 (EX)

7. AUTHOR(s): (10)
T. R. Folsom
L. B. Werner

8. CONTRACT OR GRANT NUMBER(s): (9) Nov 1 - May 54

9. PERFORMING ORGANIZATION NAME AND ADDRESS:
Headquarters Field Command
Armed Forces Special Weapons Project
Sandia Base, Albuquerque, New Mexico

10. PROGRAM ELEMENT, PROJECT, TASK AREA & WORK UNIT NUMBERS: (11) 1 Apr 54

11. CONTROLLING OFFICE NAME AND ADDRESS: (12) 88

12. REPORT DATE: April 14, 1959

13. NUMBER OF PAGES: 89

14. MONITORING AGENCY NAME & ADDRESS (if different from Controlling Office):

15. SECURITY CLASS. (of this report): Unclassified

15a. DECLASSIFICATION/DOWNGRADING SCHEDULE:

16. DISTRIBUTION STATEMENT (of this Report):

Approved for public release; unlimited distribution.

17. DISTRIBUTION STATEMENT (of the abstract entered in Block 20, if different from Report):

(15)

18. SUPPLEMENTARY NOTES:
This report has had the classified information removed and has been republished in unclassified form for public release. This work was performed by Kaman Tempo under contract DNA001-79-C-0455 with the close cooperation of the Classification Management Division of the Defense Nuclear Agency.

19. KEY WORDS (Continue on reverse side if necessary and identify by block number):
Operation CASTLE
Radioactive Fallout
Radiation Measurements
Water Sampling

20. ABSTRACT (Continue on reverse side if necessary and identify by block number):

DD FORM 1 JAN 73 1473 EDITION OF 1 NOV 65 IS OBSOLETE

UNCLASSIFIED

246420

FOREWORD

This report has had classified material removed in order to make the information available on an unclassified, open publication basis, to any interested parties. This effort to declassify this report has been accomplished specifically to support the Department of Defense Nuclear Test Personnel Review (NTPR) Program. The objective is to facilitate studies of the low levels of radiation received by some individuals during the atmospheric nuclear test program by making as much information as possible available to all interested parties.

The material which has been deleted is all currently classified as Restricted Data or Formerly Restricted Data under the provision of the Atomic Energy Act of 1954, (as amended) or is National Security Information.

This report has been reproduced directly from available copies of the original material. The locations from which material has been deleted is generally obvious by the spacings and "holes" in the text. Thus the context of the material deleted is identified to assist the reader in the determination of whether the deleted information is germane to his study.

It is the belief of the individuals who have participated in preparing this report by deleting the classified material and of the Defense Nuclear Agency that the report accurately portrays the contents of the original and that the deleted material is of little or no significance to studies into the amounts or types of radiation received by any individuals during the atmospheric nuclear test program.

Accession For	
NTIS GRA&I	X
DTIC TAB	☐
Unannounced	☐
Justification	
By (14 April 1959)	
Distribution/	
Availability Codes	
Dist	Avail and/or Special
A	

Released

UNANNOUNCED

DTIC ELECTE JUN 4 1981 S D

D

Pages 1 thru 3, deleted

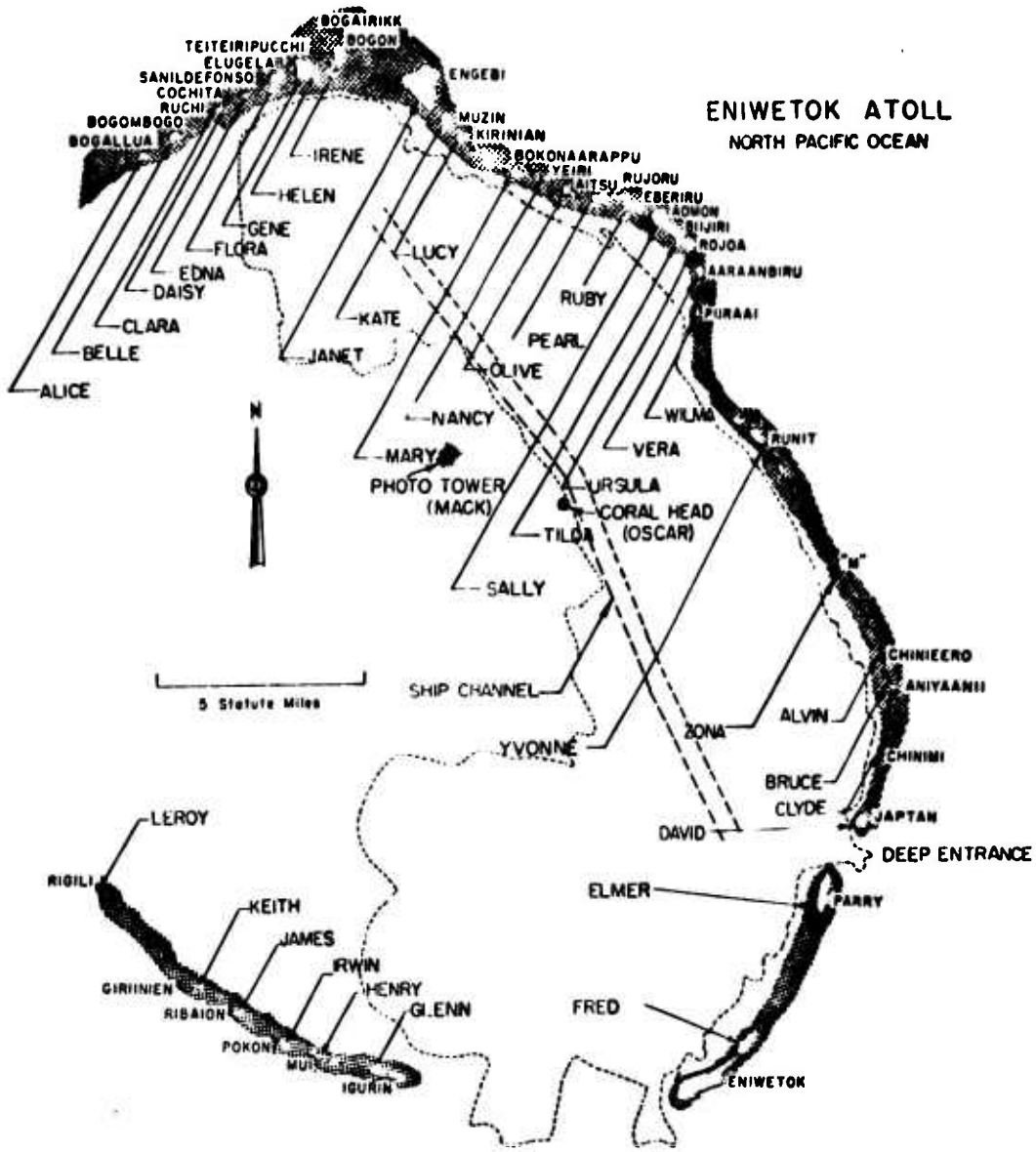

PRECEDING PAGE BLANK-NOT FILMED

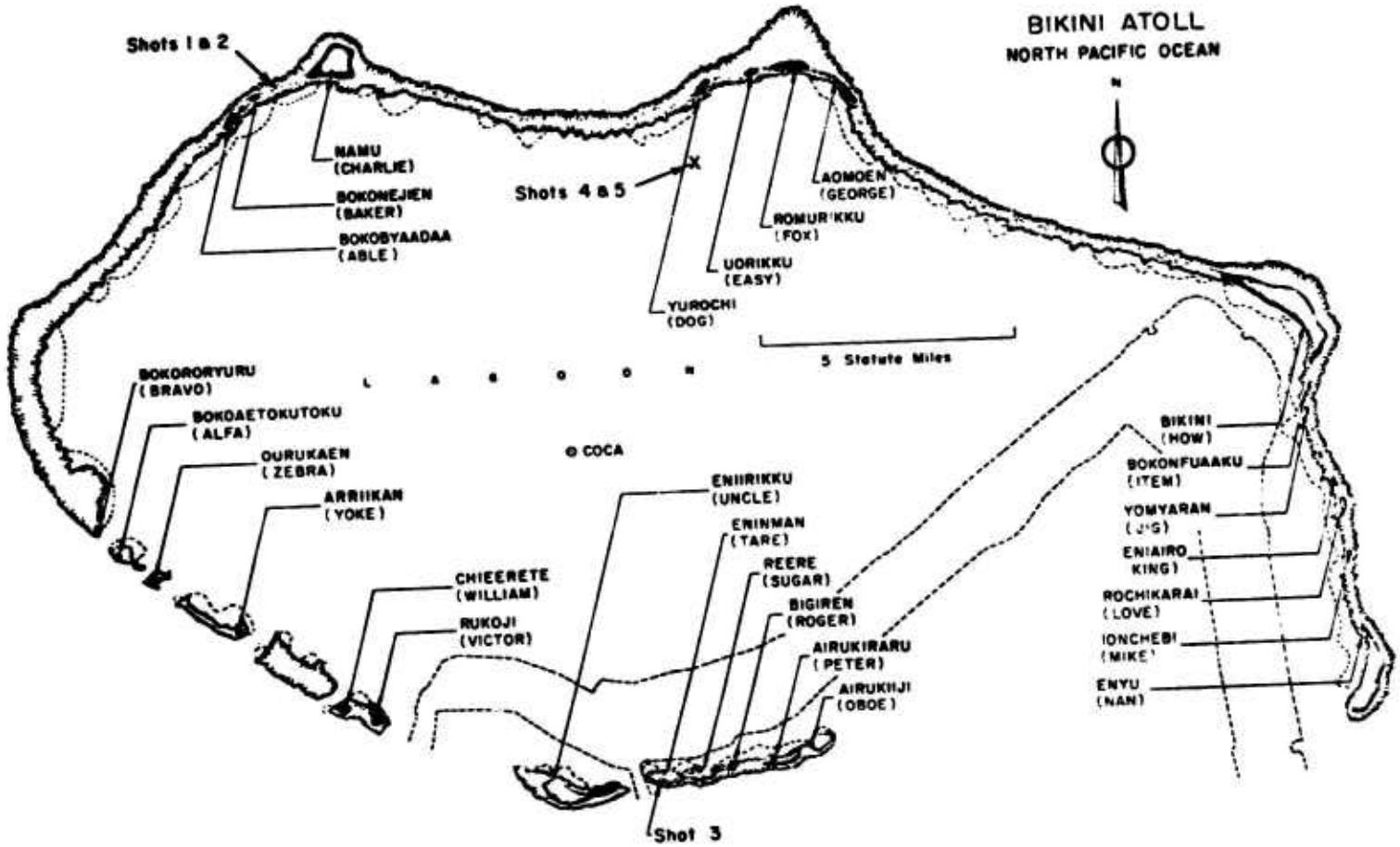
BIKINI ATOLL
NORTH PACIFIC OCEAN
N
Shots 1 & 2
NAMU (CHARLIE)
BOKONEJIEN (BAKER)
BOKOBYAADAA (ABLE)
Shots 4 & 5
AOMOEN (GEORGE)
ROMURIKKU (FOX)
UORIKKU (EASY)
YUROCHI (DOG)
5 Statute Miles
L A G O O N
BOKORORYURU (BRAVO)
BOKOAETOKUTOKU (ALFA)
OURUKAEN (ZEBRA)
ARRIIKAN (YOKE)
COCA
ENIIRIKKU (UNCLE)
ENINMAN (TARE)
REERE (SUGAR)
BIGIREN (ROGER)
AIRUKIRARU (PETER)
AIRUKIIJI (OBOE)
CHIEERETE (WILLIAM)
RUKOJI (VICTOR)
Shot 3
BIKINI (HOW)
BOKONFUAAKU (ITEM)
YOMYARAN (JIG)
ENIAIRO (KING)
ROCHIKARAI (LOVE)
IONCHEBI (MIKE)
ENYU (NAN)

GENERAL SHOT INFORMATION

	Shot 1	Shot 2	Shot 3	Shot 4	Shot 5	Shot 6
DATE	1 March	27 March	7 April	26 April	5 May	14 May
CODE NAME (Unclassified)	Bravo	Romeo	Koon	Union	Yankee	Nectar
TIME*	06:40	06:25	06:15	06:05	06:05	06:15
LOCATION	Bikini, West of Charlie (Namu) on Reef	Bikini, Shot 1 Crater	Bikini, Tare (Eninman)	Bikini, on Barge at Intersection of Arcs with Radii of 6900' from Dog (Yurochi) and 3 Statute Miles from Fox (Aomoen).		Eniwetok, IVY Mike Crater, Flora (Elugelab)
TYPE	Land	Barge	Land	Barge	Barge	Barge
HOLMES & NARVER COORDINATES	N 170,617.17 E 76,163.98	N 170,635.05 E 75,950.46	N 100,154.50 E 109,799.00	N 161,698.83 E 116,800.27	N 161,424.43 E 116,688.15	N 147,750.00 E 67,790.00

* APPROXIMATE

ABSTRACT

Oceanographic-survey and water-sampling techniques were employed to evaluate the amount and distribution of the fallout received over extended areas adjacent to nuclear detonations of high yields. The project was established as a result of the fallout phenomena observed following Shot 1. The operational and technical details had to be hastily contrived so that they could be put into effect within the latter phases of Operation Castle. Specifically, the experimental studies reported herein were conducted in connection with Shots 5 and 6.

Immediately following Shot 5, a fleet tug carrying improvised radiographic and oceanographic gear cruised the oceanic area downwind of Bikini Atoll, covering 800 miles in four days, taking samples of the water at the surface and to depths of 2,400 feet, and measuring gamma ray intensities above the sea surface and also just below the sea surface. Occasionally the gamma intensity was measured to 80 meters depth also. Two samples of open-sea plankton were netted and found to be strongly radioactive.

Following Shot 6, two tugs cruised downwind of Eniwetok Atoll taking surface water samples and measuring gamma intensity at each level; simultaneously, the area was surveyed by aircraft carrying sensitive gamma detectors.

Two survey results recommend the continued use and perfection of the novel techniques.

Analysis of data indicates that, for a surface water detonation of a high-yield weapon, an area of approximately 5,000 square miles can be covered by contamination at levels that would be hazardous to human life if the fallout had been deposited on a comparable land area; that is, over this area the total gamma ray dose accumulating during the first 50 hours would be about 250 r at a height of 3 feet above a plane fallout catchment.

PREFACE

This is a record of experimental data required following Shot 5 and Shot 6 of Operation Castle together with a careful re-evaluation of its significance.

A preliminary report was put together under great pressure just following Operation Castle (and circulated in limited numbers as ITR-935, May 1954). There had been no time for thorough consultation between the collaborating organizations; certain computations were still not completed; in fact, the final calibration of gamma instruments had not been completed because the instruments themselves disappeared for several weeks in the course of transportation.

The evaluation of the direct gamma measurements and oceanographic measurements was carried out at Scripps Institution of Oceanography; the analysis of water samples and their evaluation has been carri d out at U. S. Naval Radiological Defense Laboratory. Attempts have been made to integrate the effects at each institution.

The authors wish to accord special acknowledgment to Feenan D. Jennings of Scripps Institution of Oceanography for his outstanding contributions during the cruise and in the analyses, and to John D. Isaacs and Roger R. Revelle of the same institution for their useful guidance during the planning phases prior to Shot 5.

Appreciation is expressed to R. L. Stetson and W. B. Lane, of U. S. Naval Radiological Defense Laboratory, who assisted in planning; to D. McDonald, U. S. Naval Radiological Defense Laboratory, who participated in the Shot 5 survey; and to many individuals of the NRDL and SIO staff who assisted in this study. Mrs. Suzanne Volkmann of the SIO staff has contributed extensively during the past year to the analyses and editing of the SIO contributions.

The facilities and experience of the U. S. Bureau of Standards were made available to SIO for the calibration of the gamma devices. The authors are grateful to L. S. Taylor, Harold Wyckoff and S. W. Smith of that institution.

Finally, the success of this experiment owes much to the assistance of many individuals of Joint Task Force Seven for providing equipment and a generous amount of personal time and good will.

FOREWORD

This report is one of the reports presenting the results of the 34 projects participating in the Military Effects Tests Program of Operation Castle, which included six test detonations. For readers interested in other pertinent test information, reference is made to WT-934, "Summary Report of the Commander, Task Unit 13, Programs 1-9," Military Effects Program. This summary report includes the following information of possible general interest: (1) an overall description of each detonation, including yield, height of burst, ground zero location, time of detonation, ambient atmospheric conditions at detonation, etc., for the six shots; (2) discussion of all project results; (3) a summary of each project, including objectives and results; and (4) a complete listing of all reports covering the Military Effects Tests Program.

CONTENTS

ABSTRACT ---------- 7

PREFACE ---------- 8

FOREWORD ---------- 9

CHAPTER 1 INTRODUCTION ---------- 15

1.1 Objectives ---------- 15
1.2 Background ---------- 15

CHAPTER 2 DESIGN OF THE FIELD EXPERIMENT ---------- 17

2.1 Radiation Measurements ---------- 17
2.1.1 Instrumentation ---------- 17
2.1.2 Calibration of Instruments ---------- 18
2.1.3 Measurements Made ---------- 20
2.2 Water Sampling ---------- 21
2.2.1 Sampling Devices ---------- 21
2.2.2 Samples Collected ---------- 22
2.3 Supplementary Oceanographic Measurements ---------- 23
2.4 Plankton Sampling ---------- 25

CHAPTER 3 RESULTS OF SURFACE AND SUBSURFACE SURVEY BY RADIATION DETECTING INSTRUMENTS ---------- 26

3.1 Problems Involved in Computing a Synoptic Fallout Picture ---------- 26
3.2 Raw Measurements of Surface Gamma Intensity ---------- 26
3.3 Reduction of Readings to Roentgens Per Hour in Situ ---------- 27
3.3.1 Correction for Instrument Contamination ---------- 27
3.3.2 Running Plot of Relative Gamma Intensity In Situ ---------- 27
3.3.3 Computation of Absolute Magnitude of In Situ Intensity ---------- 32
3.4 Computation of Synoptic Picture ---------- 32
3.4.1 Vertical Extent of Activity ---------- 32
3.4.2 Conclusions Regarding Penetration Progress ---------- 35
3.4.3 Computations of Total Local Fallout ---------- 35
3.4.4 Estimate of Radioactive Decay ---------- 35
3.4.5 Local Dose at 3 Feet Elevation at the Synoptic Time H + 12 Hours ---------- 46
3.4.6 Local Dose at 3 Feet Elevation at the Synoptic Time H + 1 Hour ---------- 46
3.4.7 Effect of Time of Arrival and of Ocean Currents on Synoptic Presentation ---------- 46
3.4.8 Plotting Fallout Contours of Iso-Dose-Rate ---------- 46
3.4.9 Plotting Fallout Contours of Total Dose ---------- 52

CHAPTER 4 ANALYSIS OF CONTAMINATED SEA WATER ---------- 53

4.1 Sample Analysis ---------- 55
4.2 Calculation of A–Gamma Activity Received Per Unit Area of the Ocean Surface ---------- 58
4.3 Calculation of I/A–Ratio of Gamma Ionization Readings to Gamma Counts ---------- 63
4.4 Calculation of R/I–Ratio of Gamma Energy Emission Rate Per Unit Area to Gamma Ionization Reading Per Unit Area ---------- 63
4.5 Calculation of Reference Dose Rate, d_r ---------- 67
4.6 Calculation of Dose Rate, d ---------- 68
4.7 Calculation of Dose Rate d From Observed Gamma Field–Sample Activity Ratio ---------- 70
4.8 Fraction of Shot 5 and Shot 6 Devices in Fallout ---------- 71

REFERENCES ---------- 76

CHAPTER 5 SUMMARY, DISCUSSION AND CONCLUSIONS ---------- 77

5.1 Summary ---------- 77
5.2 Discussion and Conclusions ---------- 77

APPENDIX A COMPARISON OF COMPUTED DOSE RATE OVER THE SEA WITH CERTAIN ACTUAL MEASUREMENTS ---------- 79

APPENDIX B PROCEDURE USED IN CHAPTER 3 FOR ESTABLISHING THE CALIBRATION OF THE TOWED INSTRUMENTS FOR MEASURING GAMMA RAYS UNDERWATER ---------- 81

B.1 Calibration of Instruments in Air ---------- 81
B.2 Estimation of the Response to Underwater Radiation ---------- 83
B.2.1 Estimates of the Source Spectra ---------- 83
B.2.2 Calculations of the Underwater Dose Spectra Corresponding to the Assumed Fallout Source Spectra ---------- 83
B.2.3 Instrument Response Variation Due to Photon Energy Variation Alone ---------- 83
B.2.4 Instrument Response Variation Due to Angle of Incidence Alone ---------- 83
B.2.5 Estimates of 4 Pi Monochromatic Sensitivity ---------- 83
B.2.6 Response of Mark II to Distributed Sources Comprised of Mixed Fallout Materials ---------- 87
B.2.7 Derivation of Complete Response Curves for the Instrument Mark II When It is Used Submerged in Fallout Contaminants ---------- 87

APPENDIX C COMPUTATION OF DOSE AT THREE FEET ELEVATION ---------- 88

C.1 Computation of Dose at Three Feet Elevation From Measurements of Dose in Water ---------- 88
C.2 Numerical Computations ---------- 91
C.3 Conclusion Regarding Hypothetical Dosage at 3 Feet Elevation ---------- 91

FIGURES

2.1 Internal configuration of towed gamma detector, Mark II ---------- 19
2.2 Mark I calibration from distant point source of radium, Site Elmer Rad-Safe compound, 10 May 1954 ---------- 20
2.3 Mark II calibrations ---------- 21
2.4 Mark III calibration from distant point source of radium, Site Elmer Rad-Safe compound, 10 May 1954 ---------- 22
2.5 Response of Mark I prior to 1900 hours on 8 May 1954 ---------- 23
2.6 Ship's track, Shot 5 survey ---------- 24
3.1 Mark I, II, III, towed detector data, Shot 5 ---------- 28
3.2 "Pot" record in mr/hr showing correction for accumulated drift ---------- 30
3.3 Relative radiation intensity along ship's track, Shot 5 survey ---------- 31
3.4 Mark II vertical radioactivity profiles, Shot 5 ---------- 36
3.5 Progress of vertical mixing ---------- 36
3.6 Decay of coefficient curve ---------- 37
3.7 Accumulated dose factor ---------- 37
3.8 Estimated time of arrival of fallout from an analysis of the winds for Shot 5 ---------- 47
3.9 Ocean current vectors from Japanese hydrographic investigations, 1933-1941 ---------- 47
3.10 Ocean current buoy drift data, October-November 1952 and February-April 1954 ---------- 48
3.11 Iso-intensity contours for Shot 5 ---------- 49
3.12 Total dose from time of fallout to H + 50 hours in roentgens, Shot 5 ---------- 50
4.1 Calculated decay (d/m) for Shot 6 fallout ---------- 58
4.2 Depth of penetration of Shot 5 fallout in ocean water ---------- 61
4.3 Estimated times of arrival of fallout ---------- 62
4.4 Relative response of NRDL ion chamber with incident photon energy (Mev) (after Shelbert) ---------- 67
4.5 Calculated decay (d/m) for Shot 5 fallout ---------- 69
4.6 Estimated fallout dose rate contours for Shot 6 at H + 12 hours (r/hr) ---------- 74
A.1 Location of instruments during Shot 5 ---------- 79
B.1 Histograms of estimated source spectra ---------- 82
B.2 Histograms of degraded dose spectra ---------- 84
B.3 Experimental response of Mark II for rays at 90 degrees incidence ---------- 85
B.4 Variation in response of Mark II with angle of incidence of radiation ---------- 85
B.5 Plot of data from Table B.4 ---------- 85
C.1 Schematic of reduction of readings to dose rate (mr/hr) at 3 feet elevation ---------- 91

TABLES

3.1 Second Vertical G. M. C. Profile in Yankee Fallout ---------- 33
3.2 Third Vertical G. M. C. Profile in Yankee Fallout ---------- 33

3.3 Fourth Vertical G. M. C. Profile in Yankee Fallout ---------- 34
3.4 Estimation of Time of Arrival of Fallout From An Analysis of the Winds for Shot 5 ---------- 34
3.5 Computation of Dose Rate and Accumulated Dose 3 Feet Above a Hypothetical Plane Catching the Fallout From Shot 5 ---------- 38
3.6 Iso-dose Rate Contours at 3 Foot Elevation ---------- 51
3.7 Total Dose From Fallout Arrival Until H + 50 Hours ---------- 51
4.1 Radioactivity in Water Samples From Shot 5 ---------- 56
4.2 Radioactivity in Surface-Water Samples From Shot 6 ---------- 59
4.3 Ratio of Gamma Ionization Readings, I To Gamma Counts, A For Five Surface Water Samples From Shot 5 ---------- 63
4.4 Calculation of R/I Ratio of Gamma Energy Emission Rate Per Unit Area to Gamma Ionization Reading Per Unit Area ---------- 64
4.5 Calculation of Reference Dose Rate, d_r at Height X = 3 Feet Above An Infinitely Contaminated Plane Having a Gamma Energy Emission Rate, R = 1 Mev min^{-1} cm^{-2} ---------- 65
4.6 Dose Rate at H + 12 Hr Calculated From Water Samples From Shot 5 ---------- 65
4.7 Dose Rate at H + 12 Hr Calculated From Water Samples Collected After Shot 6 ---------- 66
4.8 Total Beta Activity in Shot 5 Fallout at 9 Days ---------- 72
4.9 Total Beta Activity in Shot 6 Fallout at 7 Days ---------- 72
4.10 Radionuclides Considered in Estimate of β/γ Ratio ---------- 73
4.11 Beta Disintegrations and Gamma Photons Per Minute Per Fission and Estimated β/γ Ratio ---------- 75
4.12 Ratio of Capture to Fission for Induced Radionuclides ---------- 76
4.13 Total Beta Activity From Devices and the Fraction of Total Beta Activity in the Fallout Shot 5 and Shot 6 at H + 218 and H + 171 Hr Respectively ---------- 76
5.1 Comparison of Shot 5 Gamma Field Intensities at 12 Hours ---------- 78
A.1 Above Surface and Below Surface Survey Data and Their Ratios ---------- 80
B.1 Estimated Source Spectra ---------- 82
B.2 Effective Response Sensitivity of Mark II to Estimated Fallout Radiation ---------- 84
B.3 Response to Uniform 4 Pi Distribution of Sources Over a Spherical Shell Relative to the Same Sources Concentrated at a Point at the Same Radius and on the Normal to the Instrument's Axis ---------- 86
B.4 Computed Responses of Mark II to Uniformly Distributed Sources of Several Different Effective Energies ---------- 86
C.1 Computation of Dose at Three Feet Elevation Above Fallout Plane By Method of AFSWP Report 502A ---------- 90

Chapter 1
INTRODUCTION

Attempts were made during Operation Castle to study the fallout patterns from nuclear devices detonated at the surface over land and water. Most of the fallout from the nuclear devices was distributed over extended ocean areas outside the atolls on which the weapons were detonated. It was desired to determine what the radiation levels would have been had the radioactive material from the test devices fallen on extended land areas.

Study of Shot 1 made clear that observation of fallout on subsequent shots over larger areas was necessary. On Shot 5 alternative methods were attempted. The Division of Biology and Medicine (DBM) of the Atomic Energy Commission used airborne gamma detectors to measure activity on rafts. Oceanographic surveys were mounted by the Scripps Institution of Oceanography (SIO) and Naval Radiological Defense Laboratory (NRDL) involving submerged counters and water sampling. Studies of these data showed need for modified techniques to give a faster synoptic survey for the remaining shot, Shot 6. This was done by limiting the observations to above-surface monitoring and surface-water sampling in conjunction with a synoptic aerial survey.

1.1 OBJECTIVES

The ultimate objective of the work described herein was to provide data for the determination of the amount and distribution of fallout received by ocean areas surrounding the site of a surface nuclear detonation. This information is of particular interest when related to the gamma field intensities which would exist if the fallout were received by land areas.

The initial objective of the work described under Project 2.7 was to evaluate the feasibility of using oceanographic surveys and sampling techniques as a means of providing radiological information. The specific objectives were to: (1) determine the distribution in ocean water of the major fallout downwind; (2) measure depth and rate of mixing of fallout; and (3) collect otherwise-unattainable specimens, technical data, and field experience essential for the success of future operational planning and instrumentation.

1.2 BACKGROUND

This study was initiated by the Headquarters, Armed Forces Special Weapons Project's (AFSWP) suggestion that water sampling and survey techniques could be used to estimate the fallout contours. The techniques adopted, following consultation between representatives of AFSWP, NRDL, and SIO, consisted of water sampling and surveys using submergible radiation instruments at several depths.

The method was based upon the existence well known by oceanographic measurements of a uniformly mixed surface-water layer. Such a layer presumably is created by the

action of wind and waves. There is evidence that mixing may be complete within a few hours to a depth, in this area, of 300 feet or more. The lower boundary of this mixed layer frequently appears as an abrupt drop in temperature. Mixing is thorough in the upper layers as evidenced by the remarkable uniformity of temperature between this boundary, called the thermocline, and the surface.

It was expected therefore that the radioactive fallout would also become evenly distributed throughout the mixing layer to an extent which might permit estimation of the amount of fallout by measurement of the radioactivity of oceanwater in the mixed layer.

The portion of the above investigations organized and performed under the direction of Task Unit 13, Program 2, was established as a separate joint SIO and NRDL project, Project 2.7. SIO has evaluated the direct gamma measurements. NRDL has analyzed the water samples. In this report an attempt has been made to construct approximate fallout contours and calculate gamma field intensities on the basis of the data obtained by these two methods.

Chapter 2
DESIGN OF THE FIELD EXPERIMENT

For the survey following Shot 5, the ATF-75 (Sioux) was hurriedly fitted with hydrographic gear and with improvised radiation detectors capable of being towed and lowered vertically to a depth of 250 feet into the sea. Between H + 6 hours and D + 4 days an 800-mile traverse of the suspected downwind area was made with sections taken near radii 30, 50, 100, 150, and 200 miles. Hydrographic casts were made at stations evidencing distinctly active water; water samples were taken to depths as great as 2,400 feet. Surface-water samples were collected frequently along the traverse while the ship was underway.

The survey following Shot 6 included taking surface-water samples from the sea in the downwind area and readings on T1B survey instruments. During this survey, 120 water samples were taken by the crews of two Task Force ships and completed at 0530, 16 May, and consequently it presents a good synoptic picture. Coverage was out to approximately 135 miles north of zero. A simultaneous aerial survey with gamma-detecting instruments was conducted by the New York Operations Office, AEC.

2.1 RADIATION MEASUREMENTS

The underwater radiation measurements for Shot 5 were made by sealed Geiger instruments which were either towed or lowered to various depths at definite points in the area. In order to assure that a record was made of regions of intensity beyond the recording capacity of the submerged GM instruments, a rough monitoring device, termed the "pot" was suspended over the side of the ship to record these high intensities. The pot was a standard ionization-chamber-type radiac set fitted in a steel tank having a gasketed lid. This steel tank was mounted on the grid floor of the hydrographer's platform 6 feet above the sea. Wire leads from the radiac set in the tank carried its output to a microammeter located on a part of the deck sheltered from the spray. The pot was set permanently on a scale of 0 to 50 mr/hr and was read every 5 to 20 minutes without resetting its drift. This surface monitoring was continued throughout the radiation survey in a relative sense rather than indicative of absolute intensity of radiation; however, the readings are valuable.

2.1.1 Instrumentation. The radiation measurements were made with three improvised underwater Geiger tube instruments. These were designated the Mark I, II, and III; they were hurriedly assembled from the parts and materials available at the forward area; none but essential details were put into the construction.

The Mark I was made by rewiring a standard Victoreen radiac Geiger counter so that it and all its appurtenances except the microammeter would fit into a cylinder. This cylinder was about 30 inches long and was made of seamless steel tubing having an outside diameter of 4 inches and a wall thickness of $\frac{1}{8}$ inch. One end of the tube was closed by brazing a disc to it, and the other end was fitted with a flange to which was fastened a gasketed cover. A piece of heavy-duty rubber-covered portable-tool "cord" about 200 feet long connected the counter with its microammeter which was located in a sheltered spot on the deck. This cord also served as the towing cable for the Mark I. A pressure-

tight gland at the point where the cord entered the cylinder prevented water from reaching the radiac instrument. The range of the radiac instrument could be set and its batteries turned on and off by manipulating a water-tight shaft that ran through another packing gland on the cylinder.

The Mark II was designed for vertical casts; it was provided with a rope line to strengthen the meter cord. The instrument was unlike the Mark I in that its cylinder was made of standard 3-inch brass pipe; the Geiger tube had thick stainless steel walls and the Mark II circuit was provided with seven range settings. Since the Mark II maintained its calibration surprisingly well and since its polished brass shell made it easy to clean, it was frequently used as a temporary standard for checking the calibration of the other instruments. A line drawing of Mark II is included in Figure 2.1.

The Mark III was encased in a copper cylinder that had a diameter of about 4 inches and a wall thickness of $^1/_{16}$ inch. Its counter was a glass Geiger tube inside a brass protective shell.

All three of these instruments were read on microammeters located on the deck and connected to the counters by long leads. The meters were located in reasonably sheltered positions on the deck and were encased in transparent plastic bags. No equipment was available for making continuous or automatic recordings of the readings. The meters were simply read at short intervals during the survey.

Figure 2.1 is a line drawing giving sectional view of Mark II and showing internal configuration and location of important parts. The Geiger tube itself had a heavy cylindrical metal wall and the thin beta window on the end was kept capped; it was located on the axis of the pressure cylinder.

This Mark II instrument was constructed from components taken mostly from a radiac device of type AN/PDR-27C. The tube was Navy type 3S-1, a type having heavy metal walls. Its responses to calibration will be discussed in detail later.

2.1.2 Calibration of Instruments. Efforts were made during the cruise and immediately after it to collect all possible data needed for establishing the calibrations of the gamma instruments.

Instruments were frequently intercalibrated at sea.

The towed instruments were compared against the ship's official radiac handsets at a few isolated intensity levels.

The instruments were taken ashore at Site Elmer immediately following the cruise and calibrated throughout their full range of response against a point source of radium of known strength.

Figures 2.2, 2.3, and 2.4 are the results of the calibration of the towed instruments at Site Elmer against radium.

Figure 2.5 is the estimated response of Mark I instrument prior to the date when its Geiger tube went bad and had to be changed. This curve was derived from the more reliable calibration of Mark II and from records of intercalibrations at sea before and after the tube was changed in Mark I.

The preliminary calibrations relate only to the use of the instruments under certain limited circumstances, the use of the instruments in air, and the measurement of fairly hard radiations. The derivation of a comprehensive calibration pertaining to the use under the actual field conditions required considerable additional experimental work and computation. The procedure used for establishment of this final realistic calibration is the subject of Appendix B.

The net outcome of the later study is the conclusion that the approximate gamma intensity under water and due to mixed fallout activity can be derived by applying to the

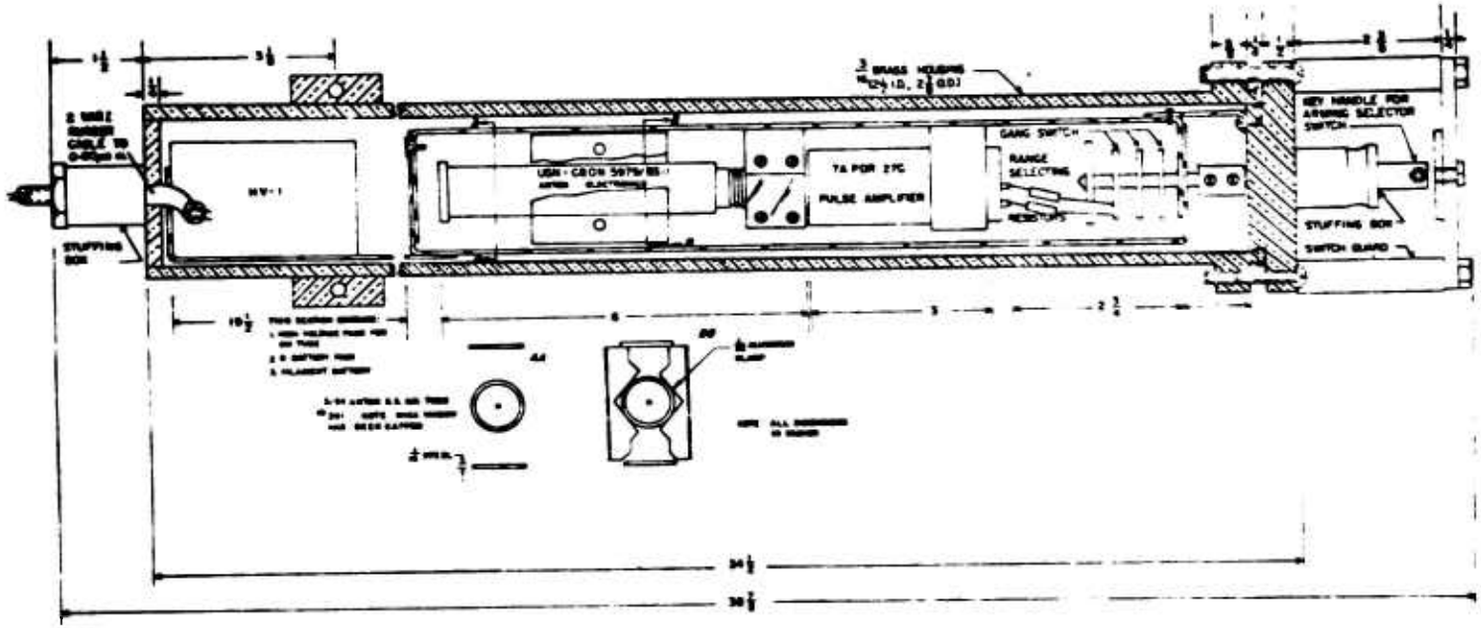

Figure 2.1 Internal configuration of towed gamma detector, Mark II.

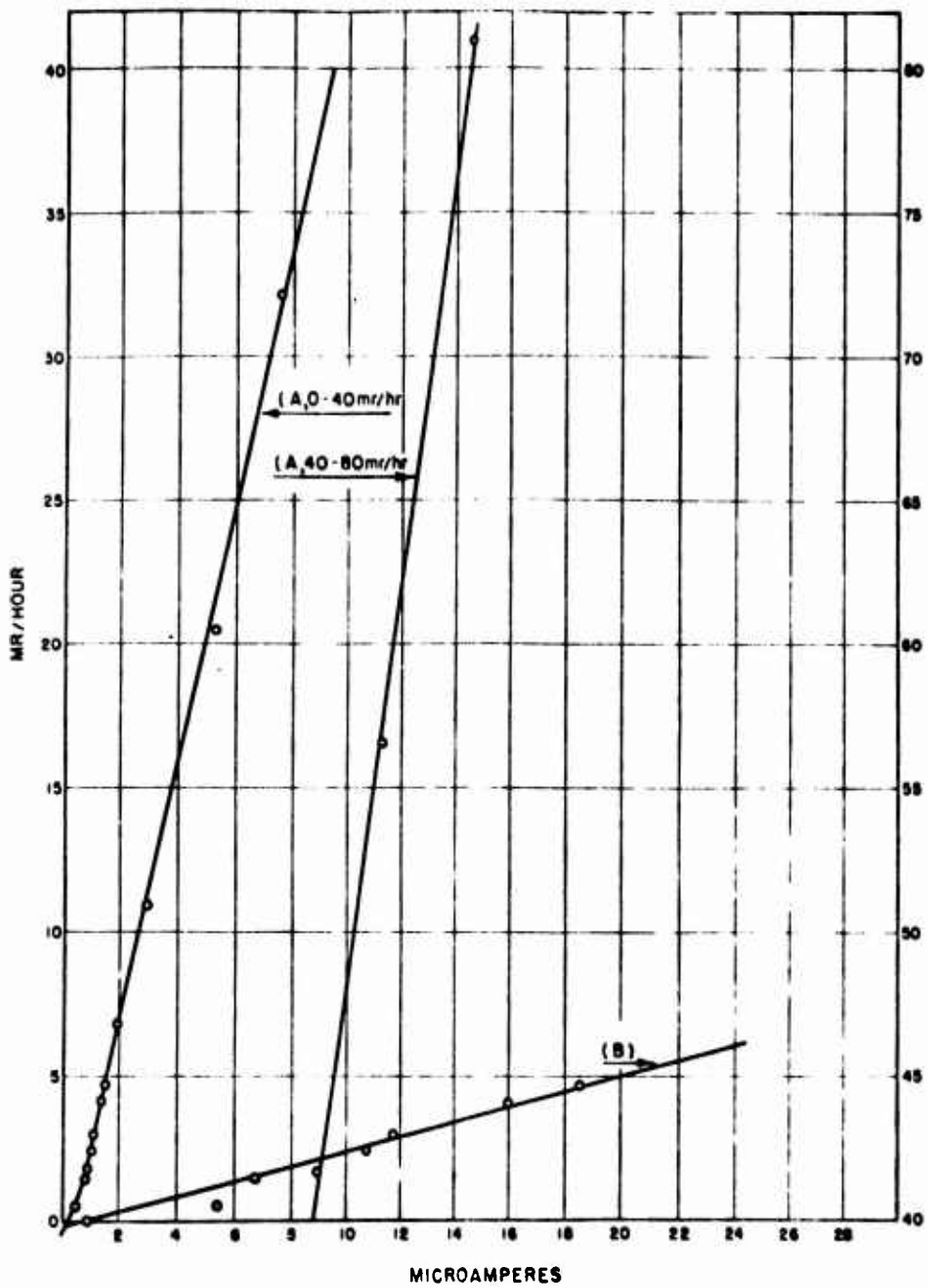

Figure 2.2 Mark I calibration from distant point source of radium, Site Elmer Rad-Safe compound, 10 May 1954. Microammeter: Weston 301, 0-20μa.

experimental field reading of Mark II the calibration curves given in Figure 2.3, but only after these latter values have been multiplied by a factor of 1.5; that is, after ordinates of the solid curves of Figure 2.3 have been displaced upward by multiplying them by the factor of 1.5.

The Mark II instrument calibrated in this manner has been used as a standard for absolute intensity of radiation underwater throughout the cruise; all other instruments used during the trip have been in effect calibrated against the Mark II response.

2.1.3 Measurements Made. About 1,000 radiation measurements were made in the survey following Shot 5. The majority of these measurements were from the Mark I, II,

and III instruments. Pot readings were taken concurrently and were used to fill the gaps in the Mark I, II, and III measurements.

At three stations, 1, 2, and 6 (Figure 2.6), vertical casts were made electronically by lowering the Mark II instrument to a depth of 250 feet and recording its readings as a function of depth. In two instances, this instrument passed through the contaminated layers and into the uncontaminated water beneath, thereby giving the extent of the mixing directly. A trial showed the need for a 150-pound weight attached to the Mark II to keep

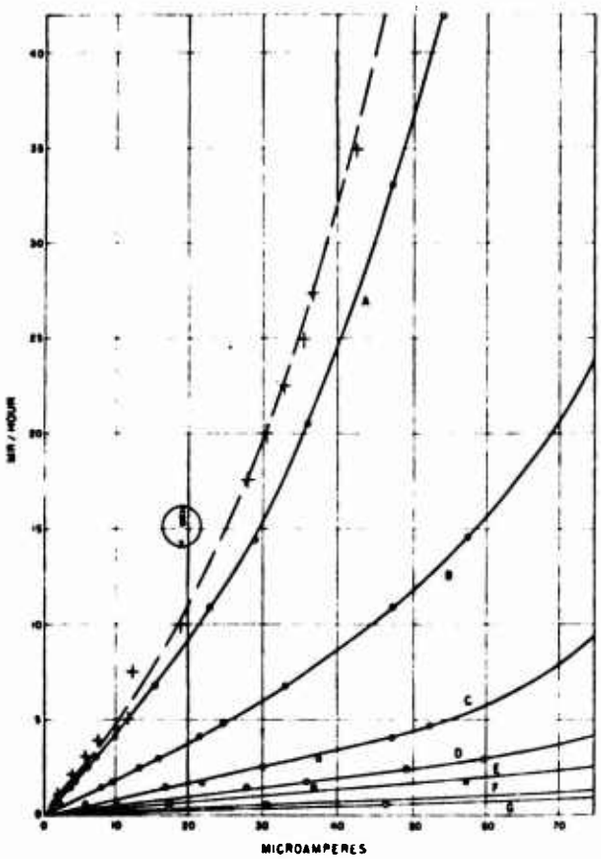

NOTES

SOLID LINES - Mark II calibration against distant point source of Radium at Site Elmer, 10 MAY 1954. The ray incidence was normal to the instrument's axis. (Block letters indicate the instrument's amplification ranges.)

DASHED LINE - Mark II calibration against point source of Radium at U S N B S several weeks later. The ray incidence here again was normal to the instrument's axis. Descrepancy between A and the dashed curve may be due to the battery voltage change or to the error in source evaluation, note, however, that it is small.

Points within Large Circle - Computed overall sensitivity of Mark II when used submerged in water which is contaminated with the fallout products whose spectrum is that assumed for the computation. This sensitivity was computed for use only of the instrument's scale-point of 19 microamps.

For the purposes of this final report, in situ intensities were therefore derived by multiplying the intensities given by the solid curves by the factor 1.5 (See Appendix B.)

Figure 2.3 Mark II Calibrations.

the hydro wire more nearly vertical. Depths were read on the meter wheel of the hydro wire. Unfortunately, the electrical wire was not long enough to follow the descent of activity to its ultimate depth.

2.2 WATER SAMPLING

Water samples were taken from both the surface and vertical casts in the survey after Shot 5. Only surface samples were taken after Shot 6. All samples were air-shipped to NRDL for analysis as quickly as possible after they were taken. For Shot 6, duplicate samples were taken everywhere; analyses were carried out both at NRDL and at NYOO, AEC.

2.2.1 Sampling Devices. Surface-water samples were taken from a bucket passed over the side while the ship was underway; either a plastic or glyptol lining was used in the bucket.

Two kinds of sampling devices were used to take the water samples in the hydrographic casts. Standard new Nansen bottles were used at a minimum of four depths simultaneously.

Since the metal Nansen bottles were suspected of absorbing radioactive materials in sea water, samples were also taken with polyethylene bottles. Inert polyethylene plastic 1-gallon bottles were filled with fresh water, 1 liter of which was squeezed out of each by compressing the sides of the bottle and then the bottle sealed with a stopper containing a breakable glass seal. After being clamped to the hydrographic wire, the plastic bottles

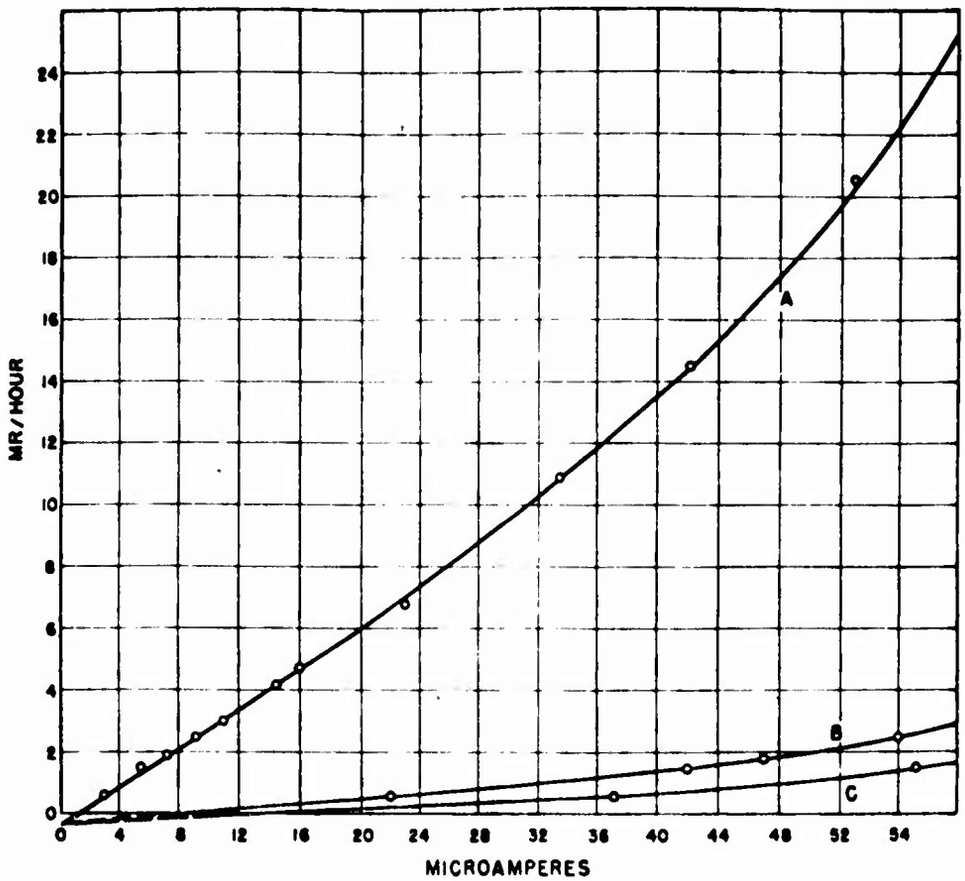

Figure 2.4 Mark III calibration from distant point source of radium, Site Elmer Rad-Safe compound, 10 May 1954. Microammeter: Western Electric Mod D-167867, 0-50μa.

were lowered to the sampling depth and then the seals were broken by dropping a messenger. After allowing time deemed sufficient for filling, the bottle was raised to the surface.

This ingenious trace-element sampling device was proposed for this cruise by John D. Isaacs who planned the field cruise and located most of the essential hydrographic gear from accessible facilities.

2.2.2 Samples Collected. Water samples were taken at 24 points along the ship's track after Shot 5. Surface samples were taken at 15 points while the ship was underway. Vertical hydrographic casts were made at the eight numbered stations as indicated in Figure 2.6. These samples were taken at the following wire depths.

1 cast: 50, 100, 150, 200, 500, and 800 m
4 casts: 25, 50, 100, 200, and 500 m
4 casts: 25, 50, 100

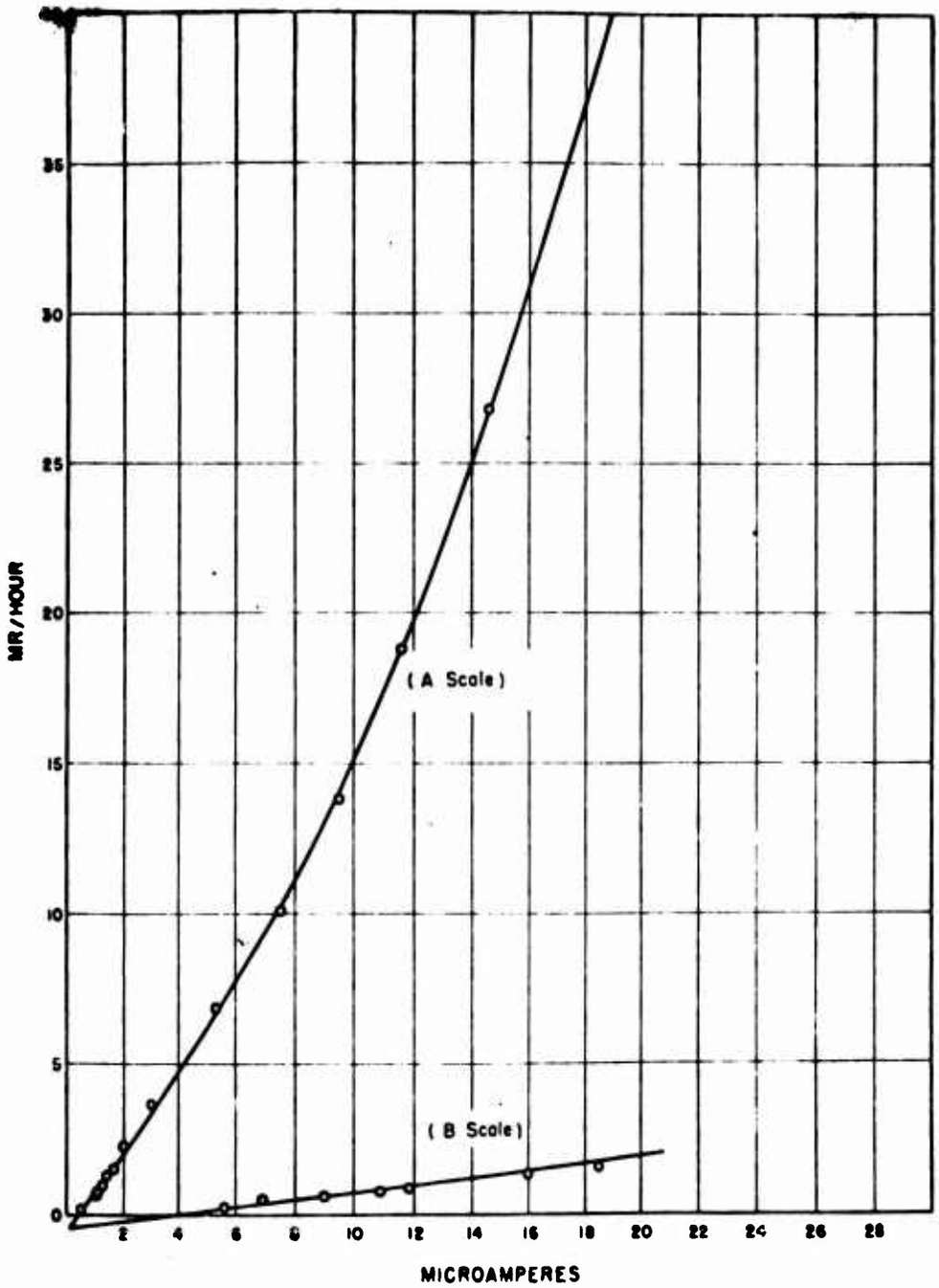

Figure 2.5 Response of Mark I prior to 1900 hours on 8 May 1954.

These wire depths required substantial corrections because of the effect of currents causing large wire angles.

Nansen water samples were divided and stored in glass pint citrate bottles. Following Shot 6, 120 surface-water samples were taken.

2.3 SUPPLEMENTARY OCEANOGRAPHIC MEASUREMENTS

Bathythermograms of the vertical temperature profile were made at 12 positions along the ship's track to a depth of about 450 feet. In making these, the ship was stopped and

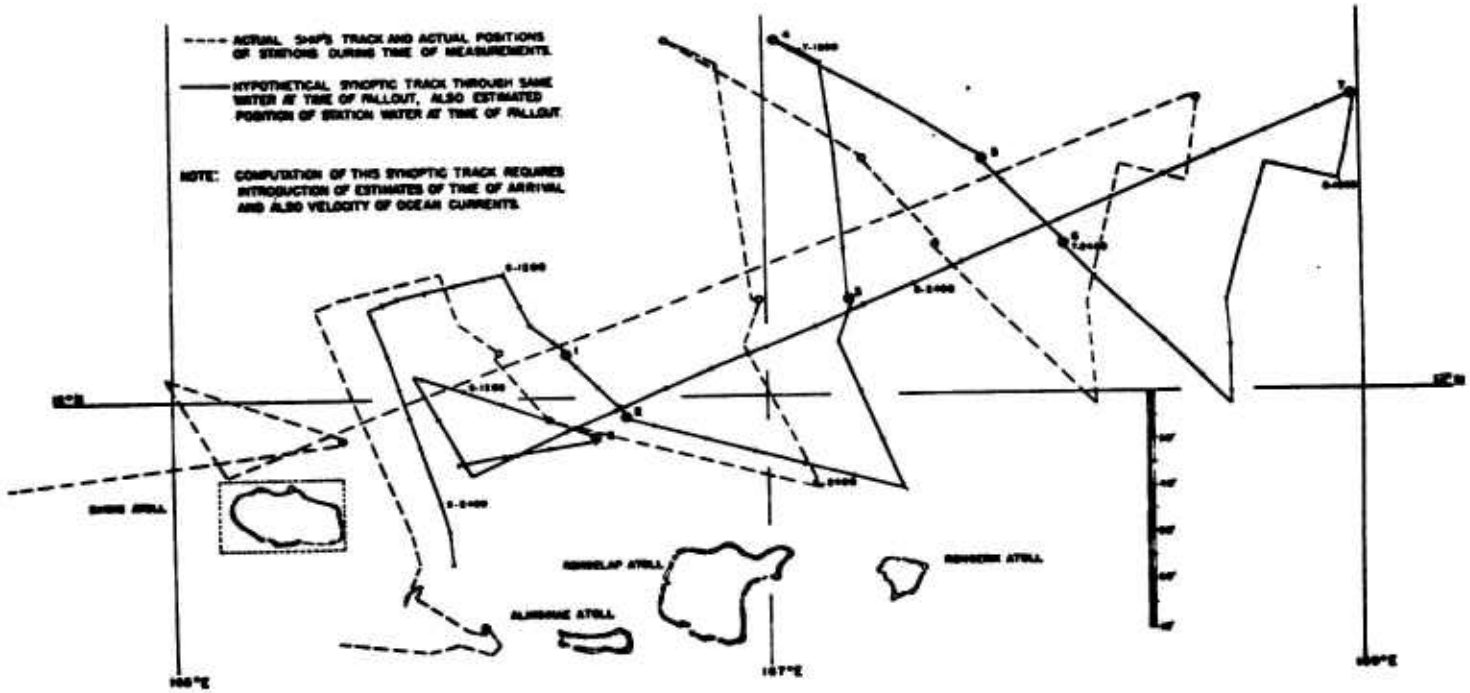

Figure 2.6 Ship's track, Shot 5 survey.

a 150-pound weight was attached to the bathythermograph (BT) to insure vertical descent so as to obtain reliable estimates of the depth of the thermocline. Four destroyers took additional bathythermograph readings. The resulting bathythermograms were used for additional knowledge of thermocline depth in the area.

Usually, oceanographers attach to each water sampling tank (Nansen bottle) a pair of precision thermometers of peculiar design, that permits them to measure and to retain a record of that temperature which existed at the moment they were turned upside down. This upsetting or "reversing" is accomplished in situ by sliding weights or "messengers" down the cable so as to strike releasing triggers. One of these pair is "protected" from the hydrostatic water pressure by a thick glass shell; it therefore records only the sea temperature. The other thermometer is "unprotected," that is, its bulb is exposed to the squeeze of the sea pressure and therefore the deviation of its reading from that of the protected thermometer records the in situ pressure and hence the depth. Temperatures can be read to $^1/_{100}$ degree centigrade, and depths to one meter or to about $^1/_{10}$ percent at 1,000 meters depth by this traditional oceanographic procedure.

Precise and well calibrated reversing thermometers took temperatures at each Nansen sampling point. Because there were no unprotected reversing thermometers available, no thermometric depth measurements could be made; so the depth of each water sample had to be computed by intercomparison with the bathythermograph measurements.

Few very-deep casts were made because of this lack of unprotected reversing thermometers such as are normally relied upon for measuring depths in hydrographic operations.

2.4 PLANKTON SAMPLING

Samples of zooplankton were recovered at two stations when a standard one-meter-diameter silk plankton net was lowered through the upper mixed water. One haul was made at night and the other in daylight. These samples were forwarded to SIO for activity analysis and examination of organisms. Some evidence of selective concentration was presented. These findings are presented in a separate paper.

It was evident—even from simple gamma measurements made on deck—that zooplankton concentrate gamma activity of several orders of magnitude. Plankton taken from a water mass, whose activity is difficult to detect with crude instruments, appear very radioactive when the detector is brought near the sample bottle holding them.

Chapter 3

RESULTS OF SURFACE AND SUBSURFACE SURVEY BY RADIATION DETECTING INSTRUMENTS

The in situ radiation intensity measurements described in Chapter 2 and the laboratory measurements of the radioactivity of water samples collected during the cruise afford two independent means for assessing the fallout. Water analyses were undertaken by NRDL; while the direct gamma measurements were evaluated at SIO with the aid of calibration data supplied by the U. S. Bureau of Standards for this purpose.

The water analyses are to be discussed in Chapter 4, and in Chapter 5 results of both methods will be compared. This present chapter describes how the direct gamma measurements were resolved into a synoptic picture.

3.1 PROBLEMS INVOLVED IN COMPUTING A SYNOPTIC FALLOUT PICTURE

A great many individual readings can be accumulated when a ship tows a gamma detector through water contaminated by fallout material. But to reduce these readings to any form of synoptic picture requires the introduction of information or assumption concerning the behavior of the fallout material after it arrived at the water surface. A slow ship sees the activity only after several agents have been acting for many hours; the debris has been moving downward and moving laterally, and it has undergone radioactive decay. Before a picture of what might have existed at any given time can be reconstructed, the time of arrival of fallout must be established, and also the rates of dispersal and of decay.

Fortunately, there is available from other sources enough information to make rough estimates of the progress of the activity in the sea; some of it comes from auxiliary measurements made during the cruise, some comes from other oceanographic and radiological sources.

In this chapter, the raw field data will first be presented; then these will be converted to consistent units (mr/hr) by application of correction and calibration data. The local data will then be used to compute a local dose rate which might have existed at 3 feet elevation if the fallout had been caught on a hypothetical fixed plane at the elevation of mean sea level. All the local dose rates will be reduced to the rate at synoptic time H + 1, and also at H + 12, and finally these synoptic dosages will be displayed in contour maps.

3.2 RAW MEASUREMENTS OF SURFACE GAMMA INTENSITY

Figure 3.1 presents the running record of raw measurements made by towing the instruments Mark I, Mark II, and Mark III behind the ship. Readings of the microammeters were made as frequently as every 5 minutes during a large part of the cruise. Two or more instruments were towed simultaneously, whenever possible, so as to give warning of instrument failure and to provide data of correcting for instrument contamination.

Stations are identified on this graph by numbers and by asterisks. It should be noticed that roughly 2 hours cruise time were expended at stations where the deep hydrographic

casts were made. A slow ship, therefore, cannot afford to undertake too many stations and must rely heavily on other means for covering large areas of the sea in a reasonable time.

A gap in the measurements made by the towed instruments appears on the chart at about midnight of the first day; activity at that time became so concentrated that all of the towed instruments deflected off scale Fortunately, during this period, the pot instrument continued to indicate gamma intensity; nevertheless, its readings had to be corrected to eliminate a continuous drift error.

Figure 3.2 gives the behavior of this ionization chamber type of gamma instrument (AN/PDR-T1B) which was supported about 6 feet outboard and about 6 feet over the sea, and was protected from spray by a pot-shaped, steel tank having ¼-inch thick walls. This instrument had been sealed inside its protective pot at about 1200 hours, 5 May; unfortunately, no provision had been made for the zero knob to be adjusted repeatedly to compensate for drift, and the drift had to be allowed to accumulate for many hours.

The actual readings are indicated by circles on Figure 3.2, and a straight line extending back to the time the instrument was last zeroed before its being sealed up is drawn to indicate what is believed to be the drift of the instrument's zero.

The net gamma dose-rate reading of the T1B instrument inside the pot after being corrected for drift is given by the solid curve below. Beyond the time 1800 on 6 May, the drift unbalance is so large that no confidence at all can be placed in the readings.

Measurements summarized by Figure 3.2 serve mainly to interpolate the measurement of surface activity through that period when the most intense peak value of the latter occurred.

3.3 REDUCTION OF READINGS TO ROENTGENS PER HOUR IN SITU

3.3.1 Correction for Instrument Contamination. The metal instruments collected measurable amounts of activity on their external surfaces while being towed through contaminated water. This was demonstrated by removing instruments, one at a time, from the sea and cleaning their surfaces with sand paper and with chemicals; the signals almost always dropped after these cleanings, giving evidence that part of the signal came from surface contamination. Figure 3.1 indicates where and when the instruments were cleaned and how much the signal decreased consequently.

It can be safely assumed that the residual signal, immediately after a thorough cleaning, was due solely to the activity in the sea. However, the law governing the rate at which an active contamination of this sort accumulates is not at present known, so that the contribution to the signal due to contamination can only be estimated except at the few points where an actual washing was carried out. It is likely that the rate of accumulation is a function of time and is also a function of concentration of active material. It is unlikely that the accumulation process is completely reversible, and it is unlikely that the surface contamination will wash away in clean water at a rate related in any simple way to that at which it has accumulated. No data was recognized as giving any lead to the nature of contamination buildup, so that a simple accumulation proportionality with the time of exposure was assumed. In Figure 3.1, the dashed curves are the results of subtracting from the raw measurements a contamination-produced signal which increased directly with time and which was independent of activity concentration in the sea.

Alternative assumptions concerning the rate of surface contamination were later considered and extensive computations made and the results then compared with the simple running correction shown in Figure 3.1. It was found numerical results were not greatly different when the correction was assumed to depend upon concentration also.

3.3.2 Running Plot of Relative Gamma Intensity In Situ. Figure 3.3 is a plot of the relative gamma intensity in the surface water derived from the readings of the towed in-

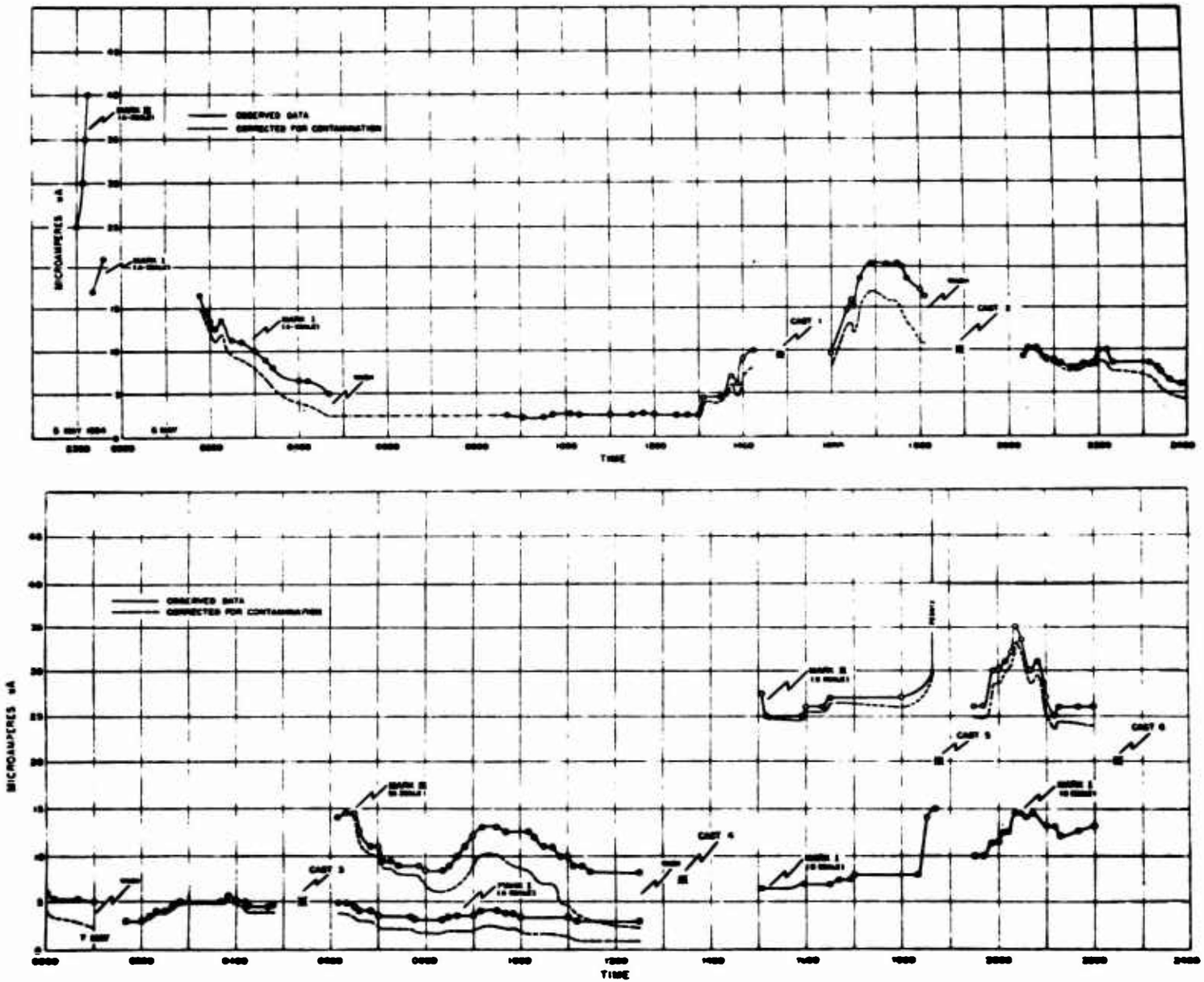

Figure 3.1 Mark I, II, III, towed detector data, *Shot 5*.

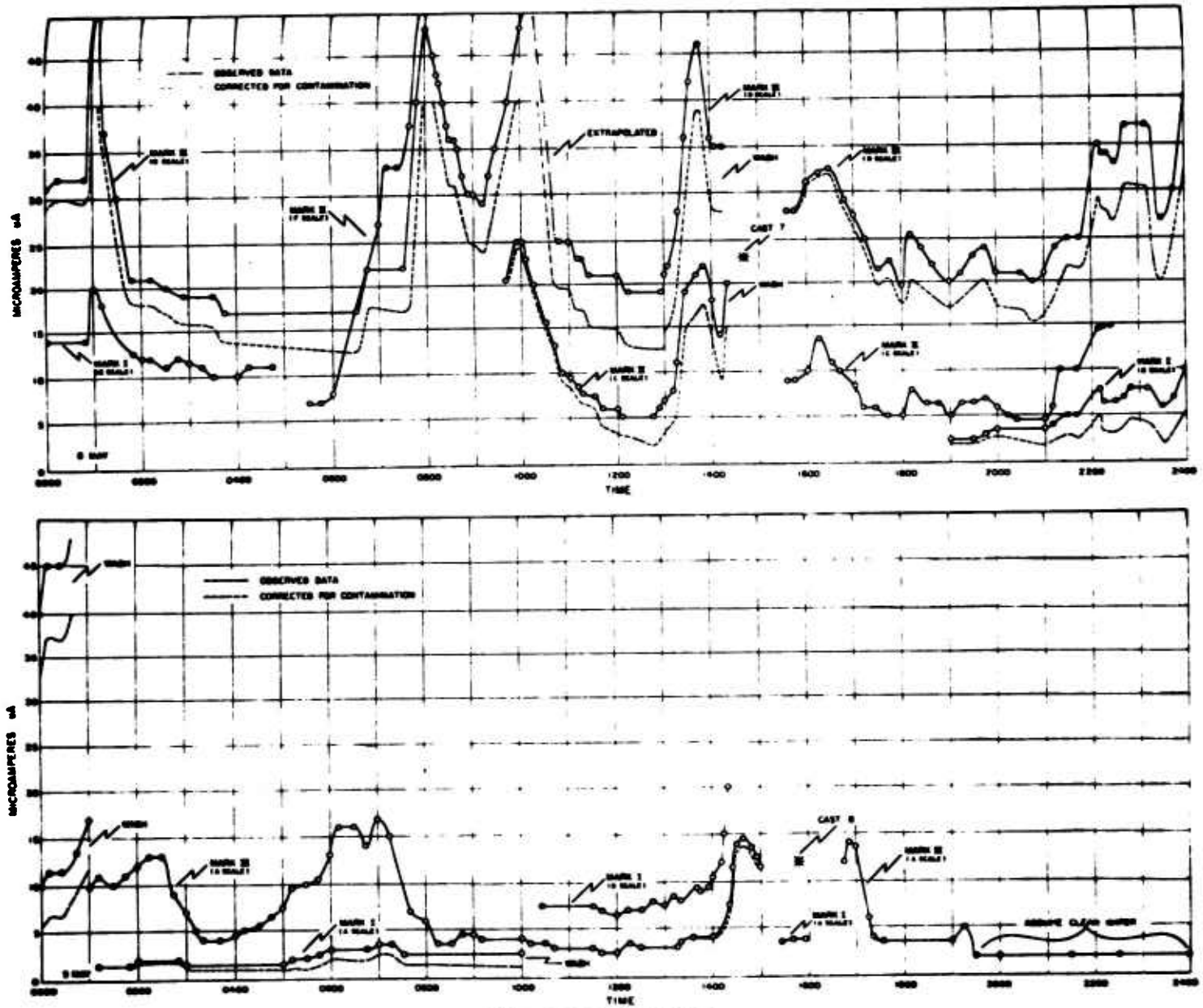

Figure 3.1 Continued.

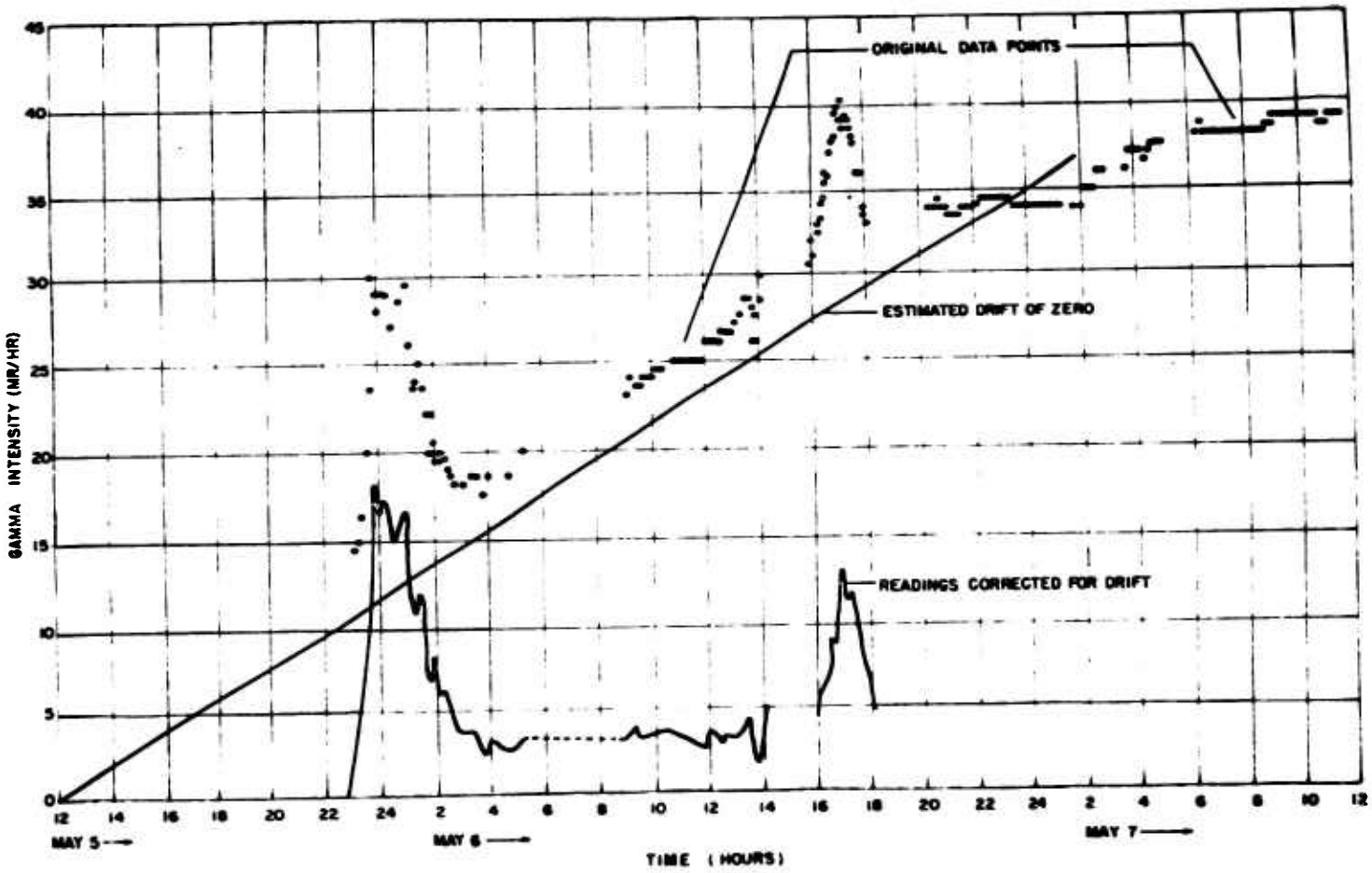

Figure 3.2 "Pot" record in mr/hr showing correction for accumulated drift.

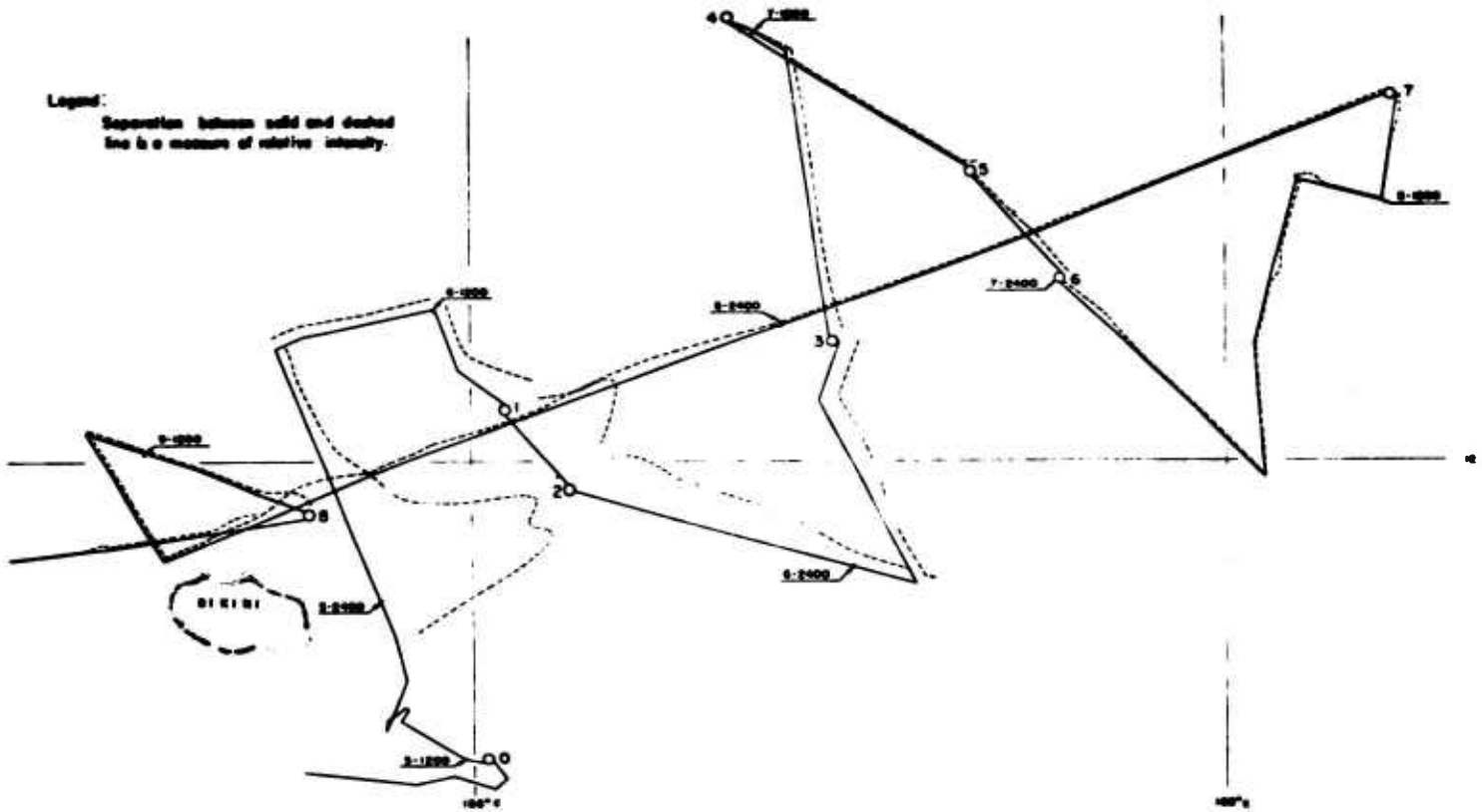

Figure 3.3 Relative radiation intensity along ship's track, Shot 5 survey.

struments after corrections were made for instrument contamination in the manner just described and followed by application of the instrument calibration data discussed in Chapter 2 with reference to Figures 2.2 through 2.5.

The relative local gamma intensity in milliroentgen per hour is plotted normal to the ship's track as base line in Figure 3.3. This is the actual ship's track; and it is the relative local gamma intensity the ship intercepted. This is what was seen from the ship; it has little in common with the synoptic method of summarizing fallout.

The values of the intensities which are shown graphically in Figure 3.3 are proportional to those tabulated in column 5 of Table 3.5, which will be discussed later.

3.3.3 Computation of Absolute Magnitude of In Situ Intensity. When instruments must be used to measure absolute gamma intensity inside a mass of water which contains radioactive sources emitting photons of several energies, an elaborate calibration procedure must be undertaken. A full calibration of Mark II has been made from data obtained in the field, and data obtained by testing the instruments later against known radioactive sources, and from estimates of the spectral nature of the radioactive material in the fallout. Details of this calibration study have been put in Appendix C.

With the aid of factors derived in Appendix B and the calibration curves of Figures 2.2 through 2.5, the value of absolute gamma intensity in milliroentgens per hour has been computed corresponding to each field measurement, and these local in situ values are plotted in Column 5 of Table 3.5. This quantity has been called ϕ_t and has the units of milliroentgens per hour.

3.4 COMPUTATION OF SYNOPTIC PICTURE

3.4.1 Vertical Extent of Activity. In preparation for computations of a synoptic picture, an estimate of the extent of penetration of the activity into the sea at any given time will now be undertaken. Numerous bathythermograph measurements taken in the area establish that the thermocline lay at about 100 meters depth during this period. The temperature discontinuity at the thermocline indicates that the water had been recently stirred to this depth, presumably because of forces originating in the winds. Such mixing presumably would force fallout material to progress downward ultimately to 100 meters even if the material had neutral buoyancy.

There is considerable evidence that the upper layers of the sea mix to a state of homogeneity, and it is known that transport by mixing becomes exceedingly small below the depth of the thermocline. However, the mechanism behind this surface mixing is still not well understood, and it has not been possible to predict the progress of mixing by oceanographic considerations alone. Fortunately, during this particular field operation, some actual measurements of the rate of penetration were acquired. These experimental data along with an estimate, made by NRDL, of the time at which fallout arrived at the sea surface permit computation of the progress downward of the contaminant.

Table 3.1 illustrates some actual penetration measurements; it lists the readings from the Mark II instrument as it was lowered at Station Y - 1. Identical readings were made as the instrument was again raised slowly. The same data is plotted (at the left with circled points) in Figure 3.4. It is believed that all the depths are accurate in Figure 3.4, except at those points indicated by crosses at the left and relating to a preliminary cast made by hand. On later casts a winch was used and a 150-pound weight was used to assure that the wire remained vertical.

Figure 3.4 indicates an abrupt decrease in activity at about 60 meters depth at Station Y - 1, and at the time the station was occupied.

Table 3.2 and the middle curve in Figure 3.4 summarize the results of lowering the Mark II instrument at Station Y - 2 three hours later. Both stations were roughly the

Table 3.1 Second Vertical G.M.C. Profile in Yankee Fallout ✓

Station Y - 1 1600 May 6, 1954

Lat: 12° 10'N Long: 166° 06' E

Depth (meters)***	Microamperes Reading	In Situ Intensity (mr/hr)
Hydro bucket *	11.0	6.8
Surface**	23.5	16.5
3.05	24.0	16.8
6.1 - 33.6	24.0	16.8
36.6	24.0	16.8
39.6	23.5	16.5
42.7	23.5	16.5
48.7	23.5	16.5
51.8	20.0	13.5
54.8	20.5	13.9
57.9	19.5	13.2
61.0	18.0	12.0
64.0	16.0	10.5
68.0	12.5	7.9
71.0	6.0	3.6
75.0	3.5	2.1
78.0	3.5	2.1
81.0	3.0	1.6

* G.M.C. on grilled floor of hydro bucket 6 ft above sea.
** G.M.C. just submerged in sea.
*** All depths measured by meter wheel on hydro wire.
✓ The first vertical cast is not tabulated since depth measurements are questionable.

Note:
Readings made after every 10 ft of line paid out, instrument was allowed to adjust itself at each depth.

Maximum depth $z_m = 68$
Average intensity $\phi_t = 14.4$ mr/hr
Decay factor $= 2.44$

Therefore at 3 feet elevation $\theta_t = 8.03$ R/hr
and $\theta_{12} = 19.59$ R/hr

Table 3.2 Third Vertical G.M.C. Profile in Yankee Fallout

Station Y - 2 1900 May 6, 1954

Lat: 11° 55.3' N Long: 166° 16.6' E

Depth (meters)***	Microamperes (Reading)	In Situ Intensity (mr/hr)
Hydro bucket *	9.0	5.4
Surface **	17.5	11.7
5	17.5	11.7
10, 20, 30, & 40	17.5	11.7
45	17.0	11.2
50	17.0	11.2
55	17.0	11.2
60	16.5	10.8
65	16.0	10.4
70	14.0	9.0
75	10.5	6.6
80	4.5	2.7
Lying on deck****	7.0	4.2

* Instrument on grid of hydro bucket about 6 ft above sea.
** Just submerged.
*** Depths read on meter wheel of hydro wire.
**** Instrument lying on ship's contaminated deck; the ship's hull shields sea radiation.

Maximum depth $z = 75$
Average intensity $\phi_t = 10.55$ mr/hr
At 3 ft elevation $\theta_t = 6.49$ r/hr
Decay factor $= 2.6$

Therefore $\theta_{12} = 16.87$ r/hr

Table 3.3 Fourth Vertical G.M.C. Profile in Yankee Fallout

Station Y - 6 2300 May 7, 1954

Lat: 12° 30' N Long: 167° 35' E

Depth (meters)***	Microamperes (Reading)	In Situ Intensity (mr/hr)
Surface *	55	1.6
5	50	1.5
10	50	1.5
20	55	1.6
30	55	1.6
40	57	1.6
50	58	1.6
60	57	1.6
70	54	1.6
80	55	1.6
End of rope and wire		

* Instrument just submerged.
*** Depths on meter wheel of hydro wire.

Maximum depth	z_m	= 100
Average Intensity	β_t	= 1.6 mr/hr
At 3 feet elevation	θ_t	= 1.3 r/hr
Decay factor		= 5.2
Therefore θ_{12}		= 6.76 r/hr

Table 3.4 Estimation of Time of Arrival of Fallout from an Analysis of the Winds for Shot 5

Approximate Distance (miles)	Mean Arrival Time (hours)*
25	1.5
35	2.3
45	2.9
55	4.3
65	5.1
85	6.7
120	9.7
135	11.0
165	15.0
215	18.0
240	19.0

* Weighted mean arrival time based upon estimated duration of fallout (2 hours) and estimated time of arrival.

same distance from ground zero, and presumably fallout arrived at both at about the same time.

A slightly greater penetration is evident at this later time.

Table 3.3 and the right hand curve on Figure 3.4 show the result of lowering the instrument to the full extent of the electric cable at a much later time at Station Y - 6. Here penetration had proceeded below 80 meters and uniform mixing above this depth was evident.

3.4.2 Conclusions Regarding Penetration Progress. From Figure 3.4 it is apparent that fairly uniform penetration to at least 80 meters was soon established, and the BT data indicates that ultimate penetration below 100 meters was highly unlikely.

To illustrate what is believed to be the extent of penetration at any time, Figure 3.5 was constructed by drawing a straight line between the estimated time of arrival (5 hours) at Stations Y - 1 and Y - 2 and the two experimental points, and continuing to the depth of the thermocline (100 meters).

This estimate of downward progress is needed for computations and is, of course, only a rough estimate; but it can be pointed out that there is still other evidence indicating that it is not absurdly inaccurate. For example, the water analyses at Station Y - 3, which was occupied about 42 hours after detonation, indicates that mixing had attained the depth of 80 to 90 meters. This datum fits the graph of Figure 3.5 well enough. Nevertheless, the fact that time of arrival and fallout at any station is not well established experimentally makes it futile to attempt to perfect the penetration estimate any further.

3.4.3 Computations of Total Local Fallout. From the knowledge of the vertical distribution of activity a process of summation leads to an estimate of how much activity might have been caught on a hypothetical plane fixed at mean sea level. From consideration of geometry, energy distribution, and scattering laws, a further estimate could be arrived at as to what radiant flux would have existed at an elevation 3 feet above the hypothetical catchment plane.

Details of the mathematical and physical considerations leading to the derivation are discussed in detail in Appendix C, and Column 6 of Table 3.5 lists the numerical values of this local datum corresponding to each field measurement.

3.4.4 Estimate of Radioactive Decay. The solid curve in Figure 3.6 is from an estimate of the progress of decay of radioactivity following Shot 5 supplied by NRDL for the purpose of making a synoptic report of these field findings; the dotted line shows, for graphical comparison, a decay proportional to time raised to the usual negative 1.2 exponent. No measurements suitable for decay evaluation were made during Shot 5. The solid line between H + 1 and H + 3 hours is based on estimates made at NRDL from calculated gamma ionization decay curve, using fission product plus induced activities. The solid line after H + 3 hours is based on measurements made by NRDL from Shot 1, How Island gamma-time-intensity record and AN/PDR-39 readings. The justification for using Shot 1 data lies in the similarity of capture to fission ratios for the two shots.

Figure 3.7 is a convenient curve for computing total dose and was derived by graphically integrating Figure 3.6. The total dose accumulated between H + 1 hour and the time t (hours) since detonation is

$$D(t) = I_1 \int_1^t f(t)\, dt = I_1 X(t)$$

where X(t) = abscissa of Figure 3.7 and, where I_1 is the dose rate at H + 1 hour, and where $I_1 f(t)$ expresses the instantaneous value of dose rate corresponding to the solid line

(Text continued on Page 46)

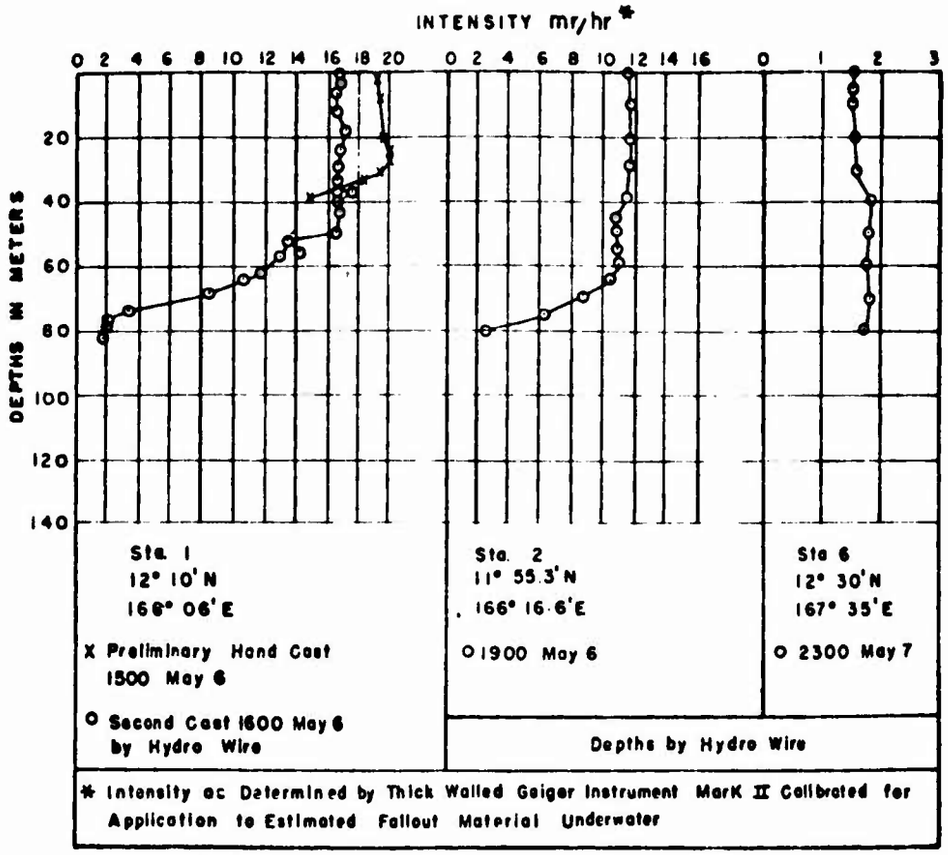

Figure 3.4 Mark II vertical radioactivity profiles, Shot 5.

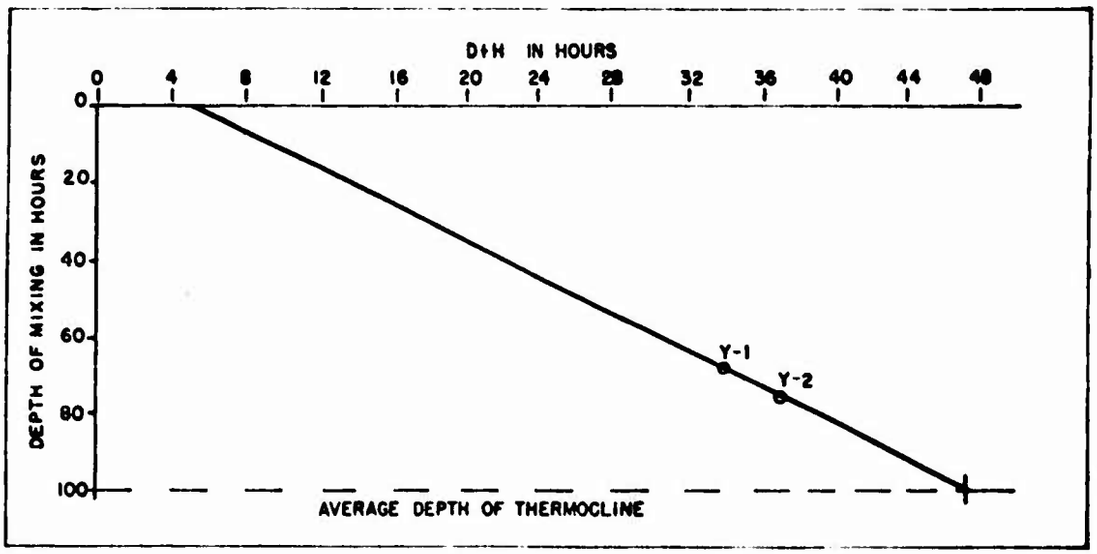

Figure 3.5 Progress of vertical mixing.

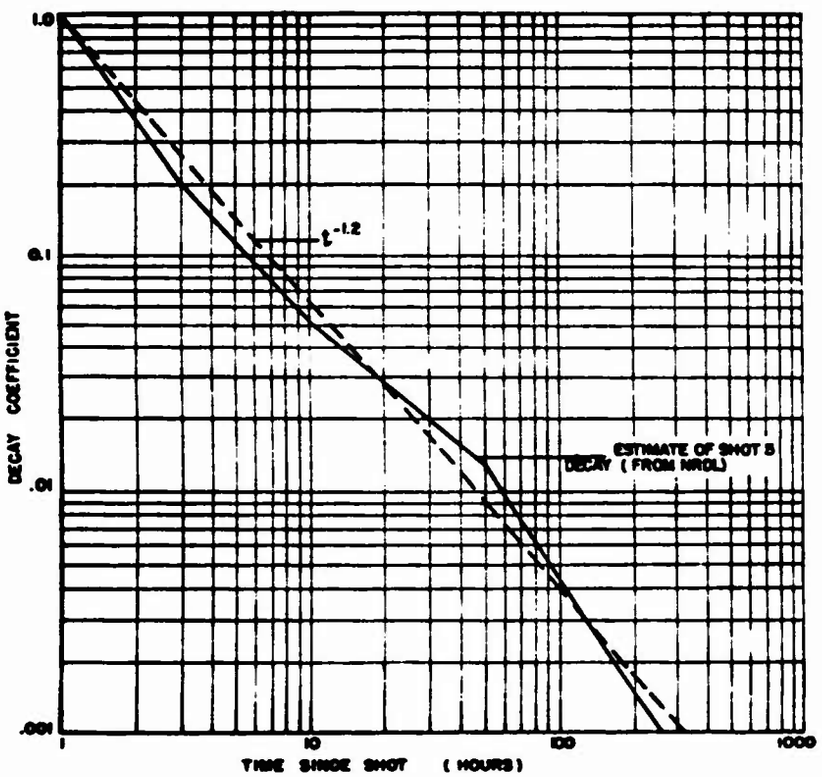

Figure 3.6 Decay of coefficient curve.

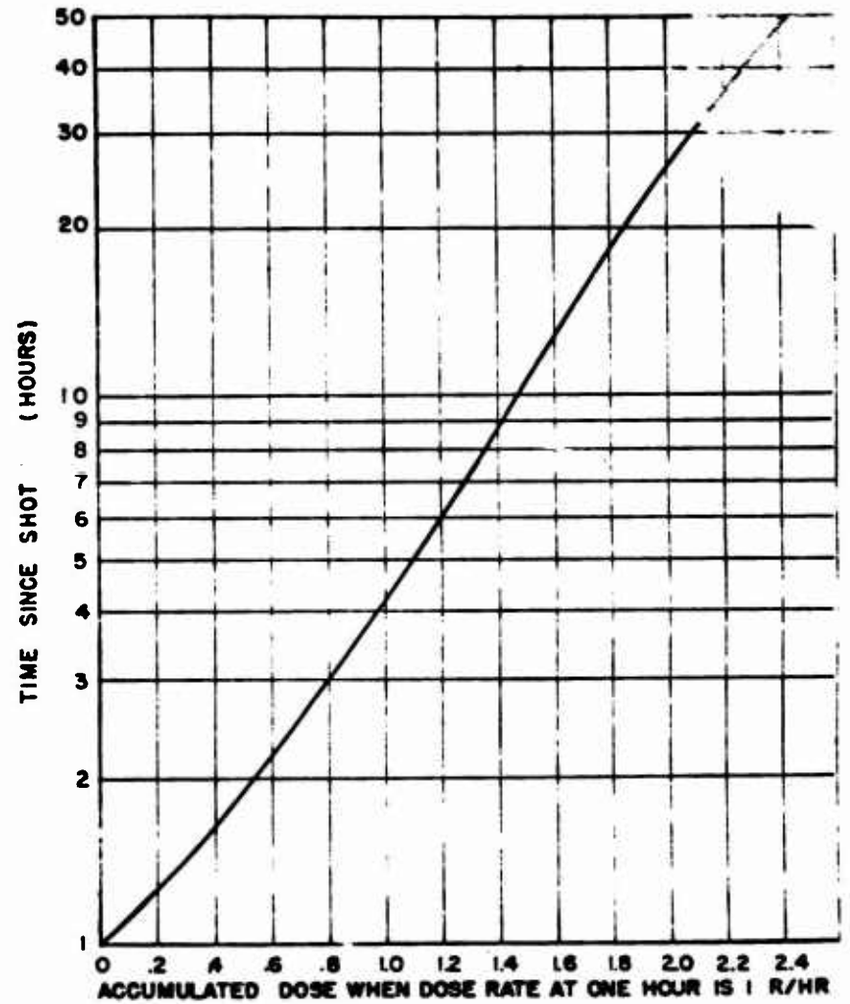

Figure 3.7 Accumulated dose factor.

TABLE 3.5 COMPUTATION OF DOSE RATE AND ACCUMULATED DOSE 3 FEET ABOVE A HYPOTHETICAL PLANE CATCHING THE FALLOUT FROM SHOT 5

Column:

1. Local time of reading (track time).
2. Hours since Shot 5 (Col 1 minus 0600/5/May).
3. Hours since fallout arrival (derived from NRDL arrival data and based upon the corrected track).
4. Depth of mixing Z in meters.
5. ϕ_t computed dose rate in situ at time t; this was derived from an average of the local μa readings (Figure 3.1) after these were first reduced to mr/hr roughly by applying the radium calibration curves (Figure 2.1 - Figure 2.4), then correcting for apparent instrument contamination, then multiplying by the factor 1.5 (Appendix B) so as to correct for use of the instruments when submerged in a 4 pi source of fallout material. In mr/hr.

Column:

6. θ_t computed instantaneous local dose rate at 3 feet elevation in r/hr (8.2×10^{-3}) (Col 4) (Col 5) Appendix C.
7. Decay coefficient to H + 12 hours (NRDL decay data).
8. θ_{12} computed local dose rate at 3 feet elevation at H + 12 (Col 7) (Col 6) in r/hr.
9. θ_1 computed local dose rate at 3 feet elevation at H + 1 (22.7) (Col 8) in r/hr.
10. Fallout time of arrival, hours after Shot 5.
11. Computational factor, the accumulated dose computed on the basis of 1 r/hr at time H + 1. (Based upon decay data from NRDL).
12. Computed dose at 3 feet elevation accumulated between fallout arrival and H + 50 = (Col 11) (Col 9).

Note: The numbers in all columns should be rounded off at two figures.

1	2	3	4	5	6	7	8	9	10	11	12
Track Time And Date	Hours Since H Hour	Hours Since Fall-Out	Depth of Mixing (Meters)	ϕ_t In Situ (mr/hr)	θ_t @ 3' R/hr	Decay Coefficient to H+12	θ_{12} @ 3' R/hr	θ_1 @ 3' R/hr	Fallout Time Hours Since H Hour	Accumulated Dose Factor	Accumulated Dose from Fallout to H+50 Roentgen
May 5 1954											
2300	17:00	15:00	35.2	11.7	3.38	1.35	4.56	103.7	2.0	1.86	193.00
2315	17:15	15:15	35.8	24.0	7.05	1.37	9.66	219.0	2.0	1.86	407.00
2330	17:30	15:30	36.4	60.0	17.90	1.39	24.88	566.0	2.0	1.86	1,052.00
2350	17:50	15:50	37.2	91.2	27.80	1.41	39.20	890.0	2.0	1.86	1,652.00
2400	18:00	16.00	37.6	83.4	25.70	1.42	36.49	806.0	2.0	1.86	1,500.00

TABLE 3.5 CONTINUED

1	2	3	4	5	6	7	8	9	10	11	12
May 6 1954											
0005	18.05		37.8	87.0	27.00	1.43	38.61	876.0	2.0	1.86	1,628.00
0015	18:15		38.4	85.5	26.90	1.44	38.74	878.0	2.0	1.86	1,630.00
0030	18:30		39.0	79.5	25.40	1.45	36.83	835.0	1.9	1.90	1,585.00
0050	18:50		39.9	84.5	27.70	1.47	40.72	924.0	1.8	1.94	1,791.00
0100	19:00	17.20	40.5	80.0	26.60	1.48	39.37	894.0	1.8	1.94	1,733.00
0115	19:15		41.1	70.0	23.60	1.50	35.40	803.0	1.8	1.94	1,558.00
0130	19:30		41.7	76.0	26.00	1.52	39.52	806.0	1.8	1.94	1,563.00
0135	19:35		41.9	70.0	24.00	1.53	36.72	833.0	1.8	1.94	1,615.00
0140	19:40		42.1	50.0	17.30	1.53	26.47	578.0	1.8	1.94	1,120.00
0150	19:50		42.5	41.8	14.60	1.54	22.48	511.0	1.8	1.94	992.00
0155	19:55		42.7	44.1	15.50	1.55	24.03	545.0	1.8	1.94	1,058.00
0200	20:00	18.20	42.9	33.0	11.60	1.55	17.98	408.0	1.8	1.94	792.00
0205	20:05		43.1	26.4	9.34	1.56	14.57	331.0	1.8	1.94	642.00
0210	20:10		43.3	29.7	10.50	1.57	16.48	374.0	1.8	1.94	726.00
0230	20:30		44.1	20.9	7.56	1.58	11.94	271.0	1.8	1.94	526.00
0300	21:00	19.20	45.1	15.2	5.62	1.61	9.05	205.0	1.8	1.94	398.00
0315	21.15		45.6	13.7	5.13	1.63	8.36	190.0	1.9	1.90	361.00
0330	21:30		45.9	11.4	4.29	1.65	7.08	161.0	2.0	1.86	300.00
0355	21:55		46.6	7.7	2.94	1.67	4.91	111.0	2.1	1.83	283.00
0400	22:00	19.9	46.8	7.4	2.64	1.68	4.44	101.0	2.1	1.83	185.00
0415	22:15		47.2	6.7	2.59	1.70	4.40	100.0	2.2	1.79	179.00
0430	22:30		47.6	6.1	2.38	1.72	4.09	93.0	2.3	1.76	164.00
0445	22:45		48.0	5.6	2.20	1.74	3.83	87.0	2.3	1.76	153.00
0500	23:00	20.6	48.6	5.3	2.11	1.75	3.69	83.7	2.4	1.74	146.00
0600	24:00	21.2	50.0	4.1	1.68	1.83	3.07	69.8	2.8	1.64	115.00
0700	25:00	21.8	51.6	4.1	1.73	1.88	3.25	73.8	3.2	1.53	113.00
0800	26:00	22.6	52.8	4.1	1.78	1.93	3.44	78.1	3.4	1.51	118.00
0845	26:45		54.5	4.1	1.83	1.98	3.62	82.2	3.6	1.49	123.00
0900	27:00		54.9	3.5	1.58	2.00	3.16	71.9	3.7	1.47	106.00
0930	27:30	23.3	55.6	3.0	1.37	2.03	2.78	63.2	3.8	1.46	92.30
0945	27:45		56.0	3.5	1.61	2.05	3.30	75.0	3.9	1.45	109.00
1005	28:05	24.0	56.5	3.4	1.58	2.07	3.27	74.4	4.0	1.42	106.00
1030	28:30		57.0	3.0	1.40	2.09	2.93	66.7	4.2	1.39	92.70
1050	28:50		57.5	3.3	1.55	2.11	3.27	74.4	4.4	1.37	102.00
1100	29:00	24.5	57.7	3.1	1.46	2.12	3.10	70.5	4.5	1.35	95.10
1130	29:30		58.4	2.5	1.20	2.16	2.59	58.9	4.6	1.34	78.80
1150	29:50		58.9	2.8	1.35	2.19	2.96	67.3	4.7	1.33	89.50

TABLE 3.5 CONTINUED

1	2	3	4	5	6	7	8	9	10	11	12
1200	30:00	25.2	59.2	2.5	1.22	2.20	2.68	61.0	4.8	1.31	79.80
1230	30:30		60.6	2.2	1.09	2.22	2.42	55.1	4.7	1.33	73.20
1300	31:00		62.0	2.0	1.02	2.24	2.28	51.8	4.6	1.34	69.5
1315	31:15		62.6	6.0	3.08	2.26	6.96	158.2	4.6	1.34	212.00
1330	31:30		63.2	5.9	3.05	2.28	6.95	158.8	4.6	1.34	213.00
1345	31:45		63.6	10.9	5.68	2.30	13.10	298.0	4.7	1.33	396.00
1350	31:50		63.7	9.5	4.96	2.31	11.46	261.0	4.7	1.33	347.00
1400	32:00	27.3	64.1	16.2	8.51	2.32	19.74	449.0	4.7	1.33	597.00
1411	32:11		64.8	19.0	10.10	2.33	23.53	535.0	4.7	1.33	711.00
	STATION Y - 1										
1600	34:00	29.1	68.2	16.7	9.33	2.44	22.77	517.0	4.9	1.30	673.00
1615	34:15		68.9	41.5	23.40	2.45	57.33	1304.0	4.9	1.30	1695.00
1625	34:25		69.2	36.2	20.50	2.46	50.43	1147.0	4.9	1.30	1490.00
1630	34:30		69.4	46.0	26.20	2.46	64.45	1467.0	5.0	1.30	1905.00
1640	34:40		69.8	52.3	29.90	2.46	73.55	1673.0	5.0	1.30	2188.00
1645	34:45		69.9	47.1	27.00	2.47	66.69	1518.0	5.0	1.30	1972.00
1650	34:50		70.2	55.9	32.20	2.47	79.53	1809.0	5.0	1.30	2350.00
1658	34:58		70.5	54.4	31.40	2.48	77.87	1770.0	5.0	1.30	2300.00
1700	35:00	30.0	70.6	63.8	37.00	2.48	91.76	2085.0	5.0	1.30	2710.00
1715	35:15		71.2	53.6	31.30	2.50	78.25	1781.0	5.0	1.30	2310.00
1720	35:20		71.4	59.0	34.40	2.51	86.34	1965.0	5.0	1.30	2555.00
1730	35:30		71.8	52.0	30.60	2.52	77.11	1753.0	5.0	1.30	2280.00
1740	35:40		72.2	40.6	24.00	2.53	60.72	1380.0	5.1	1.29	1780.00
1745	35:45		72.4	40.0	23.80	2.54	60.45	1376.0	5.1	1.29	1775.00
1750	35:50		72.5	25.8	15.30	2.55	39.02	886.0	5.1	1.29	1142.00
1800	36:00	30.9	72.9	24.0	14.30	2.56	36.61	832.0	5.1	1.29	1075.00
1805	36:05		73.2	21.2	12.70	2.57	32.64	800.0	5.1	1.29	1031.00
	STATION Y - 2										
2020	38:20		76.2	20.5	12.80	2.71	34.69	789.0	5.9	1.21	954.00
2030	38:30		76.3	22.8	14.30	2.72	38.90	884.0	6.1	1.19	1050.00
2100	39:00	32.5	76.5	16.7	10.50	2.75	28.88	657.0	6.5	1.15	755.00
2115	39:15		76.6	15.1	9.35	2.76	25.81	587.0	6.7	1.14	669.00
2130	39:30		76.7	14.7	9.24	2.77	25.59	582.0	6.9	1.12	652.00
2140	39:40		76.7	15.4	9.67	2.78	26.88	612.0	7.1	1.11	679.00
2150	39:50		76.8	15.8	9.95	2.79	27.76	632.0	7.2	1.10	695.00
2200	40:00	32.7	76.9	16.7	10.50	2.80	29.40	668.0	7.3	1.10	735.00

TABLE 3.5 CONTINUED

1	2	3	4	5	6	7	8	9	10	11	12
2210	40:10		77.0	16.8	10.60	2.81	29.79	678.0	7.4	1.09	738.00
2215	40:15		77.0	15.8	9.96	2.82	28.09	639.0	7.6	1.08	690.00
2230	40:30		77.0	14.9	9.40	2.84	26.70	607.0	7.8	1.06	644.00
2245	40:45		77.1	14.6	9.22	2.86	26.37	600.0	7.9	1.06	636.00
2305	41:05	32.8	77.1	14.1	8.90	2.87	25.54	580.0	8.2	1.03	598.00
2315	41:15		77.1	13.1	8.28	2.89	23.93	544.0	8.4	1.02	555.00
2330	41:30		77.2	10.6	6.70	2.90	19.43	442.0	8.6	1.01	447.00
2345	41:45		77.2	7.5	4.75	2.92	13.87	315.0	8.8	.99	312.00
2400	42:00	32.9	77.3	6.5	4.12	2.93	12.07	275.0	9.1	.98	269.00
May 7 1954											
0015	42:15		77.4	5.9	3.75	2.95	11.06	252.0	9.3	.97	244.00
0030	42:30		77.5	5.7	3.62	2.96	10.72	244.0	9.5	.96	234.00
0045	42:45		77.6	4.9	3.12	2.98	9.30	212.0	9.7	.95	202.00
0100	43:00	33.1	77.8	4.4	2.81	2.99	8.40	191.0	9.9	.94	179.00
0115	43:15		78.7	4.4	2.84	3.00	8.52	195.0	9.8	.94	183.00
0130	43:30		79.8	4.8	3.14	3.01	9.45	215.0	9.7	.95	204.00
0145	43:45		80.0	4.8	3.15	3.02	9.51	216.0	9.6	.95	205.00
0200	44:00	34.5	81.1	4.6	3.06	3.03	9.27	211.0	9.5	.96	203.00
0215	44:15		81.8	5.8	3.88	3.05	11.83	270.0	9.5	.96	259.00
0230	44:30		82.6	6.3	4.27	3.07	13.11	298.0	9.4	.96	286.00
0245	44:45		83.4	7.5	5.12	3.08	15.77	359.0	9.4	.96	345.00
0255	44:55		83.8	7.9	5.42	3.09	16.75	381.0	9.3	.97	370.00
0300	45:00	35.7	84.0	7.7	5.30	3.10	16.43	376.0	9.3	.97	365.00
0315	45:15		84.6	7.3	5.07	3.12	15.82	360.0	9.3	.97	349.00
0330	45:30		85.2	7.1	4.96	3.13	15.52	353.0	9.2	.97	343.00
0355	45:55		86.4	7.2	5.10	3.16	16.12	367.0	9.2	.97	356.00
0400	46:00	36.8	86.6	6.8	4.83	3.16	15.26	347.0	9.2	.97	337.00
0415	46:15		86.9	6.0	4.27	3.18	13.58	309.0	9.3	.97	300.00
0430	46:30		87.3	4.8	3.44	3.19	10.97	250.0	9.4	.96	240.00
0445	46:45		87.6	5.3	3.81	3.22	12.27	279.0	9.5	.96	268.00
	STATION Y - 3										
0615	48:15		90.7	5.3	3.95	3.28	12.96	295.0	9.6	.95	280.00
0630	48:30		91.2	5.2	3.88	3.31	12.84	292.0	9.7	.95	288.00
0645	48:45		91.7	4.4	3.31	3.33	11.02	251.0	9.7	.95	239.00
0700	49:00		92.2	2.5	1.89	3.34	6.31	143.5	9.8	.94	135.00

TABLE 3.5 CONTINUED

1	2	3	4	5	6	7	8	9	10	11	12
0715	49:15		92.6	2.0	1.52	3.37	5.12	116.5	9.9	.94	110.00
0730	49:30		93.0	2.0	1.52	3.39	5.15	117.0	10.0	.93	109.00
0745	49:45		93.4	1.8	1.38	3.42	4.72	107.5	10.1	.92	99.00
0800	50:00	39.8	93.8	1.3	1.00	3.44	3.44	78.1	10.2	.91	71.10
0810	50:10		94.0	1.2	0.925	3.46	3.20	72.6	10.2	.91	66.10
0820	50:20		94.2	1.4	1.08	3.49	3.77	85.6	10.3	.91	77.90
0830	50:30		94.5	1.6	1.24	3.51	4.35	98.8	10.3	.91	90.00
0845	50:45		94.8	2.2	1.71	3.55	6.07	137.5	10.4	.90	124.00
0900	51:00	40.5	95.2	2.0	1.56	3.58	5.58	126.5	10.5	.90	114.00
0915	51:15		95.6	2.9	2.27	3.61	8.19	185.8	10.6	.90	167.00
0930	51:30		96.0	2.5	1.97	3.63	7.15	162.2	10.7	.90	146.00
0945	51:45		96.4	2.0	1.58	3.65	5.77	131.0	10.8	.89	117.00
1000	52:00	41.1	96.8	1.5	1.19	3.67	4.37	99.0	10.9	.89	88.00
1015	52:15		96.9	1.4	1.11	3.70	4.11	93.2	11.2	.87	81.00
1030	52:30		97.1	1.3	1.04	3.73	3.88	88.0	11.4	.86	76.00
1045	52:45		97.2	1.2	0.956	3.76	3.59	81.5	11.5	.86	70.00
1100	53:00	41.4	97.4	1.0	0.798	3.79	3.02	68.6	11.6	.85	58.30
1115	53:15		98.0	0.2	0.161	3.82	0.62	14.1	11.6	.85	12.10
1130	53:30		98.6	0.2	0.162	3.84	0.62	14.1	11.5	.86	12.10
1200	54:00		99.8	0.2	0.164	3.89	0.64	14.5	11.4	.86	12.50
1230	54:30	42.6	100.0	0.2	0.164	3.93	0.64	14.5	11.5	.86	12.50
	STATION Y - 4										
1505	57:05	45.4	100.0	0.7	0.574	4.27	2.45	55.7	11.6	.85	47.30
1530	57:30		100.0	0.8	0.656	4.35	2.85	64.8	11.8	.84	54.50
1820	60:20		100.0	0.8	0.656	4.63	3.04	69.0	13.3	.79	54.50
1830	60:30		100.0	2.2	1.80	4.65	8.37	190.3	13.4	.78	149.00
1840	60:40		100.0	2.7	2.21	4.67	10.32	298.0	13.5	.78	232.00
	STATION Y - 5										
1930	61:30		100.0	1.2	0.98	4.77	4.70	107.0	13.7	.77	82.50
1945	61:45		100.0	2.3	1.88	4.80	9.02	205.0	13.8	.76	156.00
2000	62:00	48.1	100.0	2.4	1.97	4.83	9.52	216.0	13.9	.76	164.00
2015	6_:15		100	1.8	1.48	4.86	7.19	162.0	14.0	.76	123.00
2030			100	2.2	1.80	4.89	8.80	200.0	14.1	.75	150.00
2045			100	1.9	1.56	4.93	7.69	175.0	14.2	.75	131.00
2100	63:00	48.7	100	1.5	1.23	4.95	6.09	138.4	14.3	.75	104.00
2130	63:30		100	1.5	1.23	4.99	6.14	139.8	14.6	.73	102.00
2150	63:50		100	1.5	1.23	5.03	6.19	140.8	14.7	.73	103.00

TABLE 3.5 CONTINUED

1	2	3	4	5	6	7	8	9	10	11	12
	STATION Y - 6										
May 8 1954											
2400	66:00	51.4	100	1.5	1.23	5.30	6.52	148.3	14.6	.73	108.00
0015			100	1.8	1.48	5.33	7.89	179.4	14.8	.73	131.00
0045			100	1.8	1.48	5.40	7.99	181.6	15.0	.72	131.00
0100	67:00	51.8	100	2.9	2.38	5.43	12.93	294.0	15.2	.71	208.00
0115			100	1.9	1.56	5.47	8.53	194.0	15.3	.71	138.00
0130			100	1.5	1.23	5.51	6.78	154.3	15.5	.71	110.00
0145			100	0.9	0.738	5.55	4.10	93.2	15.6	.70	65.30
0200	68:00	52.3	100	0.9	0.738	5.58	4.12	93.6	15.7	.70	65.60
0230			100	0.7	0.573	5.66	3.24	73.6	15.9	.70	51.50
0400	70:00	53.6	100	0.6	0.492	5.80	2.85	64.8	16.4	.67	43.4
0500	71:00	54.2	100	0.5	0.410	5.95	2.44	55.5	16.8	.66	36.60
0530			100	0.4	0.328	6.02	1.97	44.8	16.8	.66	29.60
0600	72:00	55.2	100	0.6	0.492	6.08	2.99	68.0	16.8	.66	44.90
0630			100	0.7	0.573	6.14	3.52	80.0	16.9	.65	52.00
0645			100	0.9	0.738	6.17	4.55	103.5	16.9	.65	67.30
0700	73:00	56.1	100	0.9	0.738	6.20	4.58	104.2	16.9	.65	67.80
0730			100	0.9	0.738	6.27	4.63	105.2	17.0	.65	68.50
0745			100	1.6	1.31	6.31	8.27	188.0	17.1	.65	122.00
0800	74:00	56.8	100	3.4	2.79	6.34	17.69	401.0	17.2	.65	261.00
0815			100	2.3	1.88	6.38	11.99	272.0	17.3	.64	174.00
0830			100	1.8	1.47	6.41	9.42	214.0	17.4	.64	137.00
0900	75:00	57.4	100	1.5	1.23	6.48	7.97	181.0	17.6	.63	114.00
0920			100	1.3	1.06	6.51	6.90	157.0	17.6	.63	99.00
0930			100	1.9	1.56	6.53	10.19	231.0	17.7	.63	145.00
0945			100	3.1	2.54	6.56	16.66	378.0	17.8	.62	234.00
1000	76:00	58.2	100	3.3	2.70	6.58	17.77	403.0	17.8	.62	250.00
1030			100	2.1	1.72	6.65	11.44	260.0	17.9	.62	161.00
1100	77:00	59.0	100	1.1	0.903	6.72	6.07	138.0	18.0	.62	85.50
1130			100	0.8	0.656	6.80	4.46	101.2	18.1	.61	61.70
1200	78:00	59.8	100	0.8	0.656	6.88	4.51	102.3	18.2	.61	62.50
1230			100	0.7	0.573	6.93	3.97	90.0	18.3	.61	55.00
1300	79:00	60.6	100	0.9	0.738	7.00	5.17	117.2	18.4	.61	71.50
1310			100	0.9	0.738	7.03	5.19	117.9	18.4	.61	71.80
1330			100	1.9	1.56	7.08	11.04	251.0	18.5	.61	153.00
1350			100	2.6	2.13	7.12	15.17	344.0	18.6	.60	206.00
1400	80:00	61.4	100	2.1	1.72	7.15	12.30	279.0	18.6	.60	167.00
1420			100	1.8	1.47	7.19	10.57	240.0	18.6	.60	144.00

TABLE 3.5 CONTINUED

1	2	3	4	5	6	7	8	9	10	11	12
	STATION Y - 7										
1535			100	1.2	0.985	7.35	7.24	164.2	18.4	.61	100.00
1600	82:00	63.8	100	1.1	0.902	7.40	6.67	151.5	18.2	.61	92.50
1615			100	1.5	1.23	7.42	9.13	207.0	18.1	.61	126.00
1630			100	1.4	1.15	7.44	8.56	194.2	18.0	.62	120.00
1700	83:00	65.2	100	1.0	0.820	7.47	6.13	139.0	17.8	.62	86.00
1730			100	0.7	0.573	7.56	4.33	98.5	17.5	.63	62.00
1800	84:00	66.8	100	0.6	0.492	7.65	3.76	85.5	17.2	.65	55.50
1815			100	0.9	0.738	7.71	5.69	129.0	17.0	.65	83.80
1830			100	0.7	0.573	7.76	4.45	101.3	16.9	.65	65.80
1900	85:00	68.4	100	0.6	0.492	7.86	3.87	88.0	16.6	.67	59.00
1930			100	0.9	0.738	7.92	5.84	132.5	16.3	.67	88.80
2000	86:00	70.1	100	0.8	0.656	7.98	5.23	119.0	15.9	.70	83.30
2015			100	0.8	0.656	8.03	5.27	119.5	15.7	.70	83.70
2030			100	0.6	0.492	8.07	3.97	90.3	15.5	.71	64.10
2045			100	0.5	0.410	8.12	3.33	75.7	15.2	.71	53.80
2100	87:00	72.0	100	0.6	0.492	8.16	4.01	91.2	15.0	.72	65.70
2115			100	0.6	0.492	8.18	4.02	91.4	14.6	.73	66.60
2130			100	1.2	0.985	8.20	8.08	182.5	14.2	.75	137.00
2145			100	1.2	0.985	8.22	8.09	184.0	13.8	.76	140.00
2200	88:00	74.5	100	1.6	1.31	8.23	10.78	245.0	13.5	.78	191.00
2215			100	1.8	1.47	8.26	12.14	276.0	13.2	.79	218.00
2230			100	1.7	1.39	8.31	11.55	262.0	12.7	.81	212.00
2245			100	2.0	1.64	8.35	13.69	311.0	12.4	.82	255.00
2300	89:00	77.0	100	2.0	1.64	8.38	13.74	312.0	12.0	.84	262.00
2315			100	2.0	1.64	8.43	13.82	314.0	11.7	.85	267.00
2330			100	1.3	1.07	8.47	9.06	206.0	11.5	.86	177.00
2345			100	1.5	1.23	8.51	10.47	238.0	11.2	.87	207.00
2400	90:00	79.0	100	2.1	1.72	8.55	14.71	334.0	11.0	.88	294.00
May 9 1954											
0015			100	2.6	2.13	8.60	18.32	417.0	10.7	.90	375.00
0030			100	2.6	2.13	8.64	18.40	418.0	10.4	.90	376.00
0100	91:00	81.2	100	4.2	3.44	8.72	30.00	682.0	9.8	.94	640.00
0115			100	4.6	3.77	8.77	33.06	752.0	9.5	.96	722.00
0130			100	4.2	3.44	8.81	30.31	689.0	9.3	.97	669.00
0145			100	4.6	3.77	8.86	33.40	759.0	9.0	.98	744.00
0200	92:00	83.4	100	5.2	4.26	8.90	37.91	861.0	8.7	1.00	861.00
0215			100	5.6	4.59	8.93	40.99	932.0	8.5	1.01	942.00
0230			100	5.6	4.59	8.95	41.08	934.0	8.3	1.03	962.00
0245			100	3.6	2.95	8.98	26.49	602.0	8.2	1.03	621.00
0300	93:00	85.0	100	2.7	2.21	9.00	19.89	452.0	8.0	1.05	475.00
0330			100	1.2	0.98	9.09	8.95	394.0	7.5	1.09	430.00
0345			100	1.3	1.07	9.14	9.78	430.0	7.2	1.10	473.00

TABLE 3.5 CONTINUED

1	2	3	4	5	6	7	8	9	10	11	12
0400	94:00	87.0	100	1.5	1.23	9.18	11.25	257.0	7.0	1.10	283.00
0430			100	2.1	1.72	9.24	15.85	361.0	6.5	1.15	415.00
0500	95:00	89.0	100	2.8	2.30	9.30	21.39	486.0	6.0	1.20	584.00
0515			100	3.9	3.20	9.34	29.89	680.0	5.8	1.22	830.00
0530			100	4.1	3.36	9.37	31.48	716.0	5.6	1.23	880.00
0545			100	4.4	3.60	9.40	33.84	768.0	5.3	1.26	968.00
0600	96:00	90.9	100	5.6	4.59	9.43	43.28	985.0	5.1	1.29	1270.00
0615			100	7.0	5.73	9.46	54.21	1232.0	4.9	1.30	1602.00
0625			100	7.2	5.90	9.48	55.93	1270.0	4.7	1.33	1690.00
0645			100	6.0	4.92	9.53	46.89	1068.0	4.4	1.37	1462.00
0700	97:00	92.8	100	7.6	6.22	9.56	59.46	1353.0	4.2	1.39	1880.00
0730			100	4.2	3.44	9.63	33.13	752.0	3.7	1.47	1105.00
0745			100	2.7	2.21	9.68	21.39	486.0	3.4	1.51	734.00
0800	98:00	94.8	100	2.1	1.72	9.72	16.72	380.0	3.2	1.53	582.00
0820			100	1.2	0.985	9.76	9.61	218.0	3.0	1.59	347.00
0830			100	1.1	0.902	9.79	8.83	201.0	2.8	1.64	330.00
0845			100	1.5	1.23	9.83	12.09	275.0	2.6	1.68	462.00
0900	99:00	96.6	100	1.5	1.23	9.86	12.13	276.0	2.4	1.74	480.00
0915			100	1.2	0.985	9.89	9.74	221.0	2.4	1.74	385.00
0945			100	1.2	0.985	9.97	9.82	223.0	2.4	1.74	388.00
1000	100:00	97.6	100	0.9	0.738	10.00	7.38	167.8	2.4	1.74	292.00
1030			100	0.7	0.573	10.04	5.75	130.7	2.5	1.71	223.00
1100	101:00	98.4	100	0.6	0.492	10.08	4.96	112.8	2.6	1.68	189.00
1130			100	0.5	0.410	10.12	4.15	94.5	2.7	1.66	157.00
1145			100	0.6	0.492	10.14	4.99	113.5	2.8	1.64	222.00
1200	102:00	99.1	100	0.6	0.492	10.16	5.00	113.7	2.9	1.61	283.00
1215			100	0.5	0.410	10.18	4.17	94.8	3.0	1.59	151.00
1230			100	0.6	0.492	10.20	5.02	114.0	3.2	1.53	175.00
1245			100	0.6	0.492	10.22	5.03	114.3	3.3	1.52	174.00
1300	103:00	99.6	100	0.9	0.738	10.24	7.56	169.7	3.4	1.51	256.00
1330			100	1.0	0.820	10.28	8.43	191.8	3.7	1.47	282.00
1400	104:00	100.0	100	1.2	0.985	10.32	10.17	231.0	4.0	1.42	328.00
1420			100	2.9	2.38	10.35	24.63	559.0	4.2	1.39	776.00
1430			100	5.1	4.18	10.36	43.30	985.0	4.3	1.38	1360.00
1440			100	5.9	4.83	10.37	50.09	1140.0	4.4	1.37	1560.00
1455			100	4.8	3.93	10.39	40.83	928.0	4.6	1.34	1242.00
	STATION Y – 8										
1645			100	5.1	4.18	10.54	44.06	1004.0	4.6	1.34	1348.00
1650			100	6.0	4.92	10.55	51.91	1180.0	4.6	1.34	1580.00
1700	107:00	102.4	100	5.9	4.83	10.56	51.00	1160.0	4.6	1.34	1555.00
1715			100	3.0	2.46	10.58	26.03	591.0	4.4	1.37	810.00
1730			100	1.2	0.985	10.60	10.44	237.0	4.3	1.38	327.00
1800	108:00	104.0	100	1.1	0.902	10.64	9.60	218.0	4.0	1.42	310.00
1900	109:00	106.0	100	1.0	0.820	10.72	8.79	199.7			
1915			100	1.8	1.48						
1935			100	0.3	0.246						

in Figure 3.6 (if a simple decay proportional to $t^{-1.2}$ had been used as shown in the dotted line in Figure 3.6 then $I_1 f(t)$ would amount to simply $I_1 t^{-1.2}$).

Figure 3.7 is used only for calculating the dose accumulating between the time of arrival and H + 50 hours. This dose is, if time of arrival is t_A,

$$I_1 \int_{t_A}^{50} f(t)\, dt = I_1 \int_{1}^{50} f(t)\, dt - I_1 \int_{1}^{t_A} f(t)\, dt = I_1 \left[X(50) - X(t_A) \right]$$

Thus, the desired accumulated dose can be obtained by subtracting two abscissas of Figure 3.7.

From Figure 3.6 a computational coefficient, summarizing the effect of decay after H + 12 hours, has been taken and entered in Column 7 of Table 3.5 opposite each measurement.

3.4.5 Local Dose at 3 Feet Elevation at the Synoptic Time H + 12 Hours. Column 8 is the result of multiplying Column 7 and Column 6, that is, reducing the data of Column 6 to the synoptic time H + 12 hours.

3.4.6 Local Dose at 3 Feet Elevation at the Synoptic Time H + 1 Hour. Column 9 is the result of reducing the local data to another synoptic time, H + 1 hour; this was done by multiplying Column 8 by the common decay factor 22.7. The solid curve of Figure 3.6 shows that fallout at H + 1 hour has 22.7 times the activity present at H + 12 hours.

3.4.7 Effect of Time of Arrival and of Ocean Currents on Synoptic Presentation. Figure 3.8 and Table 3.4 are derived from an estimate supplied by NRDL of the time when fallout arrived at the sea surface as a function of distance from the point of detonation. Figures 3.9 and 3.10 summarize what is known about currents in this area.

For simplicity, the assumption was taken of a constant mean current from east to west, and the fallout time of arrival function of Figure 3.8 was utilized; the ship's track was displaced so as to present a hypothetical track indicating where the ship should have found the fallout if the water were stationary; that is, the locus of fallout on a hypothetical, firm catchment plane.

Unfortunately, local ocean currents had not been studied in detail by anyone during the immediate period, so an unknown amount of distortion is introduced here into the final fallout picture. Nevertheless, the fallout area is large, and there is evidence that the chosen velocity and direction are good representative values for the area as a whole.

The ship's track thus displaced so as to indicate where fallout would have been found on dry land, is shown as a solid line in Figure 2.5.

3.4.8 Plotting Fallout Contours of Iso-Dose-Rate. Along this "dry-land" track were distributed the measured radiation intensities given in Column 8 of Table 3.5; that is, the intensity at 3 feet elevation and H + 12 hours. Finally, contour lines showing iso-dose-rate were linked to the similar numbers.

These contour lines are in Figure 3.11.

The contours are identified by letters and the numerical values of dose rate are listed in Table 3.6. Area inside of each contour is given. The same contour map applies to

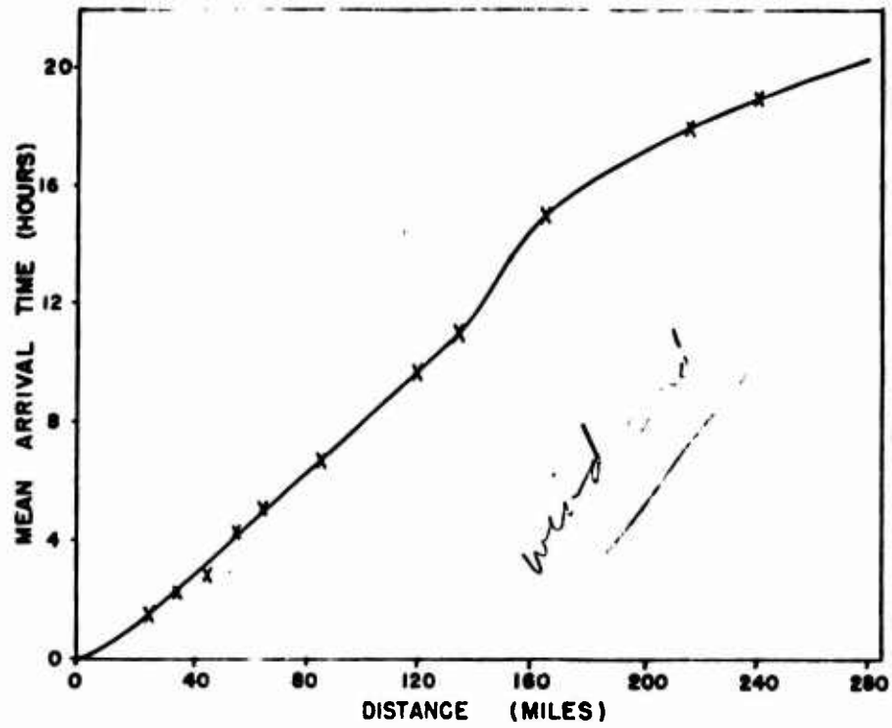

Figure 3.8 Estimated time of arrival of fallout from an analysis of the winds for Shot 5. (USNRDL data.)

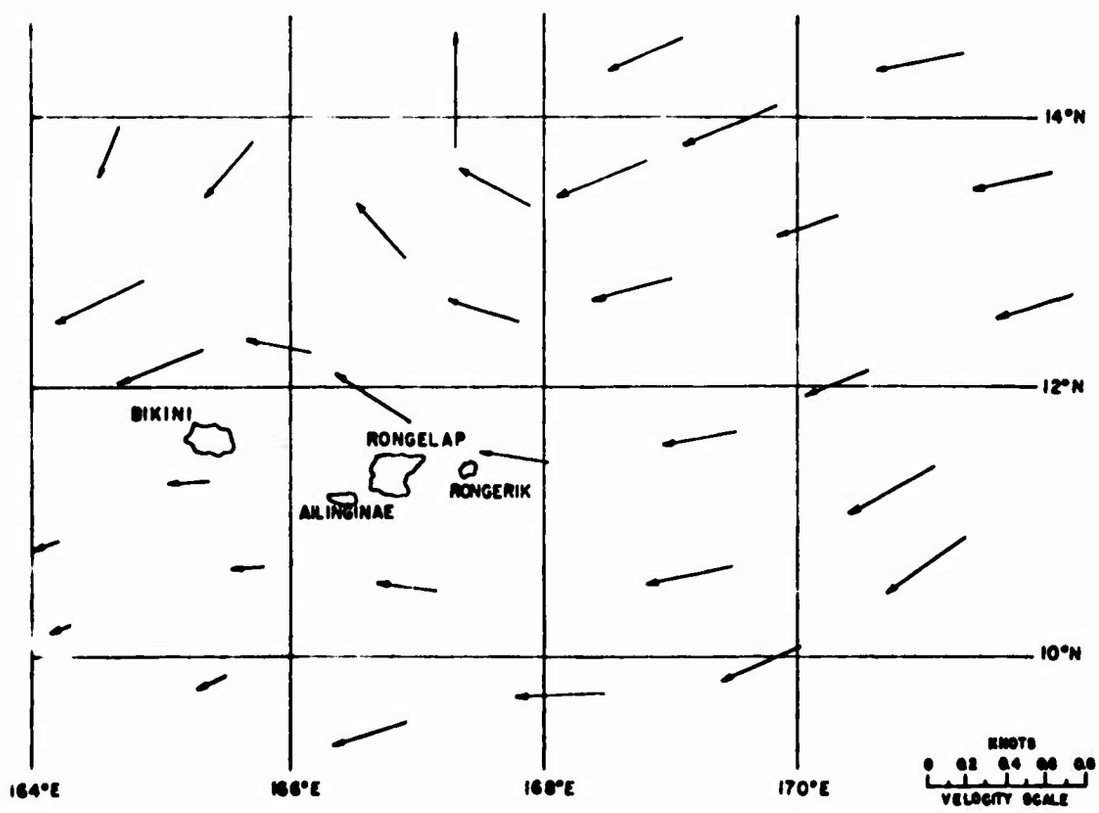

Figure 3.9 Ocean current vectors from Japanese hydrographic investigations, 1933-1941. April-September.

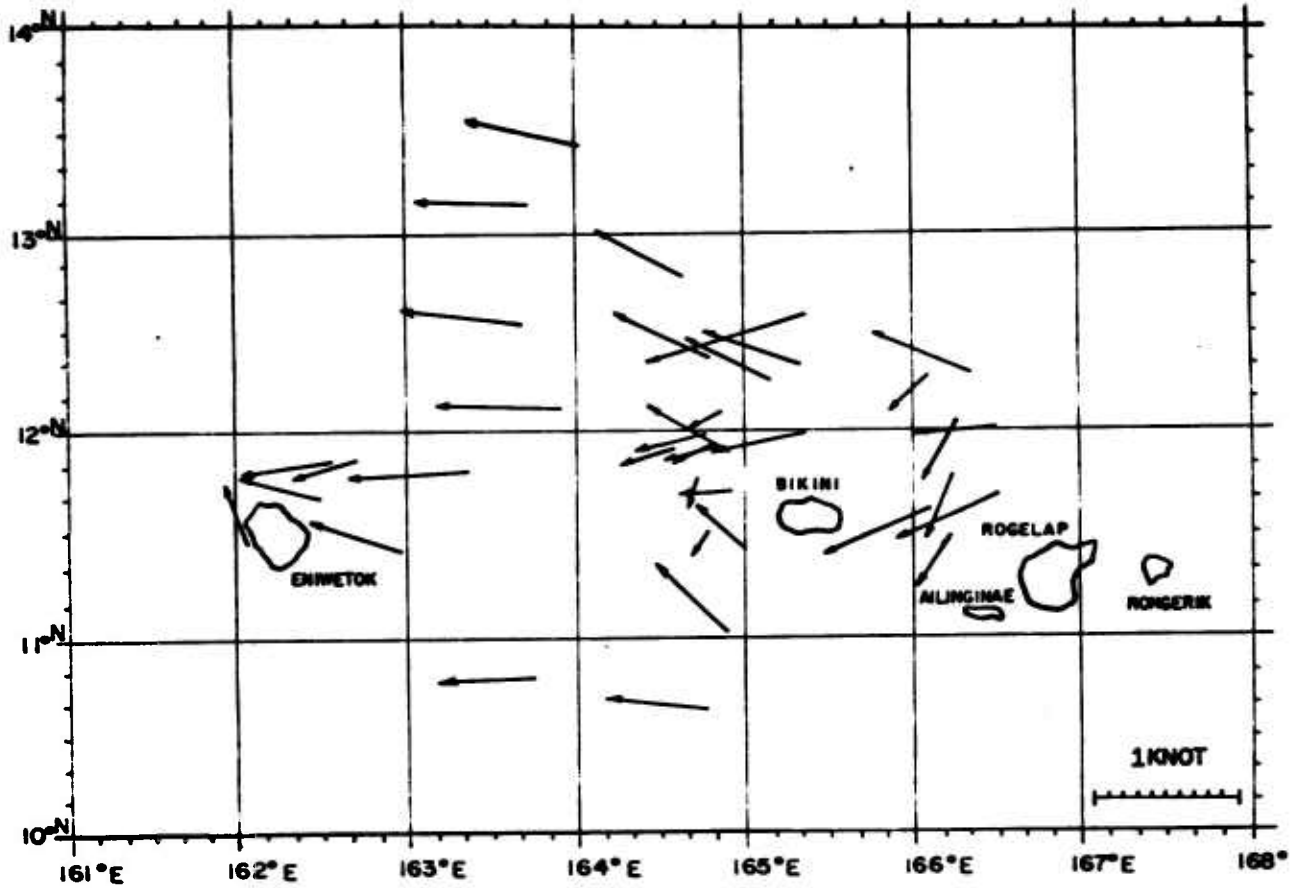

Figure 3.10 Ocean current buoy drift data, October–November 1952 and February–April 1954.

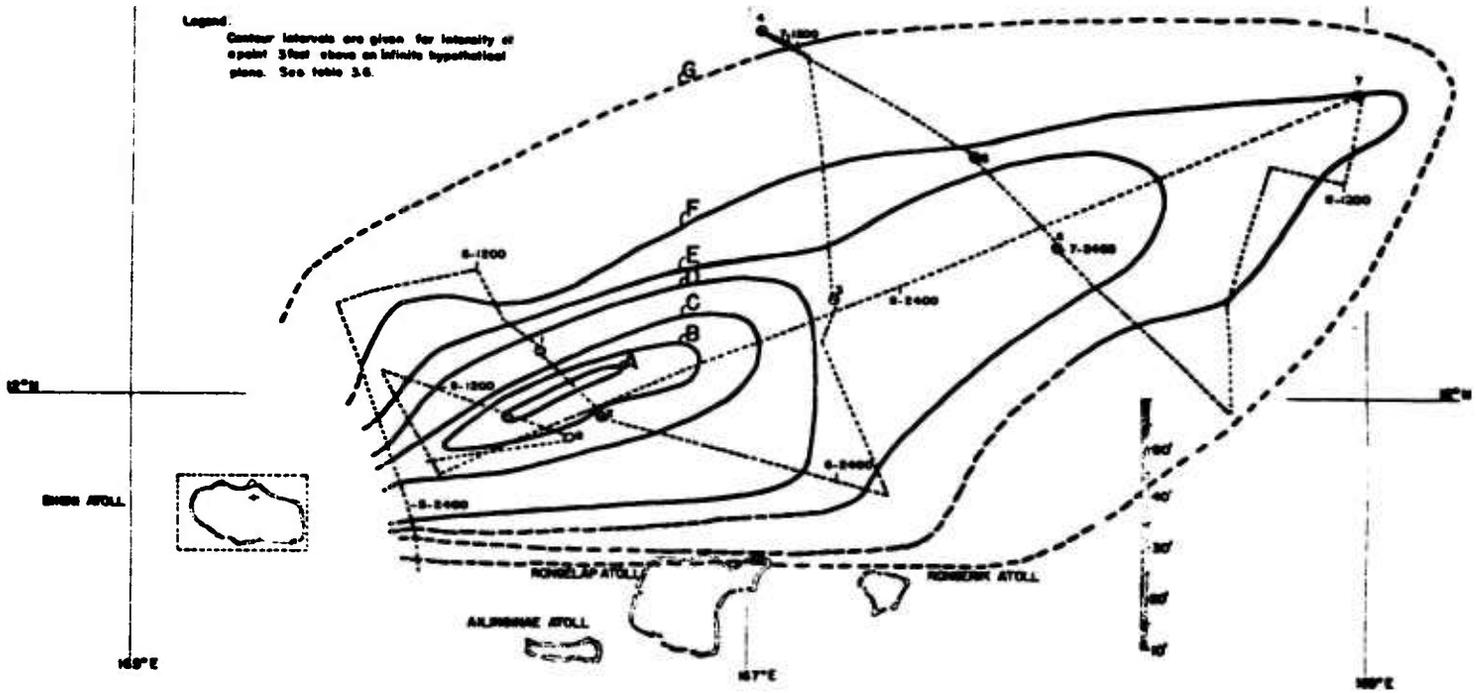

Figure 3.11 Iso-intensity contours for Shot 5.

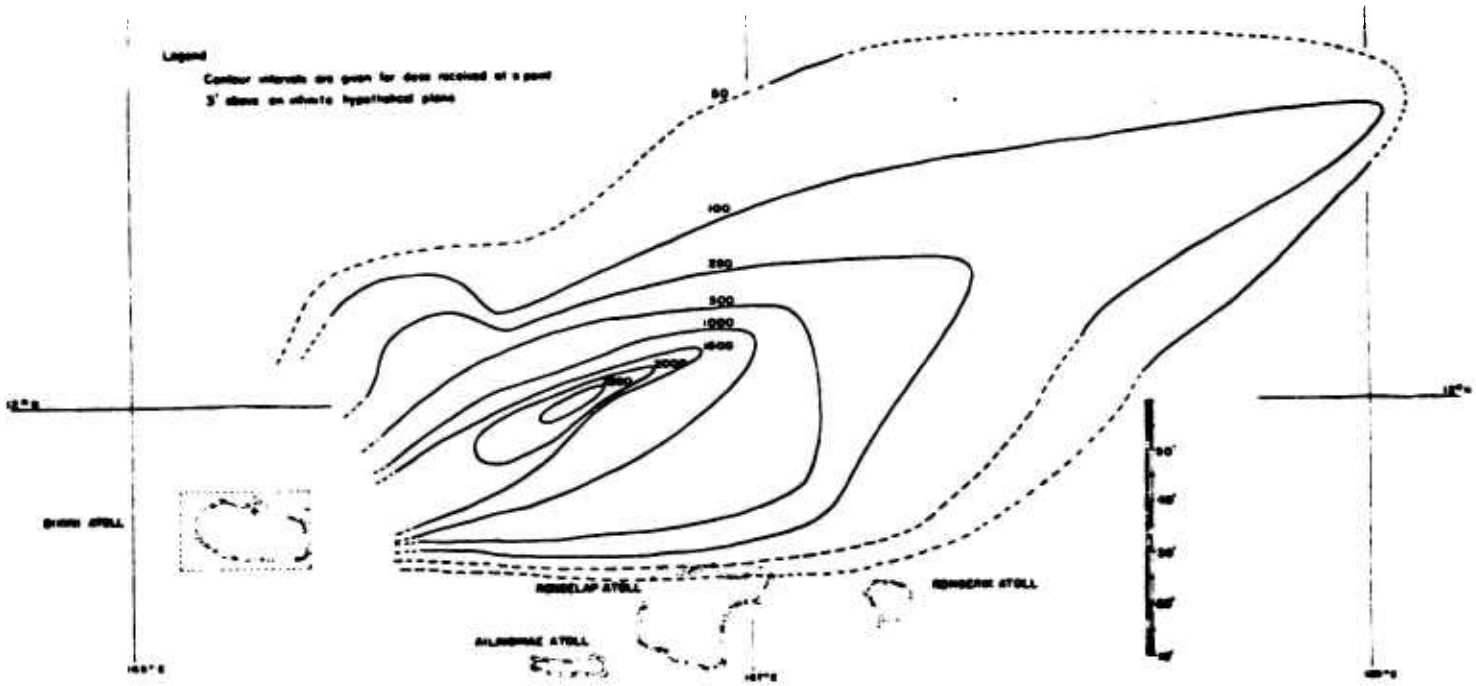

Figure 3.12 Total dose from time of fallout to H + 50 hours in roentgens, Shot 5.

Table 3.6 Iso-dose Rate Contours at 3 Foot Elevation

Contour No.	Area (Sq. Miles)	Dose Rate (R/HR) At H + 12 Hrs.	At H + 1 hr. = 22.7 x H + 12
A	45	80	1820
B	450	60	1360
C	1,190	40	910
D	3,070	20	450
E	6,320	10	230
F	10,000	5	115
G	17,850	1	25

Table 3.7 Total Dose from Fallout Arrival Until H + 50 Hours

Contour No.	Area (Sq. Miles)	Total Dose in R (Shown in Figure Itself)
Innermost	32	2500
-	210	2000
-	610	1500
-	1,400	1000
-	3,000	500
-	4,900	250
-	9,350	100
Outermost	14,350	50

estimates of dose rates at all times, so that the intensities for each area at H + 1 hour also are listed in Table 3.6.

3.4.9 Plotting Fallout Contours of Total Dose. Additional considerations enter into the construction of a contour map relating to total dosage. Time of arrival enters in a different manner. Exposure period covers only the period after the time of arrival to the arbitrary time of H + 50 hours.

This exposure period numerically is the difference between 50 hours and the arrival time listed in Column 10 of Table 3.5.

Now, for calculation of total exposure dose it is necessary to sum the intensities for all hours between fallout arrival and 50 hours. For convenience in this task, Figure 3.7 has been drafted so as to indicate accumulated dose when the dose rate at 1 hour is 1 roentgen per hour. This figure together with Columns 9 and 10 of Table 3.5 provides what is needed for computing total dosages along the dry-land track.

These dosage numbers were distributed along the track and connected as contours shown in Figure 3.12. Table 3.7 summarizes the total dose accumulated inside the contours.

Chapter 4

ANALYSIS OF CONTAMINATED SEA WATER[1]

In the previous chapter fallout dose and dose-rate contours for Shot 5 were calculated from direct measurements of gamma activity in the sea. In this chapter dose rates are calculated for a limited number of points at which samples of contaminated sea water were collected and analyzed.

Generally, the data used here are independent of those in Chapter 3, and comparison of results from the two sets of data provide a valuable basis for judging their reliability. In addition, a considerable number of samples of surface sea water collected following Shot 6 have been analyzed and dose rates calculated. Contours were drawn, and the fractions of the weapons appearing in fallout were estimated for Shots 5 and 6. Due in large part to the extremely short time in which this project was planned, executed, and samples analyzed, sufficient supporting data were not obtained to permit accurate calculations to be made. Nevertheless, a comprehensive treatment of the data has been given in order to enable the reader to judge the limitations of the data as well as to outline for future planning the manner in which more accurate results may be obtained.

As in Chapter 3, dose rate is calculated as though all the fallout had fallen upon a fixed plane at mean sea level and remained undisturbed thereon. The fallout was, in fact, both mixed with the sea water to a variable depth and transported by current action to the location at which it was sampled. For each point in the contaminated plane for which data were obtained the dose rate was calculated for 3 feet above the plane by the method of Gates and Eisenhauer (Reference 1). This method considers a source uniformly distributed upon an infinite plane. Although the actual source is not uniformly distributed, it was

[1] After Chapter 4 was completed some additional data became available which relate to the computation of gamma dose rate and fraction of device in local fallout. Revised values of the latter have been reported (Reference 12).

assumed to be so in the calculation. The total dose rate d at a height 3 feet above a uniformly contaminated infinite plane is given by:

$$d = \sum_{i=1}^{i=m} n_i d_i \tag{4.1}$$

Where: d_i = dose rate in Mev $min^{-1}cm^{-3}$ at height, x above an infinite plane emitting photons of initial energy, E_i isotropically at the rate of 1 photon $min^{-1}cm^{-2}$.

n_i = number of photons $min^{-1}cm^{-2}$ of initial energy, E_i.

The dose rate, d_i is defined by:

$$d_i = \frac{E_i\, h(E_i)}{2} \int_{t_i}^{\infty} \frac{e^{-s}}{s}\, ds\, B_i(t_i) \tag{4.2}$$

Where: E_i = initial photon energy.

$h(E_i)$ = "true" linear absorption coefficient for air or fractional energy loss per unit path length.

$t_i = \mu_i x$

x = 3 feet

μ_i = total linear absorption coefficient for photons of energy E_i.

$B_i(t_i) = \frac{1}{1 - y_i}$ = buildup factor or ratio of dose from all photons to that from unscattered photons.

y_i = fraction of dose from source energy E_i, delivered by scattered photons; y_i is obtained from Curve A, Figure 20, Reference 1.

The value of the exponential integral may be found in prepared mathematical tables (let $s = t_i$). Values of μ_i and $h(E_i)$ are compiled in Reference 1. E_i was taken as the mean energy of the i th finite energy interval in the experimentally determined spectrum (Reference 2). The actual calculations were carried out as described below.

Let R = gamma energy emission rate per unit area of the plane source in units of Mev $min^{-1}cm^{-2}$.

A = gamma activity per unit area of the plane source in units of counts $min^{-1}cm^{-2}$.

I = gamma activity per unit area of the plane source measured in a gamma ionization detector whose response at various energies is known in arbitrary units of mv cm^{-2}.

d_r = dose rate at 3 feet from a reference source for which R = 1 Mev $min^{-1}cm^{-2}$.

Dose rate, d_r is calculated from Equations 4.1 and 4.2. For any point at which the gamma energy emission rate is R:

$$d = d_r R \tag{4.3}$$

Since R cannot be calculated directly from the experimental data, d was obtained as follows:

$$d = d_r \left(\frac{R}{I}\right)\left(\frac{I}{A}\right) A \tag{4.4}$$

Values for R/I were obtained from values of R and I calculated for an arbitrary number of gamma photons. The experimentally determined gamma spectra for Shots 5 and 6 and known response of the ionization detector to various gamma photon energies were used. I/A was determined experimentally with actual water samples[2]. A was calculated from the measured activity of water samples.

Values of d thus obtained were plotted for the geographical coordinates at which fallout was received and dose rate contours were drawn.[3] Further details of the calculations are given in the following sections and illustrative calculations are provided.

4.1 SAMPLE ANALYSIS

The gamma activity of all sea water samples received was determined in general by counting 15-ml aliquots in a gamma scintillation counter (UDR–9) through approximately 1600 mg Al cm^{-2}. The UDR–9 counter was equipped with a 1½ inch by ½ inch NaI crystal detector. The overall efficiency of the instrument was estimated to be 5 to 8 percent for the sample geometry used. In some cases samples of low activity from Shot 6 were counted in a NaI crystal well counter. By counting samples in both instruments the ratio of counts in the crystal well to those from the UDR–9 was found to be ~ 12. All counting data were converted to UDR–9 counts and expressed as counts per minute at H + 218 hours for Shot 5 and H + 171 hours for Shot 6. The results are shown in Tables 4.1 and 4.2.

In the case of Shot 5 samples, decay corrections from time of counting to H + 218 hours were made by use of an experimentally determined decay curve. Shot 6 samples were received and analyzed in two separate shipments. Unfortunately from the time of analysis of the first group of samples to the time of analysis of the second group 12 or 13 days later, no decay data were recorded. It was necessary, therefore, to use a calculated decay curve based upon disintegrations per minute from a mixture of fission product and induced activities shown in Figure 4.1. The relative amounts of fission product and induced activities were consistent with the capture to fission ratio deter-

---

[2] Use was made of the gamma ionization detector since its response per gamma photon was better known as a function of photon energy than was the response of the gamma counters used. In principle, a similar calibration of the gamma counter would have permitted its use and obviated use of the gamma ionization instrument.

[3] If the fallout had been received by an actual land surface the dose rates would be decreased by the "roughness factor", and probably slightly increased by scattering from beneath the source. Neither correction has been applied. See also Section 4.7, Footnote[8].

TABLE 4.1 RADIOACTIVITY IN WATER SAMPLES FROM SHOT 6

Sampling Position	Date-Time Sampled Eniwetok or Mike	Depth*	Polyethylene Snap Sampler Data			Nansen Sampler Data			
			Volume	Date-Time Counted	Corrected Counts for 15-ml aliquot†	Volume	Date-Time Counted	Corrected Counts for 15-ml aliquot†	C‡
		meters	ml	PDT	c/m	ml	PDT	c/m	c/m/ml
11° 12' N	5/5 1630	0	3540	15 0951	Background	—	—	—	0
166° 01.5' E		47	3580	15 0959	Background	385	15 1204	Background	
		94	—	—	—	385	15 1206	Background	
		141	—	—	—	385	15 1212	Background	
		235	—	—	—	385	15 1158	Background	
		470	—	—	—	385	15 1201	Background	
		752	—	—	—	385	15 1215	Background	
12° 10' N	5/6 1436	0	4300	14 0954	4250	135	15 1431	11,800	510
166° 06' E		22	3900	15 0939	5840	188	15 1426	7,860	
(Station 1)		42	3790	15 1003	5650	118	15 1548	10,450	
		73	4300	14 1000	490	300	15 1428	7,100	
		110	—	—	—	125	15 1550	10,650	
12° 05' N	1638	0	2315	14 1120	9400	—	—	—	630
166° 08.5' E									
12° 00' N	1737	0	3550	14 1122	8630	—	—	—	575
166° 13' E									
11° 55.3' N	1840	0	4300	14 0957	4330	355	15 1420	3,230	220
166° 16.6' E		22	4300	14 1322	4220	8	20 1105	2,230	
(Station 2)		44	4300	14 1315	3660	8	20 1047	1,920	
		87	4300	14 1318	220	8	20 0949	195	
		152	4300	14 0950	300	8	20 1024	37	
		434	—	—	—	8	20 1022	Background	
11° 51' N	5/7 0130	0	4300	14 1321	82	—	—	—	5
167° 04.2' E									
12° 19.4' N	0500	0	—	—	—	355	15 1422	2,040	100
166° 57.2' E		24	4300	13 1251	1900	8	20 0946	985	
(Station 3)		44	4220	13 1503	1960	8	20 1000	900	
		80	4300	13 1305	1600	8	20 1007	1,000	
		115	4300	13 1246	125	8	20 1011	40	
13° 12' N	1300	0	2650	13 1346	53	385	15 1149	30	10
166° 40' E		22	4300	14 0924	670	8	20 0953	110	
(Station 4)		37	4300	14 1106	70	8	20 0956	128	
		52	4300	14 0940	215	8	20 0942	128	
		75	4300	13 1307	30	8	20 1106	32	
13° 00.3' N	1607	0	3950	14 1110	300	—	—	—	20
167° 00.5 E									
12° 48' N	1840	0	2315	14 1117	290	385	15 1152	300	24
167° 20' E		24	4300	14 0935	610	8	20 1030	294	
(Station 5)		43	4300	14 1005	370	8	20 1026	369	
		70	4300	14 0930	915	8	20 1017	168	
		101	4300	14 0935	215	8	20 1110	136	
12° 30' N	2225	0	3645	14 1114	520	385	15 1155	392	32
167° 35' E		19	4300	14 1325	860	385	15 1119	408	
(Station 6)		33	4300	14 1350	530	385	15 1115	408	
		52	4300	14 1100	460	385	15 1140	332	
		87	4300	14 0938	450	385	15 1052	300	
		328	—	—	—	385	15 1143	30	

TABLE 4.1 CONTINUED

Sampling Position	Date-Time Sampled Eniwetok or Mike	Depth*	Polyethylene Snap Sampler Data			Nansen Sampler Data			
			Volume	Date-Time Counted	Corrected Counts for 15-ml aliquot †	Volume	Date-Time Counted	Corrected Counts for 15-ml aliquot†	C‡
		meters	ml	PDT	c/m	ml	PDT	c/m	c/m/ml
12° 03.5' N 166° 00.5' E	5/8 0410	0	4300	14 1346	25	—	—	—	2
12° 32' N 166° 06' E	0805	0	4065	15 0942	1690	—	—	—	110
12° 45' N 166° 10.1' E	0900	0	4145	15 0948	560	—	—	—	37
12° 45' N 166° 16' E	1000	0	3900	15 0954	1830	—	—	—	120
12° 43.5' N 166° 21' E	1100	0	4200	13 1510	350	—	—	—	23
12° 43' N 166° 25' E	1200	0	3760	13 1522	150	—	—	—	10
12° 56' N 166° 27.5' E	1250	0	3920	13 1517	940	—	—	—	63
12° 56.6' N 166° 26.6' E (Station 7)	1445	0	4300	13 1352	580	385	15 1107	565	31
		21	4300	14 0946	680	385	15 1112	465	
		30	4230	13 1525	490	385	15 1146	570	
		50	4300	13 1454	640	385	15 1137	355	
		100	4300	13 1343	50	385	15 1123	23	
		347	—	—	—	385	15 1127	26	
12° 19' N 166° 30.5' E	5/9 0200	0	4300	13 1351	4700	—	—	—	310
12° 06' N 166° 10.5' E	0400	0	3520	13 1520	1100	—	—	—	73
12° 02.5' N 165° 44' E	0600	0	4300	14 1353	5480	—	—	—	360
12° 01' N 166° 16' E	1310	0	4300	13 1400	760	—	—	—	51
11° 52' N 165° 34' E (Station 8)	1525	0	4300	13 1244	4400	355	15 1417	4,910	290
		21	4300	14 1329	5550	1	20 1049	3,260	
		30	4300	13 1402	8400	1	20 1055	4,300	
		63	4300	13 1459	890	1	20 1104	3,270	
		110 reduced to	860	13 1341	170	1	20 1050	515	
		353	—	—	—	1	20 1101	43	

* Corrected for wire angle. Correction derived by SIO from analysis of oceanographic situation at time of sampling.

† Corrections have been made for dilution where applicable, and for decay during the time of analysis; counts are given as of 1200 PST 5/13/54 (H + 218 hr). Radioactivity of samples measured with gamma scintillation counter.

‡ Average of values for all water samples collected above apparent lower boundary of radioactivity in sea water. See Figure 4.2.

§ Data missing.

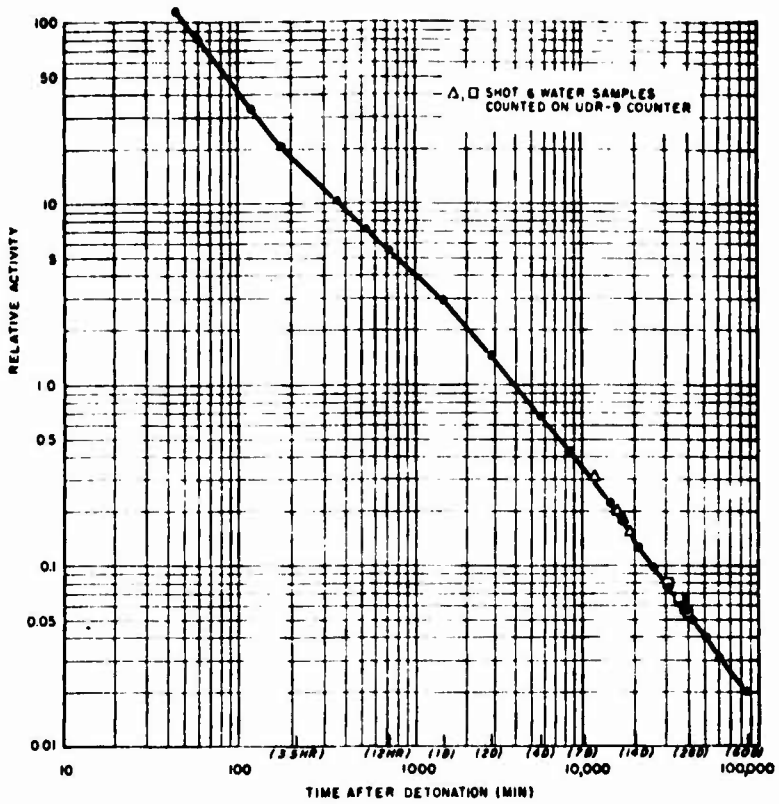

Figure 4.1 Calculated decay (d/m) for Shot 6 fallout.

mined for Shot 6. The method of calculation is described elsewhere (Reference 3).

Two experimentally determined decay curves covering short time periods fitted this calculated curve well.

4.2 CALCULATION OF A–GAMMA ACTIVITY RECEIVED PER UNIT AREA OF THE OCEAN SURFACE

A is determined as follows:

Let C = gamma counts min^{-1}.

Z = depth in cm to which the fallout has become mixed.

If C is assumed to be constant with depth, or at least represents an average value then:

$$A = CZ \tag{4.5}$$

No measurements of Z were made for Shot 6. Since it is probable the fallout had not penetrated to the thermocline at the time most of the surface samples were taken, an estimate of Z was based upon the following:

1. A mixing function estimated from Shot 5 data (Figure 4.2) which provides Z as a function of time of mixing t_m.

2. An estimated time of arrival t_a of fallout as a function of distance, l from surface zero based upon calculated small particle trajectories (Reference 4). and meteorological data (Figure 4.3).

TABLE 4.2 RADIOACTIVITY IN SURFACE-WATER SAMPLES FROM SHOT 6

Sampler Number *	Sampling Position		Date-Time Sampled Eniwetok or Mike	Date-Time Counted	Corrected Counts †	C at each Position
	Latitude	Longitude				
	north	east	5/15		c/m/ml	c/m/ml
1‡	12° 04'	162° 18'	1333	—	—	
2	12° 04'	162° 18'	1333	6/2 1300	47	47
3‡	12° 03.6'	162° 13.6'	1406	—	—	
4	12° 03.6'	162° 13.6'	1406	6/2 1300	68	68
5‡	12° 08.1'	162° 16.2'	1430	—	—	
6	12° 08.1'	162° 16.2'	1430	6/2 1300	74	74
7‡	12° 11.6'	162° 18.9'	1455	—	—	
8	12° 11.6'	162° 18.9'	1455	6/2 1300	background	0
9‡	12° 14.6'	162° 15.0'	1520	—	—	
10	12° 14.6'	162° 15.0'	1520	6/2 1300	70	70
11‡	12° 20.2'	162° 15.8'	1558	—	—	
12	12° 20.2'	162° 15.8'	1558	6/2 1300	174	174
13‡	12° 20.6'	162° 16.3'	1602	—	—	
14	12° 21.2'	162° 18.2'	1740	6/2 1300	124	124
15‡	12° 24.0'	162° 15.9'	1808	—	—	
16	12° 24.0'	162° 15.9'	1808	6/2 1300	90	90
17‡	12° 25.4'	162° 15.8'	1814	—	—	
18	12° 25.4'	162° 15.8'	1814	6/2 1300	91	91
19‡	12° 26.0'	162° 15.9'	1819	—	—	
20	12° 26.0'	162° 15.9'	1819	6/2 1300	104	104
21‡	12° 28.8'	162° 15.2'	1835	—	—	
22	12° 28.8'	162° 15.2'	1835	6/2 1300	93	93
23‡	12° 29.7'	162° 15.3'	1840	—	—	
24	12° 29.7'	162° 15.3'	1840	6/2 1300	193	193
25	12° 33.5'	162° 15.0'	1900	6/2 1300	571	300
26	12° 33.5'	162° 15.0'	1900	5/20 1400	159	
				6/2 1400	173	
27‡	12° 38.7'	162° 14.9'	1925	—	—	
28	12° 38.7'	162° 14.9'	1925	5/20 1400	131	96
				6/2 1300	60	
29	12° 45.7'	162° 14.8'	1950	5/20 1400	100	78
30	12° 45.7'	162° 14.8'	1950	5/20 1400	84	
				6/2 1300	51	
31‡	12° 51.0'	162° 14.2'	2015	—	—	
32	12° 51.0'	162° 14.2'	2015	5/20 1400	67	36
				6/2 1300	6	
33	12° 55.9'	162° 13.8'	2040	5/20 1400	53	44
34	12° 55.9'	162° 13.8'	2040	5/20 1400	45	
				6/2 1300	35	
35	13° 00.0'	162° 14.5'	2105	5/20 1400	11	33
36	13° 00.0'	162° 14.5'	2105	6/2 1300	55	
37	13° 00.0'	162° 19.0'	2130	5/20 1400	7	7.5
38	13° 00.0'	162° 19.0'	2130	6/2 1300	8	
39	13° 00.0'	162° 23.7'	2155	5/20 1400	2.5	3.0
40	13° 00.0'	162° 23.7'	2155	5/20 1400	4	
				6/2 1300	2.5	
41‡	13° 00.0'	162° 28.2'	2220	—	—	
42	13° 00.0'	162° 28.2'	2220	6/2 1300	2.6	2.5
43	12° 56.9'	162° 30.0'	2245	5/20 1400	3.5	2
44	12° 56.9'	162° 30.0'	2245	5/20 1400	2.8	
				6/2 1300	background	
45‡	12° 51.5'	162° 29.9'	2310	—	—	
46	12° 51.5'	162° 29.9'	2310	6/2 1300	1.1	1
47‡	12° 46.5'	162° 29.9'	2335	—	—	
48	12° 46.5'	162° 29.9'	2335	6/2 1300	2	2
49	12° 41.1	162° 29.8'	2400	5/20 1400	35	31
50	12° 41.1'	162° 29.8'	2400	5/20 1400	26	

TABLE 4.2 CONTINUED

Sampler Number *	Sampling Position Latitude	Sampling Position Longitude	Date-Time Sampled Eniwetok or Mike	Date-Time Counted	Corrected Counts †	C at each Position
	north	east	5/16		c/m/ml	c/m/ml
51	12° 35.8'	162° 29.8'	0025	5/20 1400	183	250
52	12° 35.8'	162° 29.8'	0025	5/20 1400	316	
53‡	12° 30.4'	162° 29.7'	0050	—	—	
54	12° 30.4'	162° 29.7'	0050	5/20 1400	217	217
55	12° 25.5'	162° 29.9'	0115	5/20 1400	194	180
56	12° 25.5'	162° 29.9'	0115	5/20 1400	164	
57	12° 20.4'	162° 29.6'	0140	5/20 1400	98	98
58‡	12° 20.4'	162° 29.6'	0140	—	—	
59	12° 15.0'	162° 29.3'	0205	5/20 1400	44	44
60	12° 15.0'	162° 29.3'	0205	5/20 1400	43	
61	12° 10.0'	162° 29.2'	0230	5/20 1400	23	24
62	12° 10.0'	162° 29.2'	0230	5/20 1400	26	
63	12° 04.9'	162° 29.2'	0255	5/20 1400	26	26
64‡	12° 04.9'	162° 29.2'	0255	—	—	
65‡	12° 00.0'	162° 29.0'	0320	—	—	
66	12° 00.0'	162° 29.0'	0320	5/20 1400	7	7
67	11° 54.6'	162° 28.9'	0345	5/20 1400	0.7	1.5
68	11° 54.6'	162° 28.9'	0345	5/20 1400	2.4	
69	11° 49.2'	162° 28.8'	0410	5/20 1400	1	0.5
70	11° 49.2'	162° 28.8'	0410	5/20 1400	background	
71	11° 44.1'	162° 28.7'	0435	5/20 1400	2.4	1.5
72	11° 44.1'	162° 28.7'	0435	5/20 1400	0.7	
			5/15			
1	13° 26.5'	161° 49.2'	1725	5/20 1400	1.1	1
2	13° 30.5'	161° 46.3'	1800	6/2 1300	1.1	
3‡	13° 30.5'	161° 46.3'	1800	—	—	
4	12° 35.2'	161° 47.6'	1830	6/2 1300	0.7	0.7
5‡	12° 35.2'	161° 47.6'	1830	—	—	
6	13° 40.2'	161° 48.8'	1900	6/2 1300	11	11
7‡	13° 40.2'	161° 48.8'	1900	—	—	
8	13° 45.5'	161° 49.7'	1930	5/20 1400	0.3	1
				6/2 1300	2	
9‡	13° 45.5'	161° 49.7'	1930	—	—	
10	13° 51'	161° 49.7'	2000	6/2 1300	1.0	1
11‡	13° 51'	161° 49.7'	2000	—	—	
12	13° 56'	161° 49.7'	2030	6/2 1300	1.2	1
13‡	13° 56'	161° 49.7'	2030	—	—	
14	13° 58.5'	161° 50.8'	2100	6/2 1300	1.0	1
15‡	13° 58.5'	161° 50.8'	2100	—	—	
16	14° 00.0'	161° 54.7'	2130	6/2 1300	background	1.5
17	14° 00.0'	161° 54.7'	2130	5/20 1400	2.6	
18	14° 01'	162° 00.0'	2200	5/20 1400	2.7	2
				6/2 1300	3.1	
19	14° 01'	162° 00.0'	2200	5/20 1400	0.5	
20	13° 26'	162° 03.0'	2230	5/20 1400	0.4	1.7
				6/2 1300	2.0	
21	13° 26'	162° 03.0'	2230	5/20 1400	2.7	
22	13° 51.7'	162° 06.0'	2300	5/20 1400	2.9	3.0
				6/2 1300	3.2	
23‡	13° 51.7'	162° 06.0'	2300	—	—	
24	13° 47.3'	162° 08.6'	2330	6/2 1300	2.4	2.4
25‡	13° 47.3'	162° 08.6'	2330	—	—	
26	13° 42.7'	162° 11.6'	2400	6/2 1300	5.5	5.5
27‡	13° 42.7'	162° 11.6'	2400	—	—	

TABLE 4.2 CONTINUED

Sampler Number *	Sampling Position Latitude	Sampling Position Longitude	Date-Time Sampled Eniwetok or Mike	Date Time Counted	Corrected Counts †	C at each Position
	north	east	5/16		c/m/ml	c/m/ml
28	13° 38'	162° 14.7'	0030	6/2 1300	1.6	1.6
29‡	13° 38'	162° 14.7'	0030	—	—	
30	13° 33.2'	162° 17.6'	0100	6/2 1300	background	0
31‡	13° 33.2'	162° 17.6'	0100	—	—	
32	13° 29'	162° 20.5'	0130	6/2 1300	3.5	3.5
33‡	13° 29'	162° 20.5'	0130	—	—	
34	13° 24.2'	162° 23.2'	0200	6/2 1300	0.6	0.6
35‡	13° 24.2'	162° 23.2'	0200	—	—	
36	13° 20'	162° 26.2'	0230	6/2 1300	2.2	2.2
37‡	13° 20'	162° 26.2'	0230	—	—	
38	13° 15.2'	162° 29'	0300	6/2 1300	background	0
39‡	13° 15.2'	162° 29'	0300	—	—	
40	13° 11'	162° 32'	0330	6/2 1300	background	0
41‡	13° 11'	162° 32'	0330	—	—	
42	13° 06.3'	162° 34.3'	0400	6/2 1300	0.7	0.7
43‡	13° 06.3'	162° 34.3'	0400	—	—	
44	13° 01.8'	162° 33'	0430	6/2 1300	2.6	2.6
45‡	13° 01.8'	162° 33'	0430	—	—	
46	12° 56.8'	162° 31.6'	0500	6/2 1300	10.5	10.5
47‡	12° 56.8'	162° 31.6'	0500	—	—	
48	12° 52'	162° 30'	0530	6/2 1300	12	12

* Samples numbered consecutively 1 through 72 were collected by the USS Molala, those numbered 1 through 48 collected by the USS Sioux.

† Corrected for decay during period of analysis, all counts referred to 1300 PST 5/20/54 (H + 171 hr). Radioactivity of samples was measured with crystal well gamma scintillation counter or with 1 1/2 inch by 1/2 inch crystal gamma scintillation counter (UDR-9), all counts referred to UDR-9. See text for conversion factor

‡ Not received at NRDL for analysis

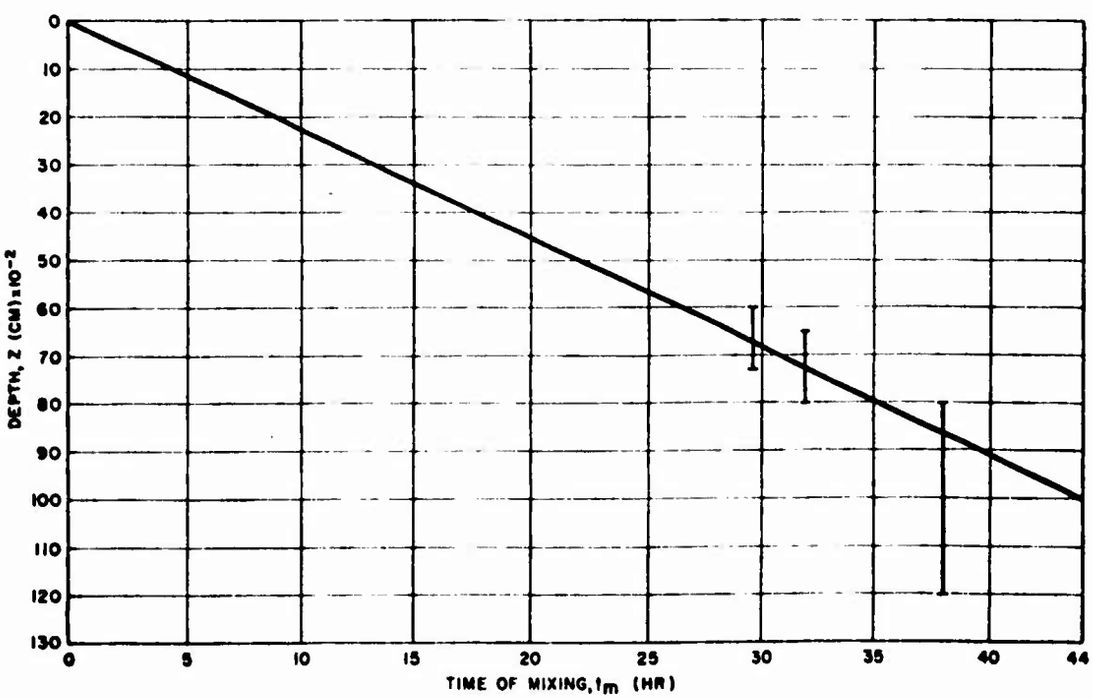

Figure 4.2 Depth of penetration of Shot 5 fallout in ocean water.

3. An approximate set and drift of the contaminated sea water east to west at 0.5 knots. If t_s is the time of sampling then:

$$t_m = t_s - t_a \tag{4.6}$$

The distance l is not the distance from surface zero to the point at which water samples were collected but rather to the geographical coordinate at which the sampled water received the fallout. It may be determined by successive approximations in the manner shown in the illustrative calculation. At t_s = 0 + 32.5 hours water samples were taken following Shot 5 at 12° 10' N 166° 06' E. Let the distance from this point to surface zero be the first approximation l. $l \simeq l_1$ = 53 miles. From Figure 4.3, t_{a_1} = 0 + 4 hours, and t_{m_1} = 32.5 - 4 = 28.5 hours. The east to west drift correction is approximately

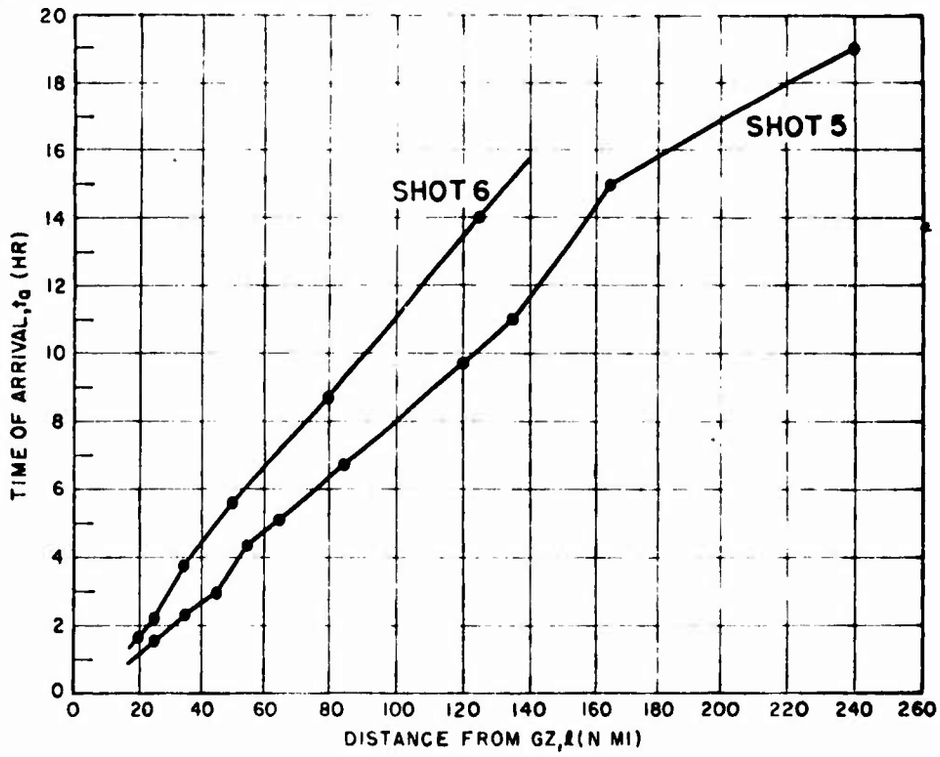

Figure 4.3 Estimated times of arrival of fallout.

$0.5t_{m_1}$ = 0.5 × 28.5 = 14.3 miles. Applying this correction and re-plotting position, it is found that the second approximation of the geographical point of fallout is l_2 = 64 miles from ground zero, and $t_{m_2} = t_s = t_{a_2}$ = 32.5 - 5 = 27.5 hours.

The second approximation of the drift correction is $0.5t_{m_2}$ = 0.5 × 27.5 = 13.8 miles: which is sufficiently close to the first estimate of the drift correction that no further improvement in the value of t_m is realized.

The geographical point of fallout is therefore established as 13.8 miles east of the point of sampling. From Figure 4.2, Z = 62 × 10^2 cm, and

$$A = CZ = 510 \times 62 \times 10^2$$
$$= 31.6 \times 10^5 \text{ counts min}^{-1}\text{cm}^{-2}$$

Values for A for other points are given in Column 3, Table 4.6 and Table 4.7. East to

west drift corrections for each sampling coordinate are given in Column 2. Values of C are taken from Column 10, Table 4.1 and Column 6, Table 4.2.

4.3 CALCULATION OF I/A–RATIO OF GAMMA IONIZATION READINGS TO GAMMA COUNTS

I/A was determined by measuring five water samples from Shot 5. These samples had sufficient activity for precise measurement in the gamma ionization instrument and in the UDR–9 gamma counter. The results are shown in Table 4.3. The ratio I/A = 1.59×10^{-6} mv counts^{-1} min was considered applicable to Shot 6 calculations as well,

TABLE 4.3 RATIO OF GAMMA IONIZATION READINGS, I TO GAMMA COUNTS, A FOR FIVE SURFACE WATER SAMPLES FROM SHOT 5

Sampling Position		$I \times \frac{15}{Z}$	$A \times \frac{15}{Z}$	$\frac{I}{A}$
Latitude	Longitude			
north	east	mv per 15 cm^3 *	c/m per 15 cm^3 †	mv counts^{-1}min
12° 10'	166° 06'	0.0057	4,250	1.34×10^{-6}
11° 55.3'	166° 16.6'	0.0071	4,330	1.64×10^{-6}
12° 05'	166° 08.5'	0.0139	9,400	1.48×10^{-6}
12° 00'	166° 13'	0.0151	8,630	1.75×10^{-6}
12° 02.5'	165° 44'	0.0095	5,480	1.73×10^{-6}
			Mean	1.59×10^{-6}

* Measured on 5/14; corrected to 1200 PST 5/13.
† Data taken from Column 6, Table 4.1.

due to the similarity in the Shot 5 and Shot 6 sample spectra at the times of analysis. The ionization measurements made in a 4-pi goemetry high pressure ionization chamber of the type described by Jones and Overman (Reference 5). The response of the instrument was calibrated[4] with standards whose photon energy and photon emission rate were known. The response-versus-energy curve for 2.22×10^6 photons min^{-1} is shown in Figure 4.4.

4.4 CALCULATION OF R/I–RATIO OF GAMMA ENERGY EMISSION RATE PER UNIT AREA TO GAMMA IONIZATION READING PER UNIT AREA

The reader is referred to Table 4.4 for a summary of the calculation of R/I. The first and second columns give respectively the mean photon energies E_i and fractional abundances:

$$n_i \Big/ \sum_{i=1}^{i=9} n_i$$

for nine energy intervals as determined by Cook (Reference 2) on samples of fallout from Shots 5 and 6. Spectra were used which were determined at the reference time of analysis

[4] Private communication from W. E. Shelberg, USNRDL.

TABLE 4.4 CALCULATION OF R/I RATIO OF GAMMA ENERGY EMISSION RATE PER UNIT AREA TO GAMMA IONIZATION READING PER UNIT AREA *

Shot 5 at D + 8 Days					Shot 6 at D + 7 Days				
E_i	$n_i / \sum_{i=1}^{i=9} n_i$	Gamma Ionization Instrument Response (2.22×10^6 photons min^{-1})	I_i (mv cm^{-2} per $2.22 \times 10^6 \times n_i / \sum_{i=1}^{i=9} n_i$ photons min^{-1})	R_i ($\times 10^{-6}$) (Mev min^{-1} cm^{-2} per $2.22 \times 10^6 \times n_i / \sum_{i=1}^{i=9} n_i$ photons min^{-1})	E_i	$n_i / \sum_{i=1}^{i=9} n_i$	Gamma Ionization Instrument Response (2.22×10^6 photons min^{-1})	I_i (mv cm^{-2} per $2.22 \times 10^6 \times n_i / \sum_{i=1}^{i=9} n_i$ photons min^{-1})	R_i ($\times 10^{-6}$) (Mev min^{-1} cm^{-2} per $2.22 \times 10^6 \times n_i / \sum_{i=1}^{i=9} n_i$ photons min^{-1})
0.05	0.261	0.08	0.0209	0.0290	0.05	0.271	0.08	0.0217	0.0301
0.15	0.245	0.12	0.0294	0.0816	0.15	0.210	0.12	0.0252	0.0700
0.25	0.140	0.16	0.0224	0.0777	0.25	0.170	0.16	0.0272	0.0943
0.35	0.016	0.21	0.0034	0.0124	0.35	0.026	0.21	0.0055	0.0202
0.45	0.095	0.25	0.0237	0.0950	0.45	0.069	0.25	0.0172	0.0690
0.65	0.087	0.34	0.0296	0.1254	0.65	0.096	0.34	0.0326	0.139
0.75	0.097	0.38	0.0368	0.1614	0.75	0.094	0.38	0.0357	0.157
0.85	0.0135	0.42	0.0057	0.0255	0.85	0.029	0.42	0.0122	0.0547
1.55	0.0455	0.70	0.0318	0.1565	1.55	0.035	0.70	0.0245	0.120
			I = 0.2037	R = 0.7645				I = 0.2018	R = 0.7543

$$\frac{R}{I} = \frac{0.7645}{0.2037} \times 10^6 = 3.75 \times 10^6 \text{ Mev min}^{-1} \text{ mv}^{-1}$$

$$\frac{R}{I} = \frac{0.7543}{0.2018} \times 10^6 = 3.74 \times 10^6 \text{ Mev min}^{-1} \text{ mv}^{-1}$$

* See Section 4.4 for explanation of Table

TABLE 4.5 CALCULATION OF REFERENCE DOSE RATE, d_r AT HEIGHT X = 3 FEET ABOVE AN INFINITELY CONTAMINATED PLANE HAVING A GAMMA ENERGY EMISSION RATE, R = 1 Mev $min^{-1} cm^{-2}$

Shot 5 at D + 8 Days					Shot 6 at D + 7 Days			
E_i	$n_i / \sum_{i=1}^{i=9} n_i$	n_i	$B_i(t_i)$	$n_i d_i \times 10^6$	E_i	$n_i / \sum_{i=1}^{i=9} n_i$	n_i	$n_i d_i \times 10^6$
0.05	0.261	0.760	≈ 2.5	≈ 7	0.05	0.271	0.796	≈ 7.3
0.15	0.245	0.713	~ 1.8	~10.5	0.15	0.21	0.617	~ 9.1
0.25	0.140	0.407	1.55	10.0	0.25	0.17	0.50	12.4
0.35	0.016	0.047	1.45	1.6	0.35	0.026	0.076	2.69
0.45	0.095	0.276	1.40	12.4	0.45	0.069	0.203	9.14
0.65	0.087	0.253	1.33	16.2	0.65	0.096	0.282	18.1
0.75	0.097	0.282	1.31	20.6	0.75	0.094	0.276	20.2
0.85	0.0135	0.039	1.29	3.1	0.85	0.029	0.085	6.96
1.55	0.0455	0.132	1.20	17.3	1.55	0.035	0.103	13.5
		n = 2.91		$d_r = 98.7 \times 10^{-6}$			n = 2.94	$d_r = 99.5 \times 10^{-6}$

TABLE 4.6 DOSE RATE AT H + 12 HR CALCULATED FROM WATER SAMPLES FROM SHOT 5

Sampling Position		Correction for East-to-West Drift	$Z \times 10^{-2}$	$A \times 10^{-5}$ at H + 218 hr*	d at H + 12 hr
Latitude	Longitude				
north	east	NM	cm	c/m per cm^{-2}	r/hr
12° 10'	166° 06' (Sta. 1)	14	62	32	49
12° 05'	166° 08.5'	15	66	42	64
12° 00'	166° 13'	15	68	40	61
11° 55.3'	166° 16.6' (Sta. 2)	16	71	15.5	24
11° 51'	167° 04.2'	17	77	0.385	0.6
12° 19.4'	166° 57.2' (Sta 3)	19	84	8.4	13
13° 12'	166° 40' (Sta. 4)	22	99	0.99	1.5
13° 00.3'	167° 00.5'	23	100	2.0	3.1
12° 48'	167° 20' (Sta. 5)	23	100	2.4	3.7
12° 30'	167° 35' (Sta. 6)	25	100	3.2	4.9
12° 03.5'	168° 00.5'	27	100	0.20	0.3
12° 32'	168° 08'	28	100	11	17
12° 45'	168° 10.1'	29	100	3.7	5.7
12° 45'	168° 16'	29	100	12	18
12° 43.5'	168° 21'	29	100	2.3	3.5
12° 43'	168° 25'	30	100	1.0	1.5
12° 58'	168° 27.5'	31	100	6.3	9.6
12° 59.6'	168° 26.6' (Sta. 7)	31	100	3.1	4.7
12° 19'	166° 39.5'	41	100	31	47
12° 08'	166° 10.5'	43	100	7.3	11
12° 02.5'	165° 44'	45	100	30	46
12° 01'	165° 16'	50	100	5.1	7.8
11° 52'	165° 34' (Sta. 8)	50	100	29	44

* See Section 4.2 for method of calculation.

TABLE 4.7 DOSE RATE AT H + 12 HR CALCULATED FROM WATER SAMPLES COLLECTED AFTER SHOT 6

Sample Number *	Sampling Position		Correction for East-to-West Drift	$Z \times 10^{-3}$	$A \times 10^{-6}$ at H+ 171 hr	d at H + 12 hr
	Latitude	Longitude				
	north	east	NM	cm	c/m per cm^{-2}	r/hr
2	12° 04'	162° 18'	14	64	3.0	2.7
4	12° 03.6'	162° 13.6'	15	66	4.5	4.0
6	12° 08.1'	162° 16.2'	14	65	4.8	4.2
8	12° 11.6'	162° 18.9'	14	65	0	0
10	12° 14.6'	162° 15.0'	14	66	4.6	4.1
12	12° 20.2'	162° 15.8'	14	65	11.3	10
14	12° 21.2'	162° 18.2'	15	69	8.6	7.6
16	12° 24.0'	162° 15.9'	14	65	5.8	5.1
18	12° 25.4'	162° 15.8'	15	69	6.3	5.6
20	12° 26.0'	162° 15.9'	15	69	7.2	6.4
22	12° 28.8'	162° 15.2'	15	69	6.4	5.7
24	12° 29.7'	162° 15.3'	15	69	13.3	11.8
25, 26	12° 33.5'	162° 15.0'	15	69	20.7	18.8
28	12° 38.7'	162° 14.9'	15	69	6.6	5.8
29, 30	12° 45.7'	162° 14.8'	15	68	5.3	4.7
32	12° 51.0'	162° 14.2'	15	68	2.45	2.2
33, 34	12° 55.9'	162° 13.8'	15	68	3.0	2.7
35, 36	13° 00.0'	162° 14.5'	15	68	2.25	2.0
37, 38	13° 00.0'	162° 19.0'	15	68	0.51	0.45
39, 40	13° 00.0'	162° 23.7'	15	69	0.20	0.18
42	13° 00.0'	162° 28.2'	15	70	0.18	0.16
43, 44	12° 56.9'	162° 30.0'	16	71	0.15	0.13
46	12° 51.5'	162° 29.9'	16	73	0.07	0.06
48	12° 46.5'	162° 29.9'	16.5	75	0.15	0.12
49, 50	12° 41.1'	162° 29.8'	17	77	2.4	2.1
51, 52	12° 35.8'	162° 29.8'	17	79	19.8	17.5
54	12° 30.4'	162° 29.7'	18	81	17.6	15.6
55, 56	12° 25.5'	162° 29.9'	18	83	14.9	13.2
57	12° 20.4'	162° 29.6'	19	85	8.3	7.3
59, 60	12° 15.0'	162° 29.3'	19	86	3.8	3.4
61, 62	12° 10.0'	162° 29.2'	19	88	2.1	1.9
63	12° 04.9'	162° 29.2'	20	90	2.3	2.0
66	12° 00.0'	162° 29.0'	20	91	0.64	0.57
67, 68	11° 54.6'	162° 28.9'	20.5	93	0.14	0.12
69, 70	11° 49.2'	162° 28.8'	21	94	0.05	0.04
71, 72	11° 44.1'	162° 28.7'	21	95	0.14	0.12
Sample Number †						
1	13° 26.5'	161° 49.2'	12	53	0.05	0.04
2	13° 30.5'	161° 46.3'	12	53	0.05	0.04
4	12° 35.2'	161° 47.6'	12	53	0.04	0.03
6	13° 40.2'	161° 48.8'	12	53	0.58	0.51
8	13° 45.5'	161° 49.7'	12	53	0.05	0.04
10	13° 51'	161° 49.7'	11	52	0.05	0.04
12	13° 56'	161° 49.7'	11	52	0.05	0.04
14	13° 58.5'	161° 50.8'	12	52	0.05	0.04
16, 17	14° 00.0'	161° 54.7'	12	53	0.08	0.06
18, 19	14° 01'	162° 00'	12	54	0.11	0.10
20, 21	13° 56'	162° 03'	12	57	0.10	0.09
22	13° 51.7'	162° 06'	13	59	0.18	0.16
24	13° 47.3'	162° 08.6	13	61	0.15	0.12
26	13° 42.7'	162° 11.6'	14	63	0.35	0.31
28	13° 38'	162° 14.7'	14	66	0.11	0.10
30	13° 33.2'	162° 17.6'	15	68	0	0
32	13° 29'	162° 20.5'	15	70	0.25	0.22
34	13° 24.2'	162° 23.2'	16	72	0.04	0.035
36	13° 20'	162° 26.2'	16	74	0.16	0.14
38	13° 15.2'	162° 29'	17	76	0	0
40	13° 11'	162° 32'	17	78	0	0
42	13° 06.3'	162° 34.3'	18	80	0.06	0.05
44	13° 01.8'	162° 33'	18	82	0.21	0.19
46	12° 56.8'	162° 31.6'	18	84	0.88	0.78
48	12° 52'	162° 30'	19	87	1.0	0.9

* These samples were collected by the USS Molala.

† These samples were collected by the USS Sioux.

of the Shot 6 water samples (7 days) and as close to the time of analysis of Shot 5 samples (9 days) as possible.

Column 3 lists the response of the gamma ionization instrument for 2.22×10^6 gamma photons min^{-1} of energy E_i as determined from the curve in Figure 4.4.

In calculating Columns 4 and 5, a source was arbitrarily chosen equivalent to 2.22×10^6 photons min^{-1} cm^{-2} of all energies. Column 4 then gives for each value of E_i

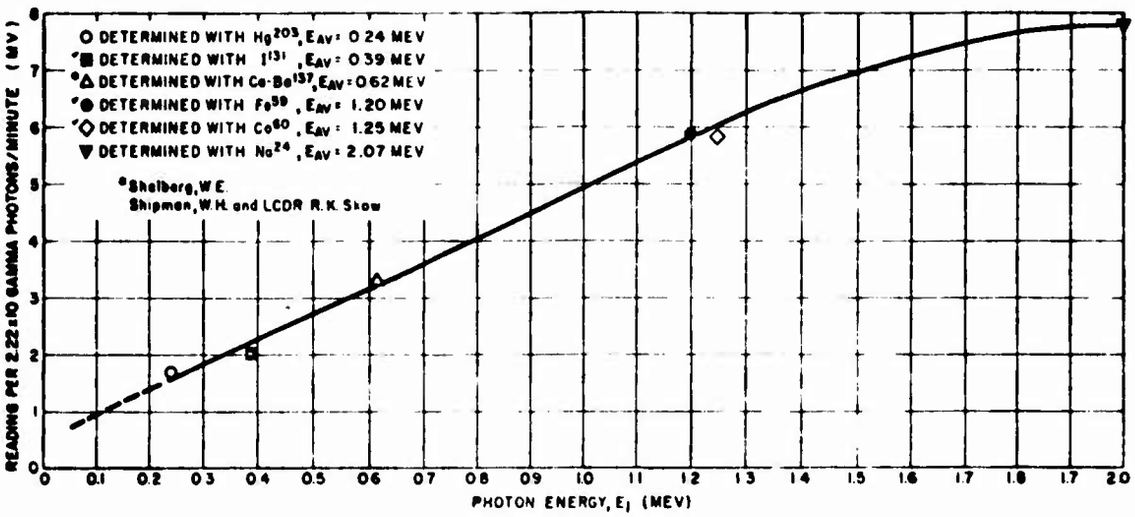

Figure 4.4 Relative response of NRDL ion chamber with incident photon energy (Mev) (after Shelbert).

the calculated gamma ionization instrument response in mv cm^{-2} for 2.22×10^6 gamma photons min^{-1} cm^{-2}. Column 5 gives the corresponding gamma energy rate in Mev min^{-1} cm^{-2} for

$$2.22 \times 10^6 \times n_i / \sum_{i=1}^{i=9}$$

photons of energy E_i in Mev min^{-1} cm^{-2}. The ratio of the Columns 5 and 4 then gives for both Shot 5 and Shot 6:

$$\frac{R}{I} = 3.75 \times 10^6 \text{ Mev min}^{-1}\text{mv}^{-1}.$$

4.5 CALCULATION OF REFERENCE DOSE RATE, d_r

The value of d_r corresponding to a gamma energy emission rate R = 1 Mev min^{-1} cm^{-2}, was calculated from Equations 4.1 and 4.2 and the gamma spectra and

abundances determined by Cook. The calculation is summarized in Table 4.5. [5] The dose rate expressed in Mev min^{-1} cm^{-3} may be converted to dose rate expressed in roentgens hr^{-1} by using the factor, 9.50×10^{-4}. [6]

Therefore:

for Shot 5

$$d_r = 98.7 \times 10^{-6} \text{ Mev min}^{-1} \text{ cm}^{-3}$$
$$= 9.37 \times 10^{-8} \text{ roentgens hr}^{-1}$$

for Shot 6

$$d_r = 99.5 \times 10^{-6} \text{ Mev min}^{-1} \text{ cm}^{-3}$$
$$= 9.45 \times 10^{-8} \text{ roentgens hr}^{-1}$$

4.6 CALCULATION OF DOSE RATE, d

Numerical values for d_r, R/I and I/A substituted into Equation 4.4 give:

$$d = 9.37 \times 10^{-8} \times 3.75 \times 10^{6} \times 1.59 \times 10^{-6} \text{ A roentgens hr}^{-1}$$
$$= 5.58 \times 10^{-7} \text{ A roentgens hr}^{-1} \text{ at H + 218 hr for Shot 5.}$$
$$d = 9.45 \times 10^{-8} \times 3.75 \times 10^{6} \times 1.59 \times 10^{-6} \text{ A roentgens hr}^{-1}$$
$$= 5.63 \times 10^{-7} \text{ A roentgens hr}^{-1} \text{ at H + 171 hr for Shot 6.}$$

Finally the dose rate was referred to H + 12 hours for both shots by applying the decay factor from H + 12 hours to the time of analysis of the H + 218 hour and H + 171 hour samples for Shot 5 and Shot 6 respectively.

No actual measurements of gamma field decay were made over these periods. Recently Miller (Reference 6) has shown a remarkable degree of agreement to exist among Rad-Safe data taken over each of the islands at Operation Castle when the calculated disintegration min^{-1} curve for each shot is used to refer readings to a common time. This appeared to provide sufficient justification for use of the calculated curve in the present calculations. Decay curves were calculated as described elsewhere (Reference 3) using experimentally determined capture-to-fission ratios for various

---

[5] Incidentally it may be shown that:

$$n = \sum_{i=1}^{i=9} n_i = 2.91 \text{ photons min}^{-1} \text{ cm}^{-2} \text{ for Shot 5 samples, and}$$

$n = 2.94$ photons min^{-1} cm^{-2} for Shot 6 samples provide a gamma emission rate, $R = 1$ Mev min^{-1} cm^{-2} since

$$\sum_{i=1}^{i=9} E_i n_i = 1 \text{ Mev min}^{-1} \text{ cm}^{-2}$$

---

[6] The dose rate in roentgens hr^{-1} is derived from dose rate in Mev min^{-1} cm^{-3} as follows: by definition 1 roentgen hr^{-1} is the absorption of 83.8 ergs per gram in air at 20°C 760 mm (or 0.101 ergs per cm^3 of air). Since 1 Mev = 1.60×10^{-6} ergs, 1 roentgen hr^{-1} is the absorption of 6.32×10^4 Mev hr^{-1} cm^{-3}, or the absorption of 1.05×10^3 Mev min^{-1} cm^{-3}. Therefore dose rate (in roentgens hr^{-1}) = dose rate (in Mev min^{-1} cm^{-3}) $\times 9.5 \times 10^{-4}$.

induced activities. The curves are shown in Figures 4.1 and 4.5.

From these curves the dose rate at H + 12 hr d_{12} for Shot 5 is:

$$d_{12} = 5.58 \times 27.4 \times 10^{-7} \text{ A roentgens hr}^{-1}$$
$$= 1.53 \times 10^{-5} \text{ A roentgens hr}^{-1}$$

and for Shot 6:

$$d_{12} = 5.63 \times 15.7 \times 10^{-7} \text{ A roentgens hr}^{-1}$$
$$= 8.85 \times 10^{-6} \text{ A roentgens hr}^{-1}$$

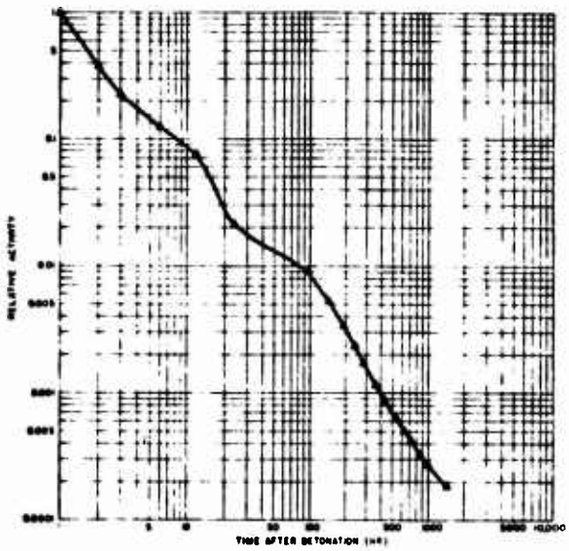

Figure 4.5 Calculated decay (d/m) for Shot 5 fallout.

Results for Shots 5 and 6 are tabulated in Tables 4.6 and 4.7 respectively.[7]

In view of the close agreement between these results for Shot 5 and those calculated independently from the water survey data (Chapter 3), contours for the water sampling results have not been drawn. Instead a comparison of the two sets of data is shown in Table 5.1.

Shot 6 results were plotted and contours drawn as shown in Figure 4.6. Aerial survey data (Reference 8) taken at H + 13 to H + 17 hours (Able flight) and H + 25 to H + 32 hours (Baker flight) were used as a rough aid in constructing contours, especially in areas where no water samples were taken. Relative intensities were read from aerial survey traces. Locations where aerial survey data and water sampling data coincide were used to normalize approximately the aerial survey traces to dose rate values calculated from water sample data. Drift corrections were applied to the latter. Baker flight traces were arbitrarily shifted 6 miles north and 6 miles east to improve the fit with Able flight and water sample data. The shift may be justifiable on the basis of errors in drift correction and position determinations. No depth of mixing calculations were made for the aerial survey data. Contours across the lagoon area were taken from Project 2.5a data (Reference 4).

[7] In this report no attempt has been made to apply a "terrain factor" to the calculated results to approximate more closely the dose rates which would have been observed over a real land area. A terrain factor has not been estimated for PPG site conditions. Ksanda (Reference 7) has estimated for Operation Jangle fallout area at NTS that observed dose rates = 0.6 × calculated dose rates.

4.7 CALCULATION OF DOSE RATE d FROM OBSERVED GAMMA FIELD-SAMPLE ACTIVITY RATIO

Schuert (Reference 4) has calculated gamma fields for certain Operation Castle shots from a relation of the following kind:

$$d = kI \tag{4.7}$$

Where: I = gamma activity of collected fallout samples per unit area of collecting surface.
k = factor calculated from gamma activity of fallout samples and gamma field intensities measured at or near the site of fallout collection.

Both measurements refer to H + 4 days. When the activity is expressed[8] in units of mv cm^{-2}, Schuert's data give for the total collector:

$$0.048 \leq k \leq 0.48 \frac{r\ hr^{-1}}{mv\ cm^{-2}}$$

and for the gumned paper collector:

$$k = 0.36 \frac{r\ hr^{-1}}{mv\ cm^{-2}}$$

Recently Miller (Reference 6) has calculated k using re-evaluation Rad-Safe gamma field data and values of gamma activity from fallout samples. From his data for Shot 1:

$k = 0.53 \pm 26$ percent (standard error).

For Shot 3:

$k = 0.34 \pm 21$ percent.

A value for k may be calculated from Equation 4.4 as follows:

$$d = d_r \left(\frac{R}{I}\right) \left(\frac{I}{A}\right) A$$

$$= d_r \frac{R}{I} I = kI$$

Where: $k = d_r \frac{R}{I}$

By substitution there results, using values based upon the spectral data for Shots 5 and 6:

$$k = 0.35 \frac{r\ hr^{-1}}{mv\ cm^{-2}}$$

---

[8] (gamma activity in mr hr^{-1}) = $\frac{\text{(gamma activity in mv)}}{5.19}$

This result and the experimental ratios calculated by Miller are in very gratifying agreement.

pgs. 72 & 73 Deleted.

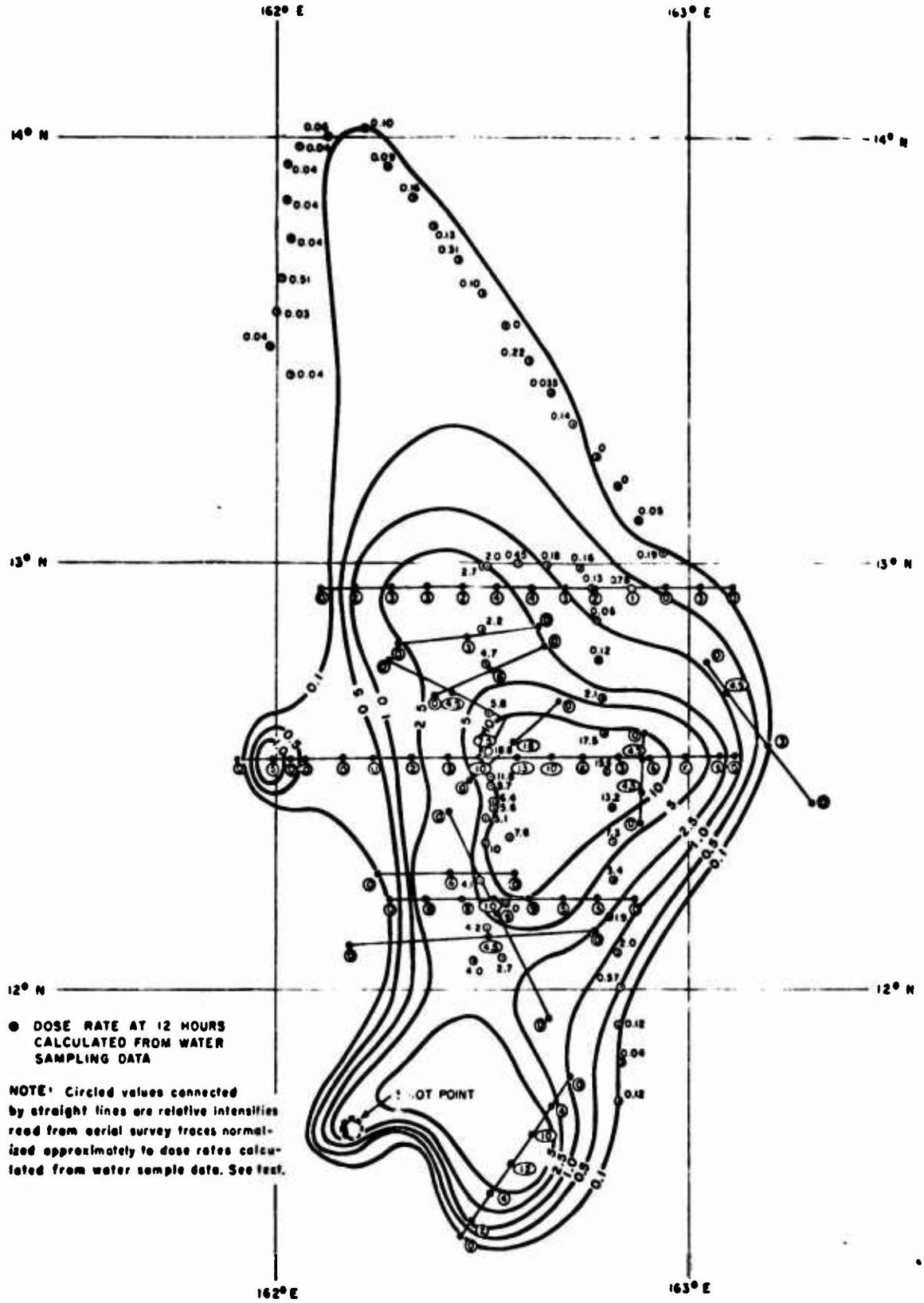

Figure 4.6 Estimated fallout dose rate contours for Shot 6 at H + 12 hours (r/hr).

PRECEDING PAGE BLANK-NOT FILMED

and sample analysis. One of the serious limitations of this work is the inability to assign limits of error.

The considerable number of data discussed in this chapter which were required for reduction and analysis of the basic water sample data and which had to be estimated indicate where improved results may be achieved in the future.

REFERENCES

1. Gates, L.D., and Eisenhauer, C.; "Spectral Distribution of Gamma Rays Propagated in Air"; TAR–AFSWP 502A and 502A Supplement.

2. Cook, C.S., and others; "Gamma Spectral Measurements of Fallout Samples from Operation Castle"; USNRDL–TR 32; U.S. Naval Radiological Defense Laboratory.

3. Tompkins, E.R., and Werner, L.B.; "Chemical, Physical and Radiochemical Characteristics of the Contaminant"; Project 2.6a, Operation Castle, WT–917.

4. Stetson, R.L., Schuert, E.A., Perkins, W.W., Shirasawa, T.H., and Chan, H.K.; "Distribution and Intensity of Fallout at Operation Castle"; Project 2.5a, Operation Castle, WT–915.

5. Jones, J.W., and Overman, R.T.; "The Use and Calibration of a 100% Geometry Ion Chamber"; AECD–2367, 20 March 1948.

6. Miller, C.F.; "Gamma Decay of Fission Products from Show Fission of U^{235}"; U.S. Naval Defense Laboratory; report in preparation.

7. Ksanda, C.F.; "Predicted Radiation Levels in Land Target Complexes after Contaminating Atomic Attacks"; USNRDL Document 009195; 15 December 1953.

8. LeVine, H.D., and Graveson, R.T.; "Radioactive Debris from Operation Castle Aerial Survey of open Sea Following Yankee–Nectar"; NYO–4618.

9. "Fallout Symposium"; AFSWP–895; January 1955.

10. "Effects of Atomic Weapons"; U.S. Government Printing Office, June 1950.

11. Ballou, N.E., and Hunter, H.F.; ADC–65.

12. "Fallout Symposium"; Rand Corporation, Santa Monica, California; 5, 6, and 7 March 1957.

pg. 75 Deleted.

Chapter 5
SUMMARY, DISCUSSION AND CONCLUSIONS

5.1 SUMMARY

In Chapters 3 and 4, independent sets of data relating to the radioactivity of sea water which had received fallout were presented. Computations were carried out so as to provide isointensity contours for Shots 5 and 6 as though the fallout had been received by a fixed plane at mean sea level. Dose rates at H + 1 hour or H + 12 hours are calculated at 3 feet above the fixed plane. Dose rate contours for Shot 5 are based upon the direct measurement of gamma activity in the sea water by towed radiation meters. A comparison of these results with those calculated from laboratory analysis of sea water samples taken at 23 locations is made in Table 5.1 and shows good agreement. Contours showing accumulated dosages at H + 50 hours were also plotted for Shot 5. One conclusion evident from these contours is that total doses of 250 r or more could have been accumulated throughout an area of about 5,000 square miles.

Contours for Shot 6 were calculated from water sample data; aerial survey traces were used to sketch in contours where water sampling was not done. Using these contours for Shots 5 and 6, the radioactivity appearing in the fallout area was summed in Chapter 4 to provide the fraction of the debris from the devices which appeared in fallout. Ten percent of the debris from Shot 5 and 8.5 percent of that from Shot 6 was accounted for within the fallout contours as drawn from radiation meter and water sample data.

5.2 DISCUSSION AND CONCLUSIONS

The agreement between the two sets of results for Shot 5 is gratifyingly good; it is recognized that the several arbitrary assumptions and approximations made in this report may have introduced systematic absolute errors which are extremely difficult to evaluate at this time. Nevertheless, it is concluded that radiation instruments submerged in the ocean and water sampling at representative locations and depths each result in data from which the fallout pattern can be determined satisfactorily for certain types of detonation. To accomplish this, supporting oceanographic and radiological data are needed. The principal deficiencies of the present work are believed to lie in the quality of the supporting data.

It is evident that on future surveys better data are needed in the following areas: (1) rate and depth of mixing of fallout; (2) physical and radiochemical characteristics of fallout, especially particulate size and radioactive decay; (3) times of arrival of fallout over the fallout area; (4) details of the action of ocean currents in dispersing fallout; (5) spectral distribution of gamma radiation from fallout; (6) relationship between intensity of a gamma radiation field and radioactivity per unit area of the source which produces the field; (7) calibration of radiation measuring devices both for field measurements and laboratory measurements and throughout the full range of gamma energies; and (8) accurate geographical positioning of all ships, planes and stations conducting surveys or collecting samples.

The two survey approaches described above give almost duplicate numerical results, but each has its inherent advantages. The direct gamma radiation meter is well suited

for rapid surveys and depth of penetration measurements, whereas the water sampling technique provides specimens for more complete gamma spectrum studies and for other physical and radiochemical studies. In relation to the depth of penetration measurements, it should be especially noted that success in either of the procedures used by this project during Castle Shot 5 is highly dependent upon reliability of estimates of fallout below the ocean surface. It is essential that the rate of descent of fallout into the mixed layer be sufficiently slow that the material is still accessible for measurement at the time of survey. It has been concluded tentatively that this requirement was met for Shots 5 and 6 since: (1) observations[1] of the fallout material from the over-water shots at Operation

Table 5.1 Comparison of Shot 5 Gamma Field Intensities at 12 Hours

(1) as Calculated from Towed Radiation Meter Data, and

(2) from Water Sample Analysis Data

Sampling Position				1*	2**
Logbook Time	Station	Latitude	Longitude	r/hr at 3 ft	r/hr at 3 ft
6 May 1500	1	12-10	166-06	23	49
1630	Surf	12-05	166-08.5	68	64
1730	Surf	12-00	166-13	65	61
1900	2	11-55.3	166-16.6	33	24
7 May 0130	Surf	11-51	167-04.2	9.5	0.6
0500	3	12-19.4	166-57.2	13	13
1400	4	13-12	166-40	1.5	1.5
1820	Surf	13-00.3	167-00.5	2.9	3.1
1900	5	12-48	167-20	7.5	3.7
2300	6	12-30	167-35	6.4	4.9
8 May 0400	Surf	12-03.5	168-00.5	2.9	0.3
0800	Surf	12-32	168-08	15	17
0900	Surf	12-45	168-10.1	8	5.7
1000	Surf	12-45	168-16	18	18
1100	Surf	12-43.5	168-21	6.1	3.5
1200	Surf	12-43	168-25	4.5	1.5
1350	Surf	12-58	168-27.5	15	9.6
1500	7	12-59.6	168-26.6	8.9	4.7
0200	Surf	12-19	166-39.5	38	47
0400	Surf	12-08	166-10.5	11	11
0600	Surf	12-02.5	165-44	43	46
1300	Surf	12-01	165-16	8	7.8
9 May 1530	8	11-52	165-34	42	44

* From Table 3.5, column 8, values at stations are interpolated. These can be identified in Table 3.5 by reference to Logbook Time.

** From Table 4.6, last column.

Castle indicated a very small particle size existed which could be expected to settle very slowly in water; (2) from the depth cast data of Shot 5 it appears that the descent of the radioactive material into the water mass comprising the mixed layer was of such a rate and uniformity as to make calculation of depth of penetration entirely feasible.

In conclusion, attention is again directed to the evidence that, following Shot 5, an area of about 5,000 square miles was covered with contamination which would be hazardous to human life had it fallen on land. For the smaller-yield Shot 6, the hazardous area was smaller. By hazardous is meant here contributing 250 r total dose during the first 50 hours. Total yield for Shot 5 was estimated at 12.5 megatons and 1.7 megatons for Shot 6. (Reference Summary Report of the Commander, Castle Report ITR-934.)

[1] Reference to Project 6.4, 2.5a reports on Operation Castle.

Appendix A

COMPARISON OF COMPUTED DOSE RATE OVER THE SEA WITH CERTAIN ACTUAL MEASUREMENTS

A few measurements were made on deck and on the bridge while underwater dosages were being obtained following Shot 5. Intercomparison of these data permits a rough test of the familiar elementary theory for making predictions of dose rate above the sea from measurements made by submerged instruments. The behavior of the several instruments can be compared also.

Figure A.1 shows the manner in which these particular measurements were made, and Table A.1 lists the measurements and also their values after being reduced to dosage rates by application of suitable calibration curves.

Column 9 is the ratio of the intensity in air to the intensity underwater-measured by the same instrument, Mark II. Column 10 is the ratio of intensity in air measured by the ship's radiac set (type AN/PDR-27C) to the intensity underwater, measured by the Mark I device.

Column 11 is the ratio which was computed by using the simplified theory summarized in Equation D.4.3, page 435 of "The Effects of Atomic Weapons" (1950, LASL), under the assumption of monochromatic

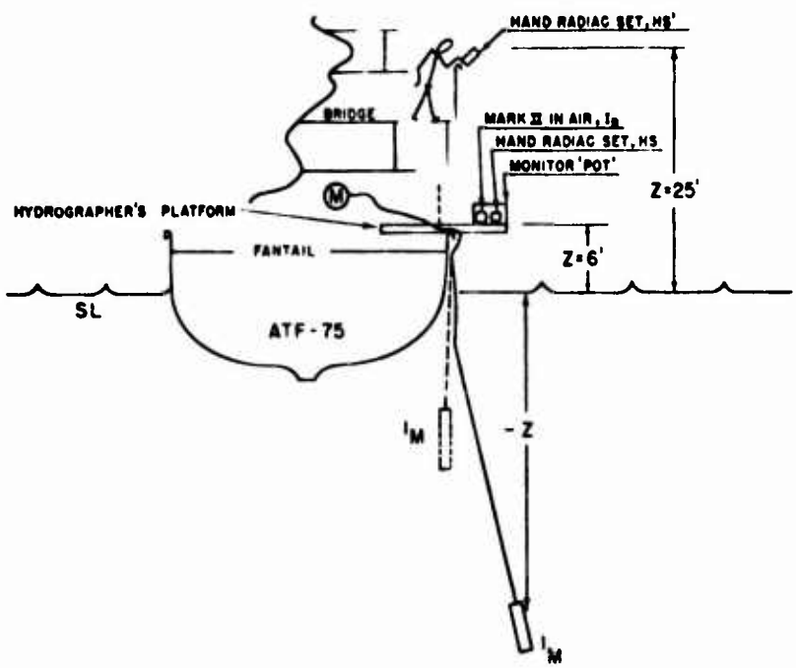

Figure A.1 Location of instruments during Shot 5. Surveys used for comparisons discussed in Appendix A.

energy of 0.7 Mev. This equation is not strictly accurate for a volume distributed source since it assumes angular distribution of unscattered radiation coming up from the water to be the same as for a plane source. However, this deficiency leads to smaller numerical error than arises from the neglect of scattered rays. It is recognized that this simple theory is deficient; there is an additional contribution due to scattering and the actual geometry including the ship cannot be treated properly.

Comparison may be made between Column 11 and Columns 9 and 10; the theoretical values agree with the experimental much better than might have been hoped for considering the geometric complications introduced by the presence of the ship. The ship filters rays coming from almost half the sea, but this is somewhat compensated for by the presence of local contamination on the deck and hull.

Table A.1 Above Surface and Below Surface Survey Data and Their Ratios

Shot 5 Station Number	Time/Date	Elevation in feet	Underwater I_M		Air I_B		Air H_S	Experimental Ratios		Theoretical Ratios
			μa	mr/hr	μa	mr/hr	mr/hr	I_B/I_M	HS/I_M	
Y - 1	1600/May 6	6	24.0*	16.9	11.0*	6.9		.40		.34
Y - 2	1900/May 6	6	17.5*	11.7	9.0*	5.4		.46		.34
On course	1621/May 6	6	15.0**	33.0			13.0		.39	.34
On course	1638/May 6	6	17.0**	51.0			21.0		.41	.34
On course	2315/May 5	25	21.0**	80.0			22.0		.27	.20
Column No. 1	2	3	4	5	6	7	8	9	10	11

Footnotes

* Mark II readings
** Mark I readings

Column No.

1. Location of measurement.
2. Time and Date of Measurement.
3. Elevation.
4. Meter Readings of Underwater Instrument.
5. Apparent mr/hr from Calibration Data Pertaining to Estimated Mixed Radiation Spectrum.
6. Meter Readings from Mark II in Air (on Hydro Platform).
7. Apparent mr/hr from Calibration for Estimated Mixed Radiation.
8. Meter Readings of Hand Set in mr/hr.
9. Experimental Ratios of $I_B:I_M$.
10. Experimental Ratios of $HS:I_M$.
11. Theoretical Ratios Based on Equation D.4.3 p. 435 in The Effects of Atomic Weapons (1950, LASL).

Appendix B

PROCEDURE USED IN CHAPTER 3 FOR ESTABLISHING THE CALIBRATION OF THE TOWED INSTRUMENTS FOR MEASURING GAMMA RAYS UNDERWATER

B.1 CALIBRATION OF INSTRUMENTS IN AIR

Initial plans called for calibrating the instruments repeatedly during the cruise against a large gamma ray source; however, no suitable source was found available at sailing date. In the absence of absolute standardization the measurements would still have been of value as interpolations of the measurements made by means of water samples at fixed stations. Nevertheless, serious efforts were continued toward establishing the calibration of the instruments without reliance upon water analyses in the laboratory.

The instruments were intercompared whenever possible; they were towed in pairs in contaminated sea water and exposed in pairs in the field of radiations which existed in the air above the ship's deck due to the contaminated materials nearby.

During the intercomparisons of instruments in the air over the deck the ship's radiac instruments were read also at the same locations. The two radiac instruments (Type AN/PDR-27C) agreed well with one another, appeared to be in good condition, and might have supported some sort of an independent calibration scheme had it not been found impossible to obtain accidental fields of activity strong enough and geometrically uniform enough to intercalibrate accurately except at a few isolated intensities.

Much pains were taken to keep the instruments in good order so that a calculation made after the cruise might be significant; the Mark II and Mark III instruments appeared to be in perfect order at the end of the trip; however, the Mark I instrument had to have a G. M. tube replaced during the cruise and therefore its calibrations pertaining to the cruise are quite different before and after this change.

Immediately after the ship returned to Parry Island the three towed instruments were taken to the open-air calibrating area which was available for standardizing radiac sets, and these were calibrated against a distant point source of radium of known activity. The results of these measurements are shown in Figures 2.1, 2.2, and 2.3 plotted in solid lines.

The instruments were then boxed and shipped to the U. S. Bureau of Standards where calibration in air and against radium was repeated. Mishap during shipping caused a delay of about one month; during this time Mark I and III apparently suffered serious battery aging or other damage so that erratic behavior was exhibited during part of their calibrations, but the Mark II instrument satisfactorily reproduced the general character and magnitude of its calibration at Site Elmer.

The dashed curve in Figure 2.2 illustrates, for example, the radium calibration made at the Bureau corresponding to the instrument scale-range A. The 20 percent discrepancy between the Elmer curve (solid) and the Bureau curve (dashed) can be attributed to the known drop in battery voltage during the intervening time.

Thus, Mark II maintained reasonable constancy of calibration (against radium) after a month of rough treatment and therefore probably was well within 10 or 20 percent of truth of its Elmer calibration during the cruise. Mark II instrument was therefore chosen as cruise standard; the Mark I, Mark III and Pot instruments' readings also may be given absolute evaluation by means of the intercalibrations against Mark II made during the cruise and at Site Elmer.

Thus far, calibration of a limited sort only has been described. The measurements summarized by the curves in Figures 2.1 to 2.4, inclusive, relate only to the hard gamma rays of radium and are strictly accurate only when the rays strike the instruments at normal incidence; that is, when the rays arrive normal to the axes of their cylindrical cases. Other information now must be introduced so that the effect of rays arriving at other angles at the surface of a submerged instrument can be predicted; and theory must be resorted to before an estimate of the activity density in the sea can be predicted from the reading coming from

(See Table B-1 for origin of these curves.)

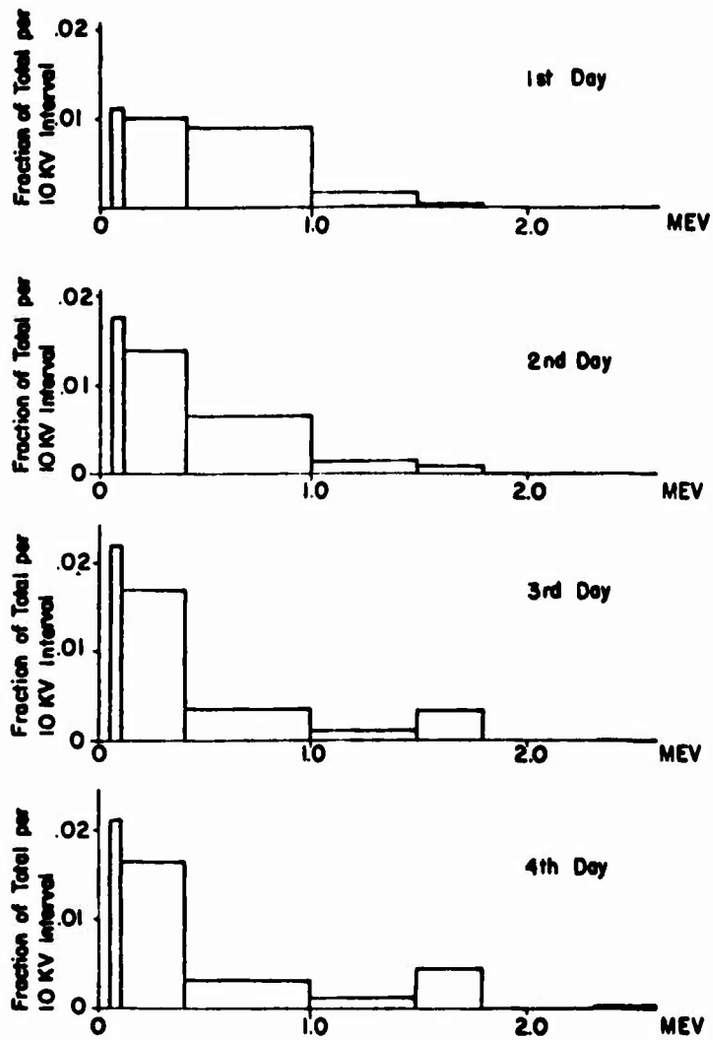

Figure B.1 Histograms of estimated source spectra.

Table B.1 Estimated Source Spectra*

Energy	Fraction of Total Source				
In MEV	D + 1	D + 2	D + 3	D + 4	Average of Four Days
0.05-0.10	.056	.088	.110	.106	.090
0.10-0.40	.302	.415	.504	.492	.428
0.40-1.00	.541	.395	.212	.191	.335
1.00-1.50	.084	.066	.060	.059	.067
1.50-1.80	.009	.029	.102	.138	.069
1.80-2.30	.005	.004	.005	.005	.005
2.30-2.60	.003	.003	.007	.009	.006

* See paragraph B.2.1 for origin of this data.

the submerged instrument. Finally, some definite assumption must be made regarding the spectral distribution of energy existing in the sea at the time of the measurement.

B.2 ESTIMATION OF THE RESPONSE TO UNDERWATER RADIATION

The spectral character of the radiation arriving at the surfaces of a submerged gamma detector depends upon the character of the radiating sources and also upon the degree to which scattering degrades the radiation before it arrives at the detector. And since response of a gamma dosimeter is never completely independent of photon energy, consideration must be made both of initial photon energy and of scattering before a practical calibration of the instrument can be established.

B.2.1 Estimates of the Source Spectra. Fortunately, estimates of the photon energy spectra of fallout material are available from other experiments. Estimated energy spectra supplied by Dr. Scoville of AFSWP were made use of in this report; Table B.1 lists these estimated spectra separately for each of the first four days. And in the right-hand column is to be found an average of the four spectra.

Numerical computations were carried out separately with each of the four spectra and the results were then averaged; however, it was later realized that the limited accuracy of the experimental measurements did not justify this detail and an average spectra might just as well have been assumed at the outset.

Figure B.1 shows the four estimated spectra reduced to histograms.

B.2.2 Calculations of the Underwater Dose Spectra Corresponding to the Assumed Fallout Source Spectra. The amount by which the emitted radiation is degraded by scattering before reaching the submerged gamma detector can be determined approximately. Measurements at sea were made under circumstances approximating the mathematically simple case of a uniform distribution of activity in an infinite body of water. This scattering problem has been investigated with the aid of modern computers, and AFSWP Report 502A (1954) presents numerical solutions in graphical form. By use of these graphs, the spectrum of energy which arrives at any point inside the large scattering medium can be derived from the spectrum of the energy emitted from the sources.

Figure B.2 shows the results when each of the four source spectra of Figure B.1 are degraded by scattering inside the large distributed source. These, therefore, must be taken to be the spectra of the gamma ray energy which the submerged instrument must measure.

These degraded spectra are given again in tabular form in Columns 3, 5, 7, and 9 in Table B.2 where their ordinates are labeled $D(E_j)$ consistent with the nomenclature of the AFSWP 502A Report. Table B.2 will be discussed further in the conclusion of this appendix.

The intervals appearing in the abscissa of the "dose" spectra of Figure B.2 were chosen arbitrarily for convenience in the computations.

B.2.3 Instrument Response Variation Due to Photon Energy Variation Alone. At the Bureau of Standards the instruments were exposed normal to their axes to several radiations; to X-rays corresponding to effective potentials of 58, 87, 132, 168, and 222 kev and also to radium and cobalt beams of known intensity.

Only the results for the Mark II instrument will be considered here in any detail. The variation in its response to rays normal to its axis is summarized in Figure B.3. It will be noted that the photon energy has relatively small influence upon the response to rays normal to the axis unless the photon energy happens to be less than about 0.080 Mev.

B.2.4 Instrument Response Variation Due to Angle of Incidence Alone. The heavy-walled instruments, of course, responded differently when the angle of incidence of the rays differed from 90 degrees. Figure B.4 shows the results of tests on Mark II in the Bureau when the incident angle was varied from 0 degrees to 180 degrees; the results $f(\theta)$ are given as response relative to that response at 90 degrees incidence.

B.2.5 Estimates of 4 Pi Monochromatic Sensitivity. From the data in Figure B.4 it can be determined what the effect would be if the radiating source were spread uniformly around the detector. It can be shown by use of the experimental values of $f(\theta)$ and by geometrical considerations that the ratio of response to a uniform distribution of sources to the response to a concentration of the sources at 90 degrees incidence will be:

$$\frac{1}{2}\int_0^{\pi} f(\theta)\ \sin\theta\ d\theta$$

Where: θ = angle of incidence in radians.

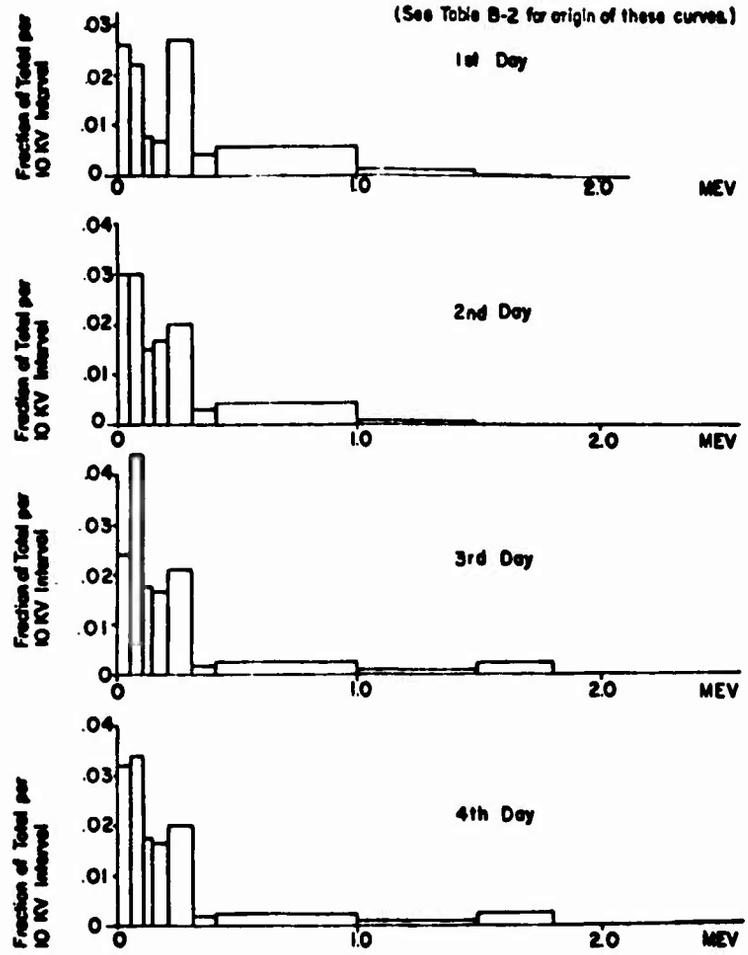

Figure B.2 Histograms of degraded dose spectra.

Table B.2 Effective Response Sensitivity of Mark II to Estimated Fallout Radiation*

E_j Energy Interval (mev)	m_j (μA/mr/hr)	D + 1 Spectrum D(Ej)	D + 1 Spectrum mj D(Ej) (μA/mr/hr)	D + 2 Spectrum D(Ej)	D + 2 Spectrum mj D(Ej)	D + 3 Spectrum D(Ej)	D + 3 Spectrum mj D(Ej)	D + 4 Spectrum D(Ej)	D + 4 Spectrum mj D(Ej)
0-0.05	0	.13	0	.15	0	.12	0	.16	0
0.05-0.10	0.40	.11	.04	.15	.06	.22	.09	.17	.07
0.10-0.14	1.05	.03	.03	.06	.06	.07	.07	.07	.07
0.14-0.20	1.45	.04	.06	.10	.15	.10	.15	.10	.15
0.20-0.30	1.55	.27	.42	.20	.31	.21	.33	.20	.31
0.30-0.40	1.60	.04	.06	.03	.05	.02	.03	.02	.03
0.40-1.00	1.75	.33	.58	.25	.44	.165	.29	.145	.25
1.00-1.50	1.90	.05	.10	.035	.07	.045	.09	.050	.10
1.50-1.80	1.95	.005	.010	.020	.04	.065	.13	.075	.146
1.80-2.30	1.98	.003	.006	.003	.006	.004	.008	.003	.006
2.30-2.60	~ 2.00	.002	~.004	.002	~.004	.004	~.008	.005	~.010
Column No. 1	2	3	4	5	6	7	8	9	10
Effective response to degraded radiation in all intervals (μA/mr/hr) $C = \sum_j m_j D(E_j) =$			1.310		1.190		1.196		1.142

Mean value of C = 1.21 μA/mr/hr

m_j = effective monochromatic response in jth interval - in μA/mr/hr (USBS)
D(Ej) = degraded spectrum - fraction of total dose (AFSWP #502A)
m_j D(Ej) = effective response to degraded radiation in jth interval - in μA/mr/hr

* See description in paragraphs B.2.2 and B.2.6

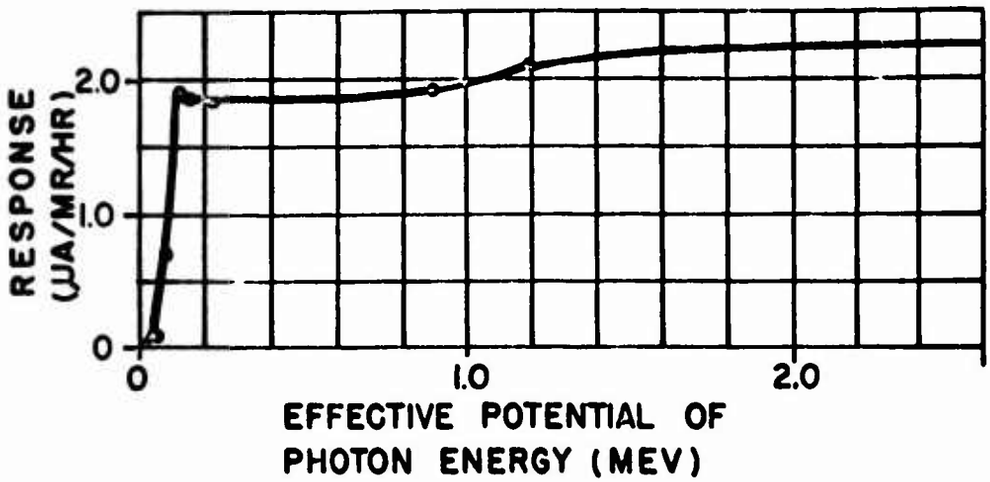

Figure B.3 Experimental response of Mark II for rays at 90 degrees incidence.

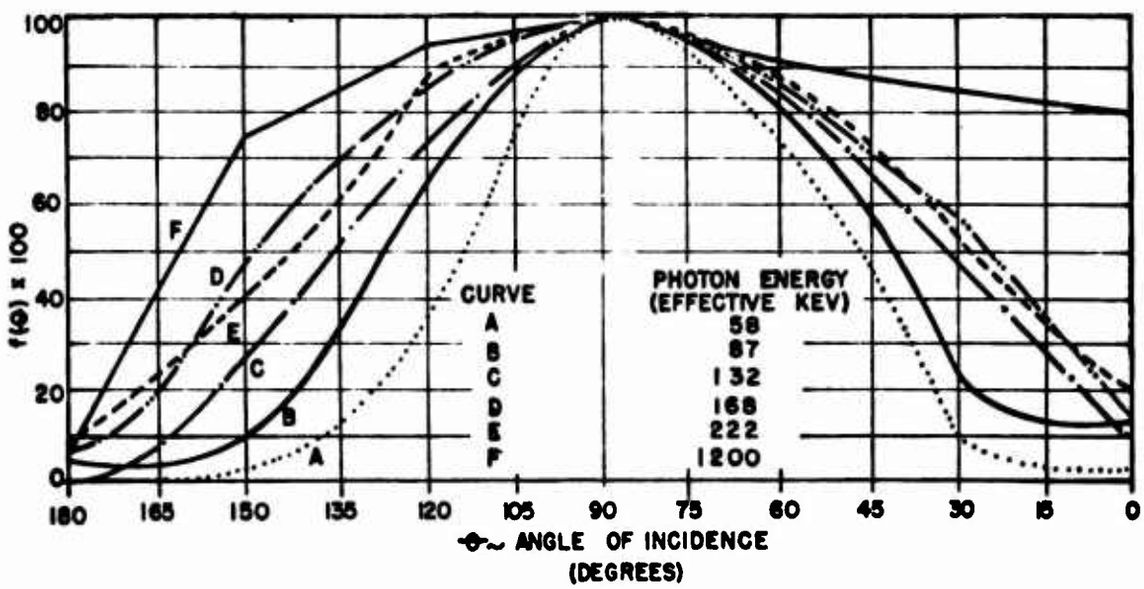

Figure B.4 Variation in response of Mark II with angle of incidence of radiation.

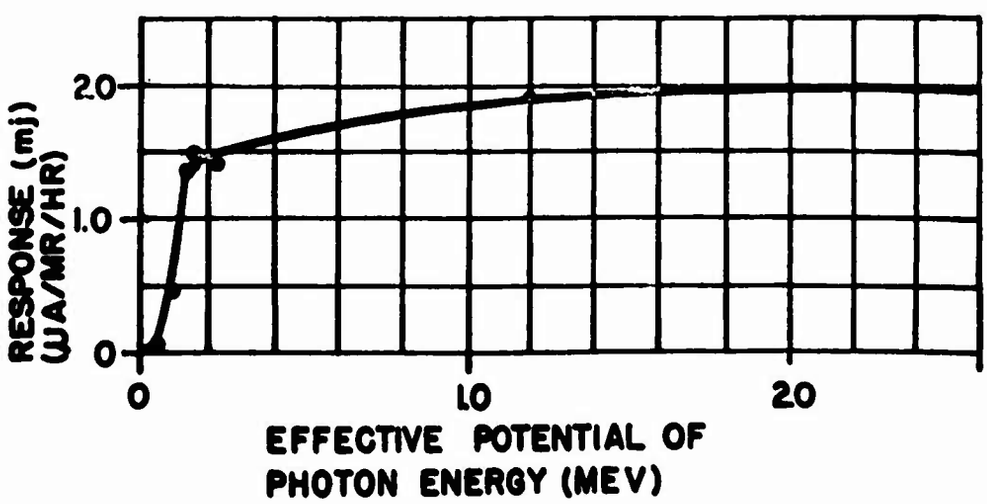

Figure B.5 Plot of data from Table B.4.

Table B.3 Response to Uniform 4 Pi Distribution of Sources Over a Spherical Shell Relative to the Same Sources Concentrated at a Point at the Same Radius and on the Normal to the Instruments's Axis*

KCVP**	75.00	100.00	150.00	200.00	250.00	Co^{60}
Effective MEV***	.058	.087	.138	.168	.222	1.20
Mark I	---	.61	.73	.73	.85	---
Mark II	.53	.64	.73	.79	.79	.90
Mark III	.71	.84	.88	.98	.93	.96

* See paragraph B.2.5.

** Kilovolt constant potential on the X-ray tube giving the beam.

*** The effective photon energy, in terms of absorbtion in light elements which the Bureau of Standards believes exists in these beams.

Table B.4 Computed Responses of Mark II to Uniformly Distributed Sources of Several Different Effective Energies*

KVCP	Effective Potential MEV	90° Response in μa/mr/hr	Response to 4 Pi Source Relative to Response to 90° Incidence	Effective Response to Distributed Monochromatic Source
75	.058	.08	.53	.04 μA/mr/hr
100	.087	.68	.64	.43 "
150	.138	1.89	.73	1.38 "
200	.168	1.85	.79	1.46 "
250	.222	1.83	.79	1.44 "
Co^{60}	1.200	2.10	.90	1.90 "

* See paragraph B.2.5

Table B.3 summarizes the effect of distribution of sources around each of the underwater instruments. Each column relates to a separate heavily-filtered radiation. For each instrument and for each radiation are listed the responses corresponding to uniform 4 π distributions of sources relative to the response to the same sources concentrated at a point on a line normal to the instruments' axes.

It can be seen here that calibration by exposure in one direction only is not sufficient when the instrument is to be used underwater.

Table B.4 combines the information in Figure B.3 and Table B.3 so as to give the absolute response to a distributed source predicted for one particular instrument, Mark II. Response is given in μa/mr/hr of each type of test radiation used.

Figure B.5 is a graphical plot of Table B.4 which will be useful in later computations. The ordinates (m_j) are the computed responses (in μa/mr/hr) to uniformly distributed sources having photon energies listed on the abscissa. The photon energies given are, of course, effective energies since truly monochromatic beams were not available.

B.2.6 Response of Mark II to Distributed Sources Comprised of Mixed Fallout Materials. An estimate now can be made of the Mark II instrument's response when it is submerged in water contaminated with active material having any given spectral character.

Let m_j represent the response to a monoenergetic source component of energy E_j and which is distributed uniformly around the detector. The ordinates of Figure B.5 approximate m_j defined here.

Let $D(E_j)$ represent the fractional dose delivered by the j, the component having energy E_j, that is the fractional dose delivered by this component per mr/hr of total dose delivered by all components together.

Then in this nomenclature of the 502A Report, the response of the Mark II instrument to a source both distributed in 4 Pi geometry and consisting of a number of constituents differing in photon energy would be

$$C = \sum_j m_j D(E_j)$$

in units of μa/mr/hr of total dose.

Table B.2 shows the final steps in deriving the overall response sensitivity C to fallout material distributed in the sea. The value of C is given for each of the four energy spectra of Table B.1.

It would appear that a mean value of C might safely be accepted here and applied to all Mark II measurements made during the cruise, or C_{ave} = 1.21 μa/mr/hr.

B.2.7 Derivation of Complete Response Curves for the Instrument Mark II When It is Used Submerged in Fallout Contaminants. The single number C is a solitary calibration factor pertaining to the single instrument Mark II. It is a mean of the estimates of the responses to the four fallout source spectra supplied by Scoville; and it strictly pertains only to one part of the instrument's range as a dosimeter. It can be seen in Figure 2.2 that the relationship between μa response on the instrument dial and dosage is not a linear one even in connection with hard radium radiation.

The value of the Factor C given above pertains strictly to the use of the Mark II instrument near 19 μa on its dial simply because the calibration experiments at the U. S. Bureau of Standards described in Figure C.3 were carried out at or near this mid-scale reading only. Complete calibration at the Bureau at all parts of the instrument's scale range would have been expensive and was believed unjustified.

It may be seen on Curve A of Figure 2.2 that 19 μa on Mark II dial corresponds to 10.2 mr/hr of radium rays, so that at this dose rate the radium calibration factor may be called $C' = 19/10.2 = 1.86$ μa/mr/hr, and by comparison of this with C it can be seen that the instrument calibration made at Site Elmer against radium must be increased by the factor $C'/C = 1.86/1.21 = 1.5$, whenever the instrument is used in mixed fallout underwater.

This correction factor was derived for points on the scale near 19 μa, but it would appear suitable for approximately correcting the radium calibration curve at all other parts of the scale. This is because there is reason to believe the shape of any of the characteristic curves such as seen in Figure 2.2 would not be radically different for photon energies effective in fallout radiation.

The final calibration adopted for the Mark II instrument, therefore, was merely the calibration against radium at Site Elmer (solid curves on Figure 2.2) but raised in numerical value everywhere by a factor of 1.5. That is, the ordinates indicated by the solid curves must be multiplied by 1.5 whenever the instrument was submerged in water contaminated by fallout debris.

Appendix C

COMPUTATION OF DOSE AT THREE FEET ELEVATION

C.1 COMPUTATION OF DOSE AT THREE FEET ELEVATION FROM MEASUREMENTS OF DOSE IN WATER

Wherever possible, the notations of AFSWP 502 will be used.

Let ϕ_t be the submerged instrument's reading converted to mr/hr after corrections by use of calibration curves which take into account all corrections for: (1) radiation coming from all angles, (2) mixed radiation having the assumed fallout spectrum of energy, and (3) contamination of instrument in the water. Then:

$$\phi_t = 1.45 \times 10^{-5} \times 1000 \times 3600 \sum_{j=0}^{j=i} h_A(E_j)\, f(E_j) = \text{mr/hr}$$

Where: there are several constituent fluxes, $f(E_j)$ each having photon energy E_j and the dose rate given by the same flux to the water will be:

$$D_t = \sum_j h_W(E_j)\, f(E_j) = \text{Mev/cm}^3\text{/sec},$$

Where: $h_A(E_j)$ is the true absorption coefficient in air, and $h_W(E_j)$ is the true absorption coefficient in water.

But these coefficients are proportional to the number of electrons per cubic centimeter, or numerically (Lauritsen AFRRT, Vol. XXX No. 3, September 1933) from:

$$\frac{h_W(E_j)}{h_A(E_j)} = \frac{860}{1}$$

which is approximately independent of energy.

So that:

$$D_t = \frac{860}{1.45 \times 10^{-5} \times 1000 \times 3600}\,\phi = 16.5\,\phi_t$$

when ϕ_t is in mr/hr, and D_t is in Mev/cm^3/sec.

But, if sources are distributed uniformly throughout a very large, homogeneous, scattering and absorbing volume, considerations of conservation of energy require that the specific rate of emission of energy is equal to the specific rate of absorption in the medium. So that the emission rate is, at time t and at depth Z,

$$I_Z = D_t$$

Therefore:

$$I_Z = 16.5\,\phi_t = \text{Mev/cm}^3\text{/sec}$$

And if the water is uniformly contaminated to the depth Z centimeters, the total amount I_F of activity in the water column per square centimeters, is

$$I_F = Z_{cm} I_Z$$

$$= 16.5\ Z_{cm}\ \phi_t = \text{Mev/cm}^2\text{/sec}$$

This can be imagined to correspond to the fallout density on a smooth, fixed plane, at time t.

If the fallout has several constituents, the fallout density can be expressed

$$I_F = \sum_i n_i E_i$$

And if P_i = the fraction of energy in the ith component

$$n_i E_i = P_i I_f$$

so that

$$n_i = \frac{P_i}{E_i} I_F$$

the dose at elevation X due to the ith constituent is,

$$n_i d_i = \frac{n_i E_i h_A(E_i)}{2} \int_{-\mu x}^{\infty} \frac{e^{-s}}{s}\, ds\ B_i\ (\mu_c\, x) = \text{Mev/cm}^2\text{/sec}$$

and the total dose in air is,

$$\sum_i n_i d_i = \sum_i \left[\frac{n_i E_i h_A(E_i)}{2} \int_{-\mu x}^{\infty} \frac{e^{-s}}{s}\, ds\ B_i\ (\mu_c\, x) \right]$$

or by substitution, the total dose at elevation X is, in Mev/cm²/sec,

$$I_F \sum_i P_i \frac{h_A(E_i)}{2} \int_{-\mu x}^{\infty} \frac{e^{-s}}{s}\, ds\ B_i\ (\mu_c\, x)$$

or,

$$16.5\ Z\phi \sum_i \frac{P_i h_A(E_i)}{2} \int_{-\mu x}^{\infty} \frac{e^{-s}}{s}\, ds\ B_i\ (\mu_c\, x)$$

Therefore a dosimeter at elevation X above the hypothetical plane would read, at time t, and in milliroentgens per hour,

$$\begin{aligned} \theta_t &= 1.45 \times 10^{-8}\ (1000)\ (3600) \sum_i n_i d_i \\ &= 52 \sum_i n_i d_i \\ &= (52)\ (16.5)\ Z\phi_t \sum_i P_i h_A(E_i) \int_{-\mu x}^{\infty} e^{-s}\ ds\ B_i\ (\mu_c\, x) \end{aligned}$$

Table C.1 Computation of Dose at Three Feet Elevation Above Fallout Plane
By Method of AFSWP Report #502A

1	2	3	4	5	6	7	8	9	10
E_i	P_i	$D_i(3',E_i)$	$B_D(3',E_i)$	$\mu_i x$	$-E_i(\mu x)$	(6)x(4)	(7)(2)	$h(E_i)$	(9)x(8)
.075	.090	.400	1.67	.0206	3.4	5.7	.518	$.29 \times 10^{-4}$	$.150 \times 10^{-4}$
.250	.428	.354	1.55	.0138	3.8	5.9	2.525	$.34 \times 10^{-4}$	.864
.700	.335	.242	1.32	.0091	4.1	5.4	1.810	.35	.634
1.250	.067	.186	1.23	.0069	4.3	5.3	.355	.348	.123
1.650	.069	.160	1.19	.0065	4.4	5.2	.358	.32	.115
2.05	.005	.143	1.17	.0058	4.5	5.3	.026	.295	.008
2.45	.005	.130	1.15	.0050	4.7	5.4	.032	.280	.009

Summed Column (10) = $\sum_i P_i h(E_i) B_D(3',E_i)[-E_i(-\mu x)]$ = 1.903×10^{-4}

KEY TO SYMBOLS

E_i - - Effective energy of photon in Mev in the ith component of the "average fallout spectrum" of Table B.1

P_i - - Fraction of energy contributed by source component i.

$D_i(3',E_i)$ - - Fraction of dose scattered from ith component reaching 3 foot elevation.

$B_D(3',E_i)$ - - Dose build up factor, defined = 1/1-Col. (3).

$h(E_i)$ - - True absorbtion coefficient (in air).

$-E_i(-\mu_i x)$ - - Exponential integral; x = 100 cm, μ for E_i.

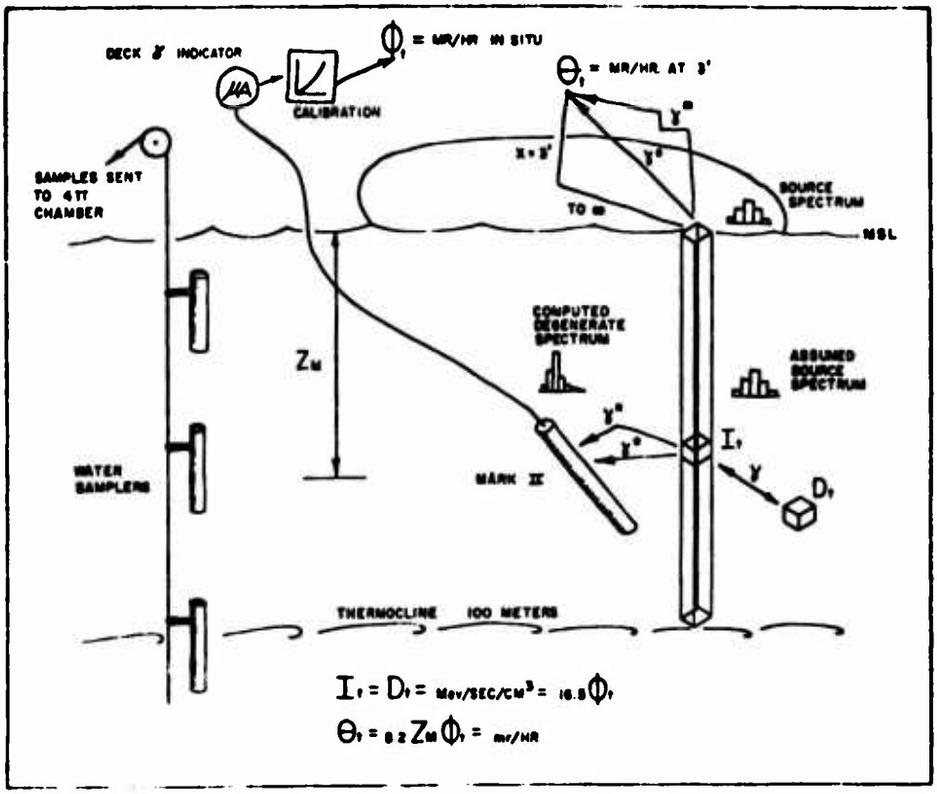

Figure C.1 Schematic of reduction of readings to dose rate (mr/hr) at 3 feet elevation.

C.2 NUMERICAL COMPUTATIONS

The numerical values of B_i (μ_c x), taken from Figure 20 of AFSWP 502A, are listed in Table C.1 for each of the seven components of an average activity spectrum that is listed in the right hand column of Table B.1.

Also shown are the tabular values of the exponential integral for the seven energy components corresponding to the elevation X = 3 feet.

It is seen from Table C.1 the computation based upon average spectrum gives the numerical value of the survey,

$$\sum_i P_i h_A(E_i) \int_{-\mu x}^{\infty} \frac{e^{-s}}{s}\, ds \;\; B_i \;\; (\mu_c\, x) = 1.90 \times 10^{-4}$$

Thus finally, the dose rate at 3 feet elevation reduces to,

$$\theta_t = (52)\,(16.5)\,(1.90 \times 10^{-4})\,(1/2)\, Z\phi_t$$
$$= 0.082\; Z\phi_t$$

where Z is in centimeters, and θ_t and ϕ_t are in milliroentgens per hour and when instead Z is in meters, ϕ_t is in milliroentgens per hour and θ is in roentgens per hour

$$\theta_t = 8.2 \times 10^{-6}\; Z\phi_t$$

C.3 CONCLUSION REGARDING HYPOTHETICAL DOSAGE AT 3 FEET ELEVATION

The numerical factor just derived, along with the calibration curves discussed in Appendix B permit the reduction of the raw gamma data (obtained in microamperes) to the desired terms. Figure C.1 schematically summarizes the whole procedure for reducing the underwater measurements to the desired hypothetical intensity at 3 feet elevation.

92 blank.